UNIVERSITÀ DEGLI STUDI DI TORINO

Doctoral School in Natural Sciences

PhD Program in Pharmaceutical and Biomolecular Sciences

XXXVI Cycle

PhD Thesis

DESIGN AND DEVELOPMENT OF A SUSTAINABLE MANUFACTURING PROCESS FOR THE PREPARATION OF ALBUMIN-BASED NANOMEDICINE ABLE TO CARRY LIPOPHILIC AND HYDROPHILIC MOLECULES

IRFAN AAMER ANSARI

Supervisor/ Coordinator: Prof. ssa Roberta Cavalli

DEDICATED TO MY PARENTS

ACKNOWLEDGEMENTS

First of all, I am deeply thankful to Almighty Allah for granting me health and the strength to pursue all my activities with vigour.

Reflecting on the emotionally charged years of my PhD journey, I am grateful for the milestones crossed, the people met, and the lasting impressions left on the shifting sands of time.

My time in the Department of Drug Science and Technology at the University of Turin, and the completion of this dissertation, were made possible by the support and guidance of several significant individuals who will forever hold a place in my heart.

I am profoundly grateful to my supervisor, **Prof. ssa Roberta Cavalli**, Professor in the Department of Drug Science and Technology, University of Turin, for her unwavering support and encouragement. I feel privileged to have had the opportunity to work under her valuable guidance. Her intelligence, motivation, and active involvement in research have not only helped me understand various aspects of my work but also fostered my development of independent thinking. Her timely advice, meticulous scrutiny, and scholarly insights have been instrumental in the completion of this task.

It is a genuine pleasure to express my deep gratitude to my mentors, **Prof. ssa Monica Argenziano** and **Prof. ssa Anna Scomparin**, also in the Department of Drug Science and Technology, University of Turin. Their dedication, keen interest, and overwhelming willingness to help their students have been fundamental to the completion of my work. I am deeply and eternally indebted to them for their advice and guidance throughout my research.

I owe a deep sense of gratitude to my collaborator **Prof. ssa Chiara Dianzani**, Department of Drug Science and Technology, University of Turin, for her keen interest in my progress at every stage of my research. Her inspiration, timely suggestions, kindness, enthusiasm, and dynamism have greatly enabled me to complete my thesis.

Special thanks to **Prof. Giancarlo Cravotto** and **Prof. ssa Katia Martina** Professor in the Department of Drug Science and Technology, University of Turin, for allowing me to use their laboratories and instruments, which were crucial for my research.

I also express my deep gratitude to **Rita Spagnolo** for providing the necessary chemicals and invaluable technical support for my dissertation**.**

I extend my heartfelt thanks to my lab mates, **Chiara Molinar, Shoeb Ansari, Ahmet Dogan Ergin, Gjylije Hoti, Ibrahim, Salah, Mohammed, Alessia,** and **Simonetta**, for always being there during the good and bad times throughout my PhD journey. Your companionship has made these years truly wonderful.

A special thanks to my elder brother, **Khalid Akhter Ansari**. Your support and encouragement mean more to me than words can express

Finally, I acknowledge the people who mean the world to me: my parents, my brothers, my sisters, and my niblings. Your love and blessings are the foundation of my strength. Thank you, Mom and Dad, for your faith in me and for giving me the freedom to pursue my dreams. I consider myself incredibly fortunate to have such a supportive family standing behind me with unwavering love and support.

Thank you.

Declaration

I Irfan Aamer Ansari declare that the work presented in this thesis, titled "Design and Development of a Sustainable Manufacturing Process for The Preparation of Albumin-Based Nanomedicine Able to Carry Lipophilic and Hydrophilic Molecules," is my original research conducted under the supervision of Prof. ssa Roberta Cavalli at Department of Drug Science and Technology, University of Turin.

I confirm that my thesis has not been submitted for any other degree or qualification. All sources of information used have been acknowledged, and appropriate citations have been included.

Signed,

Irfan Aamer Ansari

June 2024

INDEX

List of Figures 9

List of Tables 13

Introduction 15

Chapter 1: Albumin: Molecular Structure and Properties 16

1.1 Biocompatibility of Albumin 19

1.2 Denaturation of Albumin 20

1.3 Applications of Albumin in Drug Delivery 23

1.4 Challenges to Prepare Albumin Nanomedicine 25

1.5 Food Drug Administration Approved Albumin Based Nanodrugs 26

Chapter 2: Manufacturing Process of Albumin Nanocarriers 29

2.1 Coacervation Method (Desolvation method) 30

2.2 Emulsification Method 32

2.3 Nab-Technology 33

2.4 Thermal Gelation 33

2.5 Nano Spray-Drying 34

2.6 Design and Development of Albumin-Based Nanoplatforms Using Green Route 36

Chapter 3: Functionalization Approaches of albumin-based nanocarriers 39

3.1 Non-Covalent Surface Modifications 39

3.2 Covalent Surface Modifications 40

3.3 Surface modified Albumin Nanoparticles 41

3.4 Surfactant 42

3.5 Cationic Polymers 42

3.6 Chitosan 43

3.7 Thermosensitive polymers 46

3.8 Polyethylene glycol (PEG) 46

3.9 Folic acid 47

3.10 Peptides 49

3.11 Monoclonal antibodies 49

3.12 Inducible T-Cell Costimulator (ICOS) 51

Chapter 4: Development of nanomedicine as per ICH Q8 Guidelines 53

4.1 Critical Quality Attributes (CQA) 53
4.2 Critical Material Attributes (CMAs) 53
4.3 Critical Process Parameters (CPPs) 55
4.4 Development of Nanomedicine 55

Chapter 5: Aim of the work 58

Chapter 6: Preparation and Optimization of Blank Bovine Serum Albumin-Based Nanomedicine by Approaching Advanced Manufacturing Technologies 60

6.1 Formulation Components of BSA NPs and NCs 61
6.2 Preparation of BSA-NPs Using Surfactant-mediated Coacervation Method 64
6.3 Optimization of BSA-NPs Preparation by Surfactant-mediated Coacervation Method 65
6.4 Preparation of BSA-NPs Using Ultrasonication Technology (US) 67
6.5 Microwave Assisted Technology (MW) 68
6.6 Mechanisms of Microwave-Assisted Technology 70
6.7 Microwave Process Design 71
6.8 Preparation of BSA-NPs Using Microwave-Assisted Technology 72
6.9 Optimization of BSA-NPs Prepare by Microwave-Assisted Technology 73
6.10 Preparation of BSA-NPs Using Combined Microwave and Ultrasonication Technology 77
6.11 Physicochemical characterization of BSA-NPs 77
6.12 Yield of Bovine Serum Albumin Nanoparticles (BSA-NPs) 79
6.13 Anova test of BSA-NPs 80
6.14 Scanning Electron Microscopy of BSA-NPs 81
6.15 Fourier-Transform Infrared Spectroscopy of BSA-NPs 83
6.16 Release study of BSA fragments from Nanoparticles 85
6.17 Stability Study of BSA-NPs 87
6.18 Preparation of Bovine serum albumin Nanocapsules (BSA-NCs) 88
6.19 Ultrasonication Technology (US) 89
6.20 Process Characterization of Ultrasonication Technology 90
6.21 Mechanisms of Ultrasonication Technology 90
6.22 Preparation of BSA-NCs by using Ultrasonication Technology 92
6.23 Condition Optimization of Ultrasonication Technology (US) 92
6.24 Preparation of BSA-NCs by using Microwave Technology (MW) 96

6.25 Combined Microwave and Ultrasonication Technology (MW/US)..... 97
6.26 Process of Combined MW/US technology..... 100
6.27 Preparation of BSA-NCs by using combined MW/US Technology..... 102
6.28 Condition Optimization of MW/US..... 102
6.29 Physicochemical Characterization of BSA-NCs..... 107
6.30 Yield of Bovine Serum Albumin Nanocapsule (BSA-NCs)..... 107
6.31 ANOVA Test of BSA-NCs..... 108
6.32 Scanning Electron Microscopy (SEM) of BSA NCs..... 109
6.33 Fourier-Transform Infrared Spectroscopy (FTIR) of BSA-NCs..... 110
6.34 Release study of BSA Fragments from Nanocapsule..... 111
6.35 Stability Study..... 112
6.36 Chitosan Coating of Bovine Serum Albumin Nanoparticles and Nanocapsules..... 113
6.37 Conclusion..... 114

Chapter 7: Preparation of Blank Human Serum Albumin-based Nanomedicine by Approaching Advanced Manufacturing Technologies..... 117

7.1 Preparation of HSA-NPs Using Surfactant-mediated Coacervation Method..... 117
7.2 Preparation of HSA-NPs Using Microwave-Assisted Technology..... 117
7.3 Preparation of HSA-NCs by using Ultrasonication Technology (US)..... 118
7.4 Preparation of HSA-NCs by using combined MW/US Technology..... 118
7.5 Physicochemical characterisation of HSA NPs and NCs..... 118
7.6 Yield of HSA Nanoparticles and Nanocapsules..... 120
7.7 Comparison of ANOVA test of Bovine Serum Albumin (BSA) and Human Serum Albumin (HSA) Nanoparticles and Nanocapsules..... 122
7.8 Comparison of Release Study of HSA Fragments and BSA Fragments from NPs and NCs. 124

Chapter 8: Development and Optimization of Doxorubicin Albumin-based Nanocapsules by Approaching Advanced Manufacturing Technologies..... 126

8.1 Preparation and Optimization of DOX-BSA Nanocapsules using Ultrasonication Technology 128
8.2 Physicochemical Characterization of Doxorubicin loaded nanocapsules..... 129
8.3 Doxorubicin-loaded BSA-NCs by Combined Microwave and Ultrasonication Technology (MW/US)..... 133
8.4 ANOVA Test..... 135
8.5 Development of Doxorubicin loaded Human Serum Albumin Nanocapsules (DOX-HSA NCs) 137

8.6 ICOS-Fc targeted albumin-based nanocapsules as a tool for the delivery of doxorubicin in osteosarcoma cell lines 138
8.7 Preparation of Blank BSA-NCs and DOX-BSA NCs. 140
8.8 Bovine Serum Albumin Nanocapsules Conjugation with ICOS-Fc Human 140
8.9 Physicochemical Characterisation of Nanocapsules 141
8.10 Results 142
Chapter 9: Conclusion 150
References. 152

List of Figures

Figure No	Title of Figure
1.1	Structure of Albumin
1.2	Comparison of Structure of HSA and BSA
1.3	Schematic representation of Denaturation of Protein
1.4	FDA Approved Albumin Based Nanodrug
1.5	Structure of Paclitaxel
2.1	Different Manufacturing Methods of Albumin Nanoparticles
2.2	Coacervation Method
2.3	Emulsification Method
2.4	Nab Technology
2.5	Thermal gelation
2.6	Nano spray-drying
2.7	Structural Representation of Albumin-based Nanoparticles
2.8	Structural Representation of Albumin-based Nanocapsules
3.1	Non-Covalent Coating Techniques of Nanoparticles
3.2	Chemical structure of Chitin and Chitosan
3.3	Schematic representation of Surface Modification of nanocapsule with Chitosan Coating
3.4	Schematic Representation of ICOS-Fc conjugated with Nanocapsules
6.1	Chemical Structure of Kolliphor HS15
6.2	Chemical Structure of Lecithin Phosphatidylcholine (Epikuron® 200)
6.3	Chemical Structure of Caprylic /Capric Triglyceride (Miglyol® 829)
6.4	Chemical Structure of Sorbitan Sesquioleate (Span® 83)
6.5	Schematic representation of the preparation of BSA-NPs By the Optimized Surfactant-mediated Coacervation Method
6.6	Size of BSA-NPs against the BSA Concentration
6.7	Zeta Potential of BSA-NPs against the BSA Concentration
6.8	Schematic representation of the preparation of BSA-NPs Ultrasonication Technology

6.9	Microwave Single Reaction Chamber
6.10	Process Steps Involved in Microwave Technology
6.11	Schematic representation of the tuned preparation of BSA-NPs By Microwave-assisted Technology
6.12	Optimization of Temperature (°C) against the Ramp Time (Sec)
6.13	BSA Concentration Across Various Temperatures and Preparation Times
6.14	BSA Containing Kolliphor HS15 Across Various Temperatures and Preparation Times
6.15	Schematic representation of the preparation of BSA-NPs by using Combined Microwave and Ultrasonication Technology (MW/US)
6.16	Physicochemical Characteristics Variation of BSA-NPs Obtained by Surfactant-mediated Coacervation Method (CO) and Microwave Technology (MW)
6.17	BSA-NPs Particle Shape Determination by SEM
6.18	FTIR Spectra of BSA-NPs with surfactant-mediated coacervation method (CO-NPs) microwave-assisted technology (MW-NPs)
6.19	FTIR Spectra of BSA-NPs with microwave-assisted technology (MW-NPs)
6.20	Release study of BSA Fragments from Surfactant-mediated Coacervation and Microwave Nanoparticle
6.21	BSA-NPs Stability Study in Two Different Methods up to 90 Days at 4 °C
6.22	Instrument of Ultrasonication technology
6.23	Schematic representation of the US technology
6.24	Schematic representation of the involved steps in BSA-NCs preparation by using Ultrasonication Technology
6.25	BSA-NCs Size *versus* the used US Technology Frequency
6.26	Changes In the Real Temperature During Time
6.27	Size of BSA-NCs against the BSA Concentration
6.28	Changes in the Zeta Potential of BSA-NCs against the BSA Concentration
6.29	Schematic representation of the involved steps in BSA-NCs preparation by using Microwave Technology
6.30	Combined Microwave and Ultrasonication Technology (MW/US)
6.31	Flow Chart of Main Properties of MWUS

6.32	Process Steps involved in combined MW/US
6.33	Schematic representation of the involved steps in BSA-NCs preparation by using MW/US
6.34	Size of BSA-NCs against the BSA Concentration
6.35	Changes in the Zeta Potential of BSA-NCs against the BSA Concentration
6.36	Size and Zeta Potential of BSA-NCs against the Preparation Time
6.37	Physicochemical Characteristics Variation of BSA-NCs Obtained by Using the Different Manufacturing Methods
6.38	BSA-NCs Particle Shape Determination by SEM
6.39	FTIR Spectra of BSA-NCs with Ultrasonication Technology (US)
6.40	FTIR Spectra of BSA-NCs with Combined Microwave Ultrasonication (MW/US)
6.41	Release study of albumin from different types of Nanocapsule
6.42	BSA-NCs Stability Study in Two Different Methods up to 90 Days at 4 °C
7.1	Comparison of Physicochemical Characteristics Variation of Surfactant-mediated Coacervation BSA and HSA Nanoparticles
7.2	Comparison of Physicochemical Characteristics Variation of Microwave-assisted Technology BSA and HSA Nanoparticles
7.3	Comparison of Physicochemical Characteristics Variation of Ultrasonication BSA and HSA Nanoparticles
7.4	Comparison of Physicochemical Characteristics Variation of Combined Microwave and Ultrasonication BSA and HSA Nanoparticles
7.5	Comparison of Physicochemical Characteristics Variation of Combined Microwave and Ultrasonication BSA and HSA Nanoparticles
7.6	Comparison of Release study of BSA and HSA Fragment from different types of Nanocapsules
8.1	Chemical Structure of Doxorubicin Hydrochloride (DOX-HCl)
8.2	Mechanism of action of doxorubicin
8.3	In vitro release study of DOX-BSA NCs with different concentrations of Doxorubicin hydrochloride
8.4	In vitro release study of DOX-BSA NCs with two different manufacturing methods

8.5	Physicochemical Characteristics Variation of DOX-BSA-NCs Obtained by Using the Different Manufacturing Methods
8.6	In vitro release study of DOX-HSA NCs with MW/US Technology
8.7	Representative scheme of the preparation by utilizing the Ultrasonication technique (20KHZ, 500W) to prepare the DOX-BSA- NCs
8.8	Particle size distribution analysis of DOX-BSA NCPSs by the Nanocapsule tracking analysis instrument (Nano Sight Amesbury, United Kingdom), 1) Average particle concentration/size 2) Intensity/size, for experiment
8.9	Fourier Transform Infrared Spectroscopy FTIR spectra of free DOX, DOX-loaded Nanocapsules (DOX-BSA NCs), Blank BSA Nanocapsules (Blank BSA-NCs) and both with ICOS-Fc
8.10	In-vitro release study of Dox-BSA NCs, Dox-BSA ICOS-Fc and Dox-free solution as a release up to 8 hours and 50 hours
8.11	The mathematical modelling of doxorubicin release from Dox-BSA NCs and Dox-BSA ICOS-Fc NCs was performed by plotting the data and determining the preference of each kinetic model.
8.12	Haemolysis Study of DOX-BSA NCs
8.13	The Viability Inhibition and Invasion on Osteosarcoma Cells Line U2OS

List of Tables

Table No	Title of Table
1.1	Applications of Albumin in Drug Delivery
2.1	Albumin nanoparticles for cancer treatment prepared by coacervation method
2.2	Albumin Nanoparticle for cancer treatment prepared by different methods
6.1	Parameters of Quality Target Critical Attributes
6.2	Optimise the Process Parameters of BSA-NPs Obtained by MW Technology
6.3	Physicochemical Characteristics of BSA-NPs Obtained by Different Manufacturing Technologies
6.4	Yield of BSA NPs Obtained by Different Manufacturing Technology
6.5	BSA standard dilution scheme for the solution preparations
6.6	Optimise Process Parameters of BSA-NCs Obtained by US technology
6.7	Optimise Process Parameters of BSA-NCs Obtained by Combined MW/US
6.8	Physicochemical Characterization Of BSA-NCs Obtained by Different Manufacturing Process
6.9	Yield of BSA NCs Obtained by Different Manufacturing Technologies
6.10	Physicochemical Characterization of BSA NPs and NCs Coated with Chitosan Obtained by Different Manufacturing Technologies
7.1	Physicochemical Characteristics of Blank-HSA NPs Obtained by Surfactant-mediated Coacervation Method and Microwave-assisted Technology
7.2	Physicochemical Characteristics of Blank-HSA NCs Obtained by Ultrasonication Technology and Combined Microwave and Ultrasonication Technology
7.3	Yield of HSA NPs Obtained by Surfactant-mediated Coacervation Method and Microwave-assisted Technology
7.4	Yield of HSA-NCs Obtained by Ultrasonication Technology and Combined Microwave and Ultrasonication Technology
8.1	Physicochemical Characterization, Encapsulation efficiency (EE%) and Drug loading (DL%) of Different concentrations of DOX-BSA NCs obtained by Ultrasonication Technology
8.2	Physiochemical Characterization of DOX-BSA NCs with Two Different

	Manufacturing Technology
8.3	Encapsulation Efficiency and Drug Loading of DOX-BSA NCs obtain by Different Manufacturing Process
8.4	Physicochemical Characterization, Encapsulation Efficiency and Drug Loading of DOX-HSA-NCs
8.5	Physicochemical Characterization of Nanocapsules
8.6	Encapsulation efficiency and Drug loading of Nanocapsules

Introduction

The PhD research was focused on the development of albumin-based drug nanodelivery systems taking into account the evaluation and the optimisation of innovative manufacturing technologies for their preparation. In particular, it focuses on two types of nanostructures: nanoparticles and nanocapsules. Albumin, a naturally occurring globular protein in blood plasma attracted much research attention in medicine, supporting both environmental sustainability and human health safety.

Indeed, it exhibits a number of advantageous properties, including biocompatibility, biodegradability, non-immunogenicity, and the ability to bind a variety of drugs. In addition, albumin shows interesting processibility, making the protein easy to manipulate and adapt for various uses for biomedical applications.

These characteristics render albumin an optimal component for the development of nanocarriers as drug delivery systems. In this context, Abraxane®, albumin-bound paclitaxel approved by FDA in the 2005, paved the way for albumin-based nanomedicines. Various manufacturing methods for the preparation of albumin nanocarriers have been described in the literature. The research considered two types of protein: Bovine Serum Albumin (BSA) and Human Serum Albumin (HSA). BSA is a commonly used research tool due to its availability and cost-effectiveness. In contrast, HSA is preferred for clinical applications due to its compatibility with human physiology. The development of improved manufacturing techniques able to assure the quality of the nano delivery systems is a key factor for industrial production and safe administration.

Considering this challenging research area the thesis project will investigate new albumin-based nano formulations as well as the optimization of the manufacturing process.

Chapter 1: Albumin: Molecular Structure and Properties

Serum albumin, globular proteins, constitutes approximately 60% of all proteins present in blood plasma and is highly solubilised in water [1]. There are three types of albumin including human serum albumin (MW 66 kDa), bovine serum albumin (MW 66.5 kDa), and ovalbumin (egg white, MW 44.5 kDa) [2]. Factors that affect albumin coagulation include heating, pH levels close to its isoelectric point, and salt concentration. In human blood plasma, albumin has an average half-life of 19 days albumin is synthesised in the liver, with an adult liver producing approximately 12 grams daily. The normal albumin concentration in adult humans is within the range of 3.4 to 4.7 g/dL, accounting for approximately 60% of the total plasma protein [3]. One of the albumin's principal functions as a plasma protein is to maintain osmotic pressure, thereby preventing fluid leakage from blood vessels into surrounding tissues. It maintains plasma osmotic pressure at approximately 70 to 80% [4].

Osmotic pressure is a consequence of varying water concentrations within the body, which are influenced by the salt content and the presence of other nutrients. Furthermore, albumin plays a role in maintaining the body's acid-base balance due to its numerous negative electrical charges [5].

Albumin is a protein composed of a single polypeptide chain consisting of 583 amino acids for bovine serum albumin and 585 amino acids for human serum albumin. Approximately 67% of its secondary structure is composed of α-helices, which are a common structural motif in proteins. The protein contains 17 disulfide bridges, which are strong covalent bonds formed between two cysteine amino acids through oxidation. These bridges play a crucial role in stabilising the protein's overall structure [6]. Albumin's structure is organized into three homologous domains, each of which contains two subdomains (A and B) as illustrated in Figure 1.1.

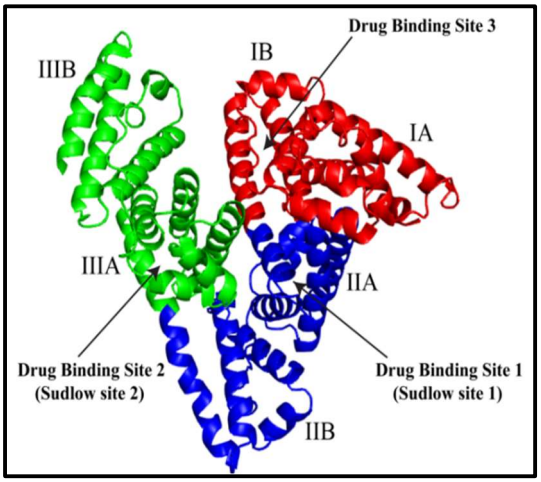

Figure 1.1. Structure of Albumin [7]

Domain I comprises amino acids 1-195, which are further divided into two subdomains: IA (amino acids 1-112) and IB (amino acids 113-195).

Domain II spans amino acids 196-303 and includes subdomain IIA. Amino acids 196-303 correspond to Subdomain IIB, while amino acids 304-383 correspond to Domain III. Subdomain IIIA encompasses amino acids 384-500, and Subdomain IIIB encompasses amino acids 501-585. These domains and subdomains contribute to the overall structure, stability, and function of the protein. The flexibility and compactness of albumin's structure are key factors in its ability to maintain oncotic pressure, transport molecules, and regulate pH [8,9].

Bovine Serum Albumin (BSA) and Human Serum Albumin (HSA) are the two most commonly used types of albumins. The difference in tryptophan content between BSA and HSA is evident in their structures, as shown in Figure 1.2.

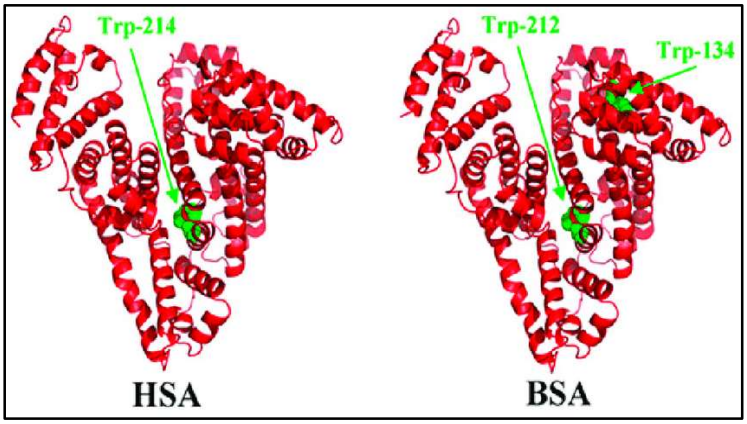

Figure 1.2. Comparison of Structure of HSA and BSA [10]

BSA has two tryptophan residues, while HSA has only one. This difference in tryptophan composition highlights the unique structural differences between the two albumin variants [10].

Bovine Serum Albumin (BSA) and Human Serum Albumin (HSA) are crucial proteins with slight differences in their molecular weights and specific applications. BSA has a molecular weight of approximately 66,430 Daltons (Da) and consists of 583 amino acids. HSA has a molecular weight of approximately 66,500 Daltons (Da) and is composed of 585 amino acids [11]. Both BSA and HSA exhibit high solubility in water, with concentrations typically reaching 40-50 mg/mL at room temperature. The solubility of these proteins is influenced by a number of factors, including pH and ionic strength. These properties are of significant importance for numerous applications in the fields of biochemistry and pharmaceutical sciences, where precise control of protein solubility is essential for effective usage and formulation [12].

The isoelectric point of a protein is the pH at which the albumin carries no net electrical charge. The isoelectric point of bovine serum albumin and human serum albumin is typically situated between pH 4.4 and pH 4.9 [13]. At this pH range, albumin molecules exhibit an equal number of positive and negative charges, resulting in a net zero charge. At a pH of 8, which is above the isoelectric point of albumin, the protein will exhibit a net negative charge. This occurs because, at a pH higher than its isoelectric point, the amino acid residues in albumin that can lose protons (such as carboxyl groups) will be deprotonated, resulting in a negatively charged protein [14]. Consequently, albumin in a solution with a pH of 8 will exhibit a greater number of negative charges on its surface compared to positive charges. The pH of the protein solution is one of the most prominent parameters influencing the particle sizes of protein-based nanoparticles [15]. While protein molecules are coagulated due to the decrease in the net charge of the protein when the pH of the protein solution is close to the isoelectric point of the protein, it has been determined that the particle size decreases as the pH of the solution increases [16]. In the study conducted by Sebak et al., when the pH of the solution dropped below 8.0, the particle size and poly- dispersity index increased [17].

1.1 Biocompatibility of Albumin

Bovine serum albumin (BSA) and human serum albumin (HSA) are widely studied and used proteins in biomedical and pharmaceutical applications due to their high biocompatibility. BSA, derived from cows, and HSA, obtained from human blood plasma, exhibit a high degree of structural similarity, with only minor differences in their sequences. The biocompatibility of BSA and HSA is derived from their natural abundance in blood plasma and their crucial roles in maintaining osmotic pressure and transporting various endogenous and exogenous substances, including drugs, hormones, and fatty acids. This inherent compatibility with biological systems ensures minimal immunogenicity and toxicity, rendering them optimal candidates for use in drug delivery, medical diagnostics, and tissue engineering [7,18]. In the field of drug delivery, both BSA and HSA can act as carriers for therapeutic agents, enhancing their solubility, stability, and bioavailability. Their capacity to bind to a diverse range of pharmaceuticals enables the controlled release and targeted delivery of drugs, thereby reducing the incidence of adverse effects and enhancing the efficacy of therapeutic interventions [19]. Furthermore, HSA, a human-derived protein, exhibits superior biocompatibility compared to BSA in clinical applications due to the reduced risk of cross-species immunogenic responses. Nevertheless, BSA remains a valuable and cost-effective [20].

Both proteins are biodegradable, undergoing degradation primarily through enzymatic and microbial pathways. Key enzymes like trypsin, pepsin, and chymotrypsin are essential in breaking down these proteins into smaller peptides and amino acids within biological systems [21,22]. These proteins are rapidly degraded by proteolytic enzymes, which is vital for regulating protein levels and recycling amino acids in the body [23]. *In vitro*, controlled enzymatic digestion is employed to investigate their behaviour, particularly in drug formulations [11]. The environmental degradation of both BSA and HSA is contingent upon a number of factors, including pH, temperature, and microbial activity. The proteins are most stable at neutral pH. Extreme pH levels or temperatures can result in the denaturation of proteins, rendering them more susceptible to enzymatic degradation. The use of protease inhibitors can serve to slow down the aforementioned degradation process, while adsorption to surfaces may temporarily protect the proteins from breakdown [24].

1.2 Denaturation of Albumin

Denaturation is a biochemical process that involves any modification in the secondary, tertiary, or quaternary structure of a protein molecule, which ultimately leads to the disruption of covalent bonds. In their native states, the majority of known proteins are folded into well-defined, rigid three-dimensional structures. Changes in a protein's structure are typically accompanied by alterations in its chemical, physical, and functional properties. A significant number of studies have demonstrated that certain proteins or enzymes can lose their activities, either irreversibly or reversibly, when exposed to a variety of natural or artificial conditions. For example, glyceraldehyde phosphate dehydrogenase and lactate dehydrogenase are two enzymes that lose their properties when subjected to lower temperatures [25,26]. Denaturation may involve the ionisation of carboxylic, amino acid or phenolic groups. Such alterations can result in the rearrangement of molecular structures, accompanied by the liberation of sulfhydryl or disulfide groups. Consequently, the protein structure is disrupted, resulting in denaturation. This can result in a reduction in protein solubility, which may subsequently lead to the loss of specific biological activities [27].

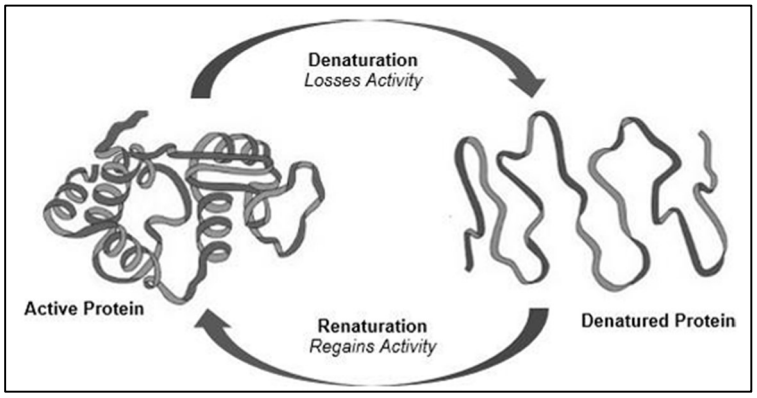

Figure 1.3. Schematic representation of Denaturation of Protein [25]

Denaturation of albumin usually lead to the following changes [25,26,28]. Protein denaturation frequently results in a reduction in solubility, with denatured proteins precipitating upon the addition of small amounts of neutral salts. This reduction in solubility has been extensively studied and is considered a key indicator of denaturation. When a protein denatures, it loses its native structure, which leads to an increase in hydrophobic interactions that cause the proteins to aggregate and precipitate, particularly in the presence of neutral salts or organic solvents.

Denaturation can result in the loss of some of the biochemical activities of proteins or enzymes. It has been demonstrated that proteolytic enzymes become inactivated when exposed to heat or treated with alkali. It has been observed that viruses lose their proteolytic enzymes, which are necessary for the causation of disease, and certain hormones lose specific regulatory functions are shown in the Figure 1.3. A significant proportion of globular proteins are capable of forming crystals. Nevertheless, upon undergoing denaturation, these proteins are unable to form crystals due to alterations in their structural and morphological characteristics.

Proteins are maintained in their 3-D structure through a variety of non-covalent interactions, which are crucial for their stability and functionality. Hydrogen bonds are formed between the amides of the protein backbone and the carbonyl groups, as well as between certain side chains, providing significant structural support. Ionic bonds, or salt bridges, arise between positively and negatively charged side chains, thereby further stabilising the protein's conformation [29]. Hydrophobic interactions occur as non-polar side chains aggregate to avoid contact with water, driving the folding process. In addition, van der Waals forces, though individually weak, collectively contribute to the overall stability by acting between all atoms within the protein. When a protein undergoes denaturation, the non-covalent interactions that stabilise its structure are disrupted, causing the protein to unfold and lose its functional conformation. This disruption can be triggered by a number of factors, including changes in pH, temperature, or the presence of denaturing agents, which ultimately impair the protein's biological activity [30,31].

Heat/High Temperature

When a protein solution is heated to a temperature close to its isoelectric point, the protein will coagulate. Increasing the temperature by ten degrees can accelerate this heat coagulation process by approximately 600 times. Heat is the most commonly known agent for protein denaturation. Proteins denatured by heat become more prone to aggregation, which depends on factors such as pH, dielectric constant, and ionic strength of the medium. Both acids and alkalis can dissolve heat-coagulated proteins [32]. Furthermore, substances such as urea, guanidine hydrochloride, detergents, and salicylate can dissolve heat-coagulated proteins even at the isoelectric point. Heat-denatured proteins can slowly return to their original soluble

form upon cooling. However, irreversible denaturation occurs when proteins are heated for extended periods, or heated for shorter periods at their isoelectric point [25,27]. Daniel et al. have conducted research into the instability of the tertiary structure of proteins. The researchers examined the stability of enzymes at elevated temperatures by subjecting the enzyme to a heating process, followed by a rapid cooling period, and subsequently evaluating its residual activity at a lower temperature [33].

Pressure

In the presence of high pressure, the hydrophobic interactions within a protein are weakened, initiating the process of protein denaturation. While moderate pressure may not fully unfold the protein, it can cause structural changes that result in a loss of protein activity [34]. Neurath et al. have demonstrated that protein denaturation can occur at high pressures of approximately 6000 kg/cm², while protein coagulation can take place at pressures around 10,000 kg/cm² [27]

Irradiation

Protein molecules exposed to ultraviolet (UV) light undergo coagulation through two primary methods: proper light denaturation and a photochemical reaction that is independent of temperature. This is followed by flocculation of the denatured protein. The UV-induced coagulation has a high temperature coefficient. Irradiation can alter the aggregation state of protein solutions, potentially leading to a loss of biological activity. Furthermore, the pH of the solutions tends to shift towards the isoelectric point of the protein [25].

Sound waves

Protein molecules subjected to high-intensity mechanical vibrations, such as those produced by ultrasonic or sonic waves, exhibit a loss of enzymatic activity and the formation of protein coagulate [25].

Denaturation by Chemical Agents

Acid/Low pH

The behaviour of proteins at low pH levels is influenced by a number of factors, including temperature. Some proteins retain their native conformations at extremely low pH levels when the temperature is maintained at a low level, whereas others undergo unfolding. For the latter group, a reduction in pH can result in significant

conformational alterations. A significant proportion of proteins exhibit properties that lie between these two extremes. Lysozyme is an illustrative example of a protein that remains unperturbed by low pH even at room temperature. Other proteins that are resistant to acid denaturation include β-lactoglobulin and ribonuclease. Conversely, yeast glyceraldehyde-3-phosphate dehydrogenase exhibits marked alterations in enzymatic activity and molecular weight in response to low pH and low-temperature conditions. This protein exhibits a transition between pH 4 and pH 11, although a highly cooperative transition occurs below pH 4. At this point, the protein loses enzymatic activity, dissociates into subunits, and the conformation of these subunits becomes thoroughly disorganized [35].

Alkali/High pH

Some proteins exhibit denaturation at alkaline pH values similar to those observed at acidic pH values, while others follow a different course during alkaline denaturation. The stability of haemoglobin and myoglobin is greater at alkaline pH than at acidic pH. The denaturation of proteins at alkaline pH is particularly complex for those containing thiol groups or disulfide bonds [36]. In addition to chemical modifications, the products of alkaline denaturation are as diverse as those resulting from acid denaturation. At pH levels above 10 or 11, buried tyrosyl residues tend to become exposed, resulting in a lesser tendency to retain residual structure at very high pH compared to a very low pH. Nevertheless, it is challenging to conduct meaningful experimental studies due to the prevalence of chemical instability at high pH [37].

1.3 Applications of Albumin in Drug Delivery

Albumin is a protein with a number of important pharmaceutical applications. Its properties include the ability to bind and transport various substances, a long half-life, and biocompatibility. [38]. In Drug Delivery Systems, albumin enhances the solubility and stability of lipophilic drugs, as exemplified by paclitaxel albumin-bound nanoparticles (Abraxane), which are used in cancer treatment. A bovine serum albumin (BSA) nanosuspension was formulated for parenteral delivery with the objective of targeting delivery to the lung, reducing toxicity and the side effects of etoposide [39] Zhang et al. have successfully employed the emulsification method to synthesize BSA nanoparticles loaded with a combination of paclitaxel and sorafenib.

This approach has resulted in the reduction of myelosuppression, hemolysis, and low blood pressure issues commonly associated with nanoparticle-based systems [40]. The cellular uptake and cytotoxic effect of paclitaxel-loaded HSA-PEG nanoparticles have been demonstrated in certain cancer cell lines [41]. Clinically, albumin is utilized as a plasma volume expander for patients with hypovolemia, burns, and hypoalbuminemia, helping to maintain blood volume and pressure [42]. It also acts as a stabilizing agent in pharmaceutical formulations, including vaccines, to prevent aggregation and denaturation of active ingredients. In diagnostics, radiolabelled albumin assists in imaging for evaluating blood volume and cardiac output, while serum albumin levels serve as biomarkers for various diseases [43].

The various applications of albumin in drug delivery, focusing on different aspects such as drug types, mechanisms, and benefits as discussed below in Table 1.1.

Table 1.1. Applications of Albumin in Drug Delivery

Applications	Drug Type	Mechanism	Benefits	Reference
Albumin-bound Nanoparticles	Anticancer drugs	Albumin binds to lipophilic drugs forming nanoparticles that enhance drug solubility and stability	Improved bioavailability and tumor targeting	[8]
Albumin-based nanocarriers	Anticancer drugs	Albumin nanoparticles act as carriers, facilitating drug delivery to cancer cells	Enhanced permeability and retention effect in tumors	[44]
Albumin-coated Liposomes	Antibiotics, Antifungals	Albumin coating stabilizes liposomes and prolongs circulation time	Reduced clearance, improved drug accumulation at infection sites	[45]
Albumin Conjugates	Peptides, Small Molecules	Covalent binding of drugs to albumin prolongs their half-life	Extended circulation time, reduced dosing frequency	[46]
Albumin Microsphere	Proteins, Peptides	Encapsulation of drugs in albumin microspheres for controlled release	Sustained release, improved patient compliance	[47]
Albumin Hydrogels	Hydrophilic drugs	Albumin forms hydrogels that can	Localized delivery, reduced systemic	[48]

		encapsulate drugs for local delivery	side effects	
Albumin-coated Nanogels	Gene therapy vectors	Albumin coating on nanogels enhances stability and cellular uptake	Improved transfection efficiency, targeted gene delivery	[49]
Albumin-stabilized Emulsions	Lipophilic drugs	Albumin stabilizes emulsions, enhancing the solubility and bioavailability of lipophilic drugs	Enhanced drug absorption, reduced irritation	[50]
Albumin-based Drug Carriers	Hormones, Vaccines	Albumin acts as a carrier, improving the stability and delivery of biologics	Enhanced stability, prolonged release	[51]

1.4 Challenges to Prepare Albumin Nanomedicine

Preparing albumin nanomedicine presents several challenges, mainly due to the complex nature of the albumin protein and the required nanoscale manipulation. These challenges include [19,52,53].

Stability Issue

To deliver therapeutic agents effectively, albumin nanocarriers must maintain their structural integrity under physiological conditions. Stability is crucial to prevent premature drug release and ensure the carrier reaches its target site. Factors such as pH, temperature, and the presence of enzymes can affect the stability of albumin nanomedicines.

Controlled Particle Size and Distribution

Achieving a uniform and controlled particle size and distribution is crucial for predictable pharmacokinetics and biodistribution. Smaller particles may facilitate deeper tissue penetration and faster clearance, while larger particles may offer prolonged circulation times. However, creating a consistent particle size distribution is technically challenging.

Loading Efficiency

Efficient drug loading into albumin nanocarriers is crucial for maximising therapeutic efficacy. The challenge is to encapsulate a sufficient amount of the lipophilic and hydrophilic drug without compromising the structural and functional integrity of the

albumin or the drug itself. This requires optimising the drug-to-carrier ratio and ensuring that the drug remains stable and bioavailable.

Scalability and Reproducibility

Scaling up the production of albumin nanomedicines from laboratory to industrial scale while maintaining product quality and efficacy is a significant challenge. This requires consistent particle size, distribution, and drug loading efficiency, as well as cost-effectiveness and adherence to regulatory standards. Reproducing the same quality and characteristics of albumin nanomedicines batch after batch is challenging due to the complexity of their preparation processes. Minor variations in the manufacturing process can lead to significant differences in the final product, affecting its safety, efficacy, and regulatory approval.

Biological Compatibility

Although albumin is typically biocompatible and biodegradable, any changes to its structure or the inclusion of therapeutic agents can impact its compatibility. Therefore, it is crucial to ensure that albumin nanomedicines do not cause unintended immune responses or toxicity to guarantee their safe use in clinical applications.

Surface Modification

Modifying albumin nanocarriers to target specific tissues or cells, enhance circulation time, or improve drug release profiles is technically challenging. It requires precise control over the chemistry and orientation of the molecules attached to the albumin surface without affecting its biocompatibility or functionality.

Denaturation of Albumin

The manufacturing process of albumin nanocarriers can lead to denaturation, where the albumin protein loses its native structure. Protein denaturation dynamics are governed by general physical and chemical parameters, like pH, and temperature.

1.5 Food Drug Administration Approved Albumin Based Nanodrugs

The Food Drug Administration approved the albumin-based nanodrugs currently available on the market. The first is Abraxane, which contains the active ingredient paclitaxel (Nab technology) The second is FYARRO, which contains the active

ingredient sirolimus (Coacervation method). FYARRO® (sirolimus protein-bound particles for injectable suspension) (albumin-bound) is a medication designed to treat adults with malignant perivascular epithelioid cell tumors (PEComa) that are either metastatic or locally advanced and cannot be surgically removed [54].

Albumin-bound paclitaxel, commercially known as ABRAXANE® First FDA approved a novel formulation of paclitaxel, a chemotherapy drug used for the treatment of various cancers [55,56]. Abraxane®, in clinical use against metastatic breast cancer, HSA with paclitaxel, and generates an annual revenue of ~1 billion US $ [57]. Abraxane® is an albumin-bound form of paclitaxel that is manufactured using Nab technology. Abraxane is formulated with albumin, a human protein [58]. Fyarro® and Abraxane® both formulations are designed to enhance the delivery and efficacy of their respective drugs as shown in Figure 1.4. The particle size for both is around 130 nm.

Figure 1.4. FDA Approved Albumin Based Nanodrug [53,54]

Abraxane is primarily used in the treatment of metastatic breast cancer, particularly in scenarios where combination chemotherapy is required or where alternative treatments have failed. It is also approved for the treatment of non-small cell lung cancer and advanced pancreatic cancer, typically in combination with other pharmacological agents. [56,57]. Abraxane is generally thought to take advantage of albumin's increased delivery to tumors through receptor-mediated transport via Gp60, an albumin receptor on the surface of vascular endothelial cells [59,60]. In an advanced treatment study using an orthotopic breast cancer xenograft mouse model, Abraxane was found to reduce breast cancer stem cells, whereas Taxol was observed to increase breast cancer stem cells [61].

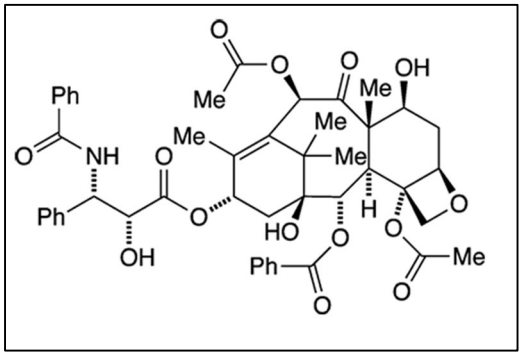

Figure 1.5. Structure of Paclitaxel [62]

Abraxane's innovative nanoparticle formulation significantly enhances the efficiency of drug delivery to cancer cells, potentially increasing its effectiveness in tumour reduction [63]. In addition, its unique formulation eliminates the need for solvents required in the traditional intravenous administration of paclitaxel. This feature significantly reduces the incidence of severe hypersensitivity reactions and other solvent-related side effects [64]. In addition, patients typically have a higher tolerance to Abraxane compared to standard paclitaxel, which could lead to more favourable outcomes. Another advantage of Abraxane is its administration protocol; unlike solvent-based paclitaxel, Abraxane generally does not require pre-medication with steroids and antihistamines, streamlining the treatment process and improving patient compliance [65].

The main limitations of the use of Abraxane in clinical treatments include several adverse side effects, despite a reduction in solvent-related issues. Patients may experience neutropenia, anaemia, thrombocytopenia, nausea, vomiting, diarrhoea, alopecia, and peripheral neuropathy. Additionally, although less common, some patients may have allergic reactions to the components of Abraxane. Cost considerations are significant, as Abraxane tends to be more expensive than traditional chemotherapy drugs, potentially affecting accessibility and affordability [66]. The immunosuppressive effects, particularly the reduction of white blood cell counts, increase the risk of infection. These side effects can also significantly impact the quality of life during treatment. Furthermore, Abraxane is not suitable for everyone, as it is not recommended for patients with certain pre-existing medical conditions or those who have had severe hypersensitivity reactions to albumin [67]

Chapter 2: Manufacturing Process of Albumin Nanocarriers

The manufacturing of albumin-based nanoparticles for drug delivery systems has been extensively studied in the literature, with a particular focus on the utilisation of specialised nanotechnology methods. These methods include coacervation (desolvation), emulsification, thermal gelation, nano-spray drying, and nanoparticle albumin-bound (nab) technology as shown in the Figure 2.1. This overview presents a summary of the various methods discussed in the available research literature.

The preparation of albumin nanoparticles necessitates the achievement of a balance between the attractive and repulsive forces within the protein. It is widely acknowledged that enhancing protein unfolding and reducing intramolecular hydrophobic interactions are key factors in the formation of albumin nanoparticles [68,69]. During the formation of nanoparticles, proteins undergo conformational changes, which involve the unfolding of their structures. This process results in the exposure of interactive sites, such as disulfide bonds, thiol groups, and hydrophobic regions, to the exterior. The extent of these conformational changes is contingent upon the protein's composition, concentration, preparation conditions (including pH, ionic strength, and solvent), and the crosslinking methods employed [69,70]. These changes result in an increase in intramolecular crosslinking and a decrease in hydrophobic interactions. Thermal or chemical crosslinking facilitates the formation of a network, resulting in the manufacturing of cross-linked nanoparticles that can encapsulate drug molecules [69].

Drug entrapment is typically associated with the manufacturing of albumin nanoparticles, although it can also be a distinct stage in the overall manufacturing process. Two principal techniques are employed for the entrapment of drugs: passive and active trapping. In passive trapping, the drug and carrier are co-dispersed in the same medium, allowing the simultaneous formation of nanoparticles and drug loading. This method frequently necessitates the utilisation of organic solvents, sonication, or elevated temperatures. In contrast, active trapping involves the loading of the drug after the nanoparticles have been formed, a technique that is predominantly employed for the encapsulation of hydrophilic drugs [71].

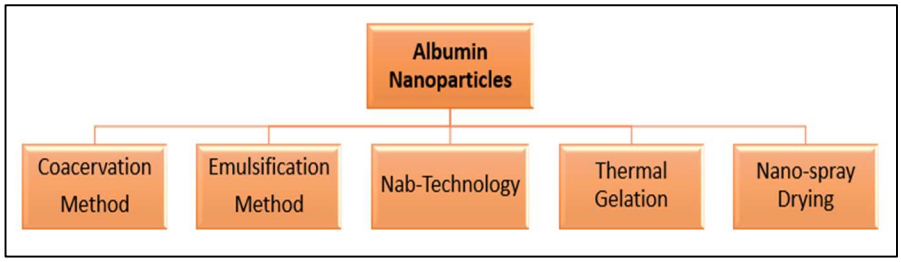

Figure 2.1 Different Manufacturing Methods of Albumin Nanoparticles

2.1 Coacervation Method (Desolvation method)

The coacervation method is a process that involves preparing an albumin solution from sources such as BSA or HSA. The albumin solution is then adjusted to alter its properties by changing its pH. Coacervation, which is the core step, is induced by methods such as adding salts, changing temperature, or altering pH [70,72]. This leads to phase separation into a protein-rich coacervate and a supernatant. Within the coacervate phase, albumin aggregates to form nanoparticles, a process that is influenced by temperature and stirring conditions. Optionally, cross-linking agents such as glutaraldehyde may be added to stabilise the nanoparticles, as shown in Figure 2.2. The study conducted by Li et al. demonstrated that higher concentrations of glutaraldehyde result in a reduction in the size of albumin nanoparticles due to enhanced protein cross-linking. Nevertheless, this phenomenon also results in a reduction in the encapsulation efficiency of hydrophilic active substances due to the carrier becoming more hydrophobic [73]. The increase in the ionic strength of the dispersion medium resulted in a reduction in electrostatic repulsion forces between albumin molecules, which in turn led to an increase in particle size [74]. Doxorubicin-loaded bovine serum albumin nanoparticles (NPs) were efficiently synthesized via the desolvation technique. These nanoparticles were then stabilized through crosslinking via Schiff base bonds, creating a pH-sensitive system for DOX delivery. The nanoparticles are then isolated, usually through centrifugation, to remove any unreacted materials and by-products [75,76]. This is followed by drying and collection methods, such as lyophilisation [2].

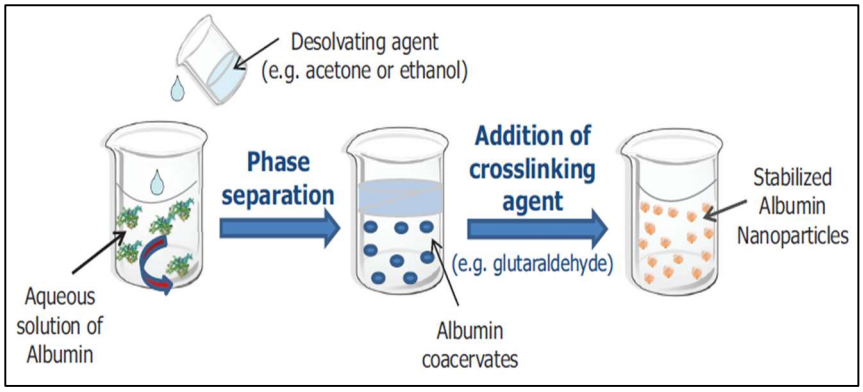

Figure 2.2. Coacervation Method [70]

Table 2.1. Albumin nanoparticles for cancer treatment prepared by coacervation method

Drug	Preparation Method	Cancer Type	Result	Reference
Doxorubicin	Coacervation	Cervical Cancer	The enhanced cellular internalisation observed in the present study is in contrast to that observed in non-targeted Nanoparticles.	[77]
Docetaxel	Coacervation	Lung, breast, colon and gastric cancer	The proliferation of cancer cells was inhibited in a concentration-dependent manner.	[78]
Coumarin-6	Coacervation	Lung and breast cancer	The cellular internalization of the nanoparticles was approximately twice that of unmodified BSA nanoparticles.	[79]
siRNA	Coacervation	Breast cancer	The delivery system is characterised by efficient transfection, retention of siRNA function, and low cytotoxicity.	[80]
Paclitaxel	Coacervation	Prostate cancer	The desired surface properties in favour of cellular uptake and targeting include increased water solubility.	[81]
Doxorubicin	Coacervation	Neuroblastoma	The objective of this study is to investigate the efficacy of a novel approach to overcoming transporter-mediated drug resistance in drug-adapted neuroblastoma cells.	[82]

2.2 Emulsification Method

High-energy emulsification techniques employ specialised mechanical equipment to produce nanometric emulsions. The process commences with the formation of droplets, which are subsequently deformed and broken down into micrometric droplets. Finally, surfactants are adsorbed onto the droplet interfaces in order to ensure steric stabilization [83]. High-pressure homogenisers and ultrasound generators are high-efficiency devices, with only a very low amount of the mechanical energy produced being used for emulsification [84]. Low-energy methods exploit the stored chemical energy within the system, utilising the intrinsic physicochemical properties of surfactants, co-surfactants, and excipients in the formulation. This process results in the formation of emulsion droplets within the nanometric range [85].

The emulsification method starts with preparing an albumin solution. The albumin protein is dissolved in an aqueous buffer. At the same time, an oil phase is prepared, often using biocompatible oils like soybean oil [86,87]. The two phases are then mixed under specific conditions, such as stirring or sonication, to produce an emulsion in which the albumin molecules aggregate into tiny droplets in the oil phase [88]. To stabilise these droplets into nanoparticles, a crosslinking agent, such as glutaraldehyde, is added shown in Figure 2.3. This facilitates bonds between albumin molecules and solidifies their structure [89]. Subsequently, the nanoparticles are separated from the oil phase, usually through centrifugation, and then washed to remove any residual oil and chemicals. The final step involves drying, often through lyophilisation (freeze-drying), to obtain the nanoparticles in a powder form [23,90].

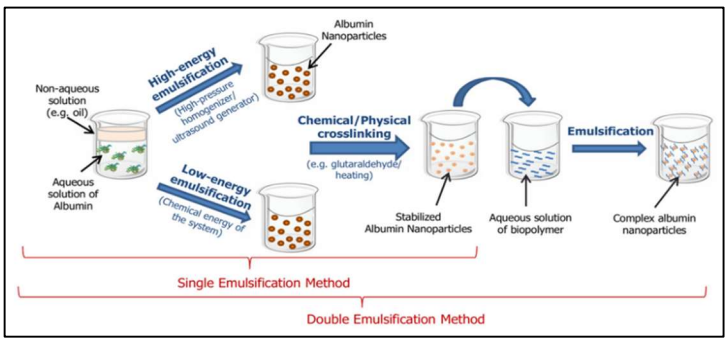

Figure 2.3. Emulsification Method [70]

2.3 Nab-Technology

Nab (nanoparticle albumin-bound) technology is a sophisticated process used to manufacture albumin nanoparticles, The process begins with preparing a concentrated albumin solution using BSA or HSA. The technology is based on binding therapeutic agents to albumin molecules, which is achieved through high-pressure homogenization or ultrasonic cavitation shown in Figure 2.4 [19,91]. These methods create an environment that enables the drug to attach effectively to the albumin molecules, forming nanoparticles typically ranging from 100-200nm in diameter. The nanoparticles are stabilized, typically through cross-linking, to maintain their structure and ensure sustained drug release. Following stabilization, a purification process removes any unbound drug or albumin [53]. A number of nanoparticle albumin-bound (nab) drugs are currently in development, including ABI-008 (nab-docetaxel) and ABI-009 (nab-rapamycin). It is understood that the preparation procedures can be similarly applied with suitable minor modifications [2,8].

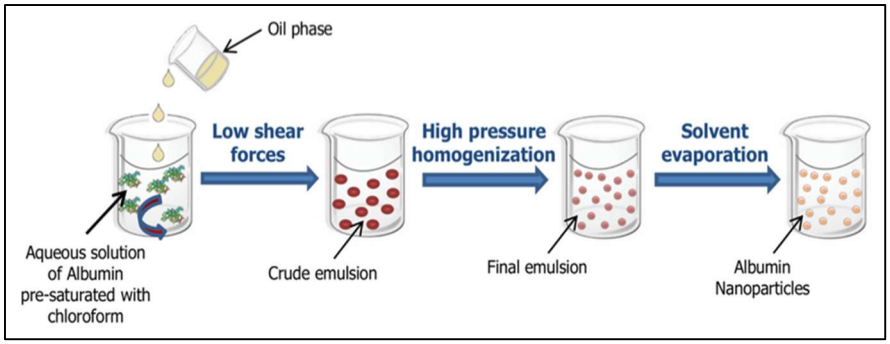

Figure 2.4. Nab Technology [70]

2.4 Thermal Gelation

The thermal gelation process is initiated by heat-induced conformational changes in proteins, which cause some polypeptide segments to unfold. This is then followed by protein-protein interactions, which include hydrogen bonding, electrostatic interactions, hydrophobic interactions, and disulfide-sulfhydryl interchange reactions [2,92,93]. First, a solution of albumin, is prepared in an aqueous buffer. The solution then undergoes thermal gelation, a critical step where it is heated to a specific temperature that causes the albumin to coagulate, forming a network of

interconnected nanoparticles is shown in Figure 2.5 [2,94]. The size of the nanoparticles is carefully controlled by adjusting factors such as albumin concentration, heating temperature, and the duration of heat exposure. After the nanoparticles are formed, the solution is cooled to stabilize them and prevent further growth or aggregation [95].

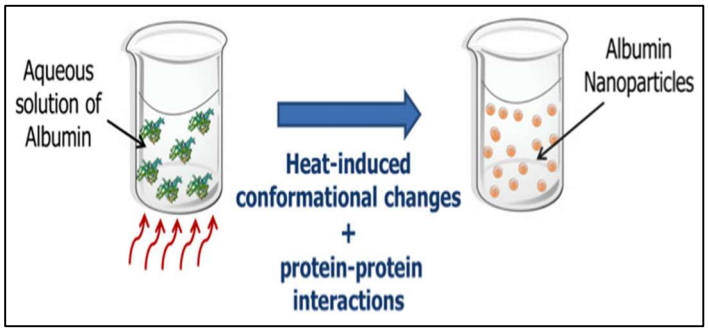

Figure 2.5. Thermal gelation [70]

2.5 Nano Spray-Drying

The spray drying process involves the generation of droplets from a solution containing the protein and the drug. This method is a common practice in the pharmaceutical industry, whereby a dry powder is produced from a liquid phase [2,95].

The typical spray drying process comprises four fundamental steps: atomising the feed into a spray, contacting the spray with air, drying the spray, and separating the dried product from the drying air. This method offers the advantage of a continuous and scalable single-step process for both drying and particle formation, as illustrated in Figure 2.6 [2,87]. The size and properties of the particles can be controlled by adjusting the drying conditions, such as air temperature, feed rate, nozzle size, and solution concentration. After spray-drying, the nanoparticles are typically collected using a cyclone separator or filter and may undergo further processing, such as sieving for size uniformity or additional drying [70,96].

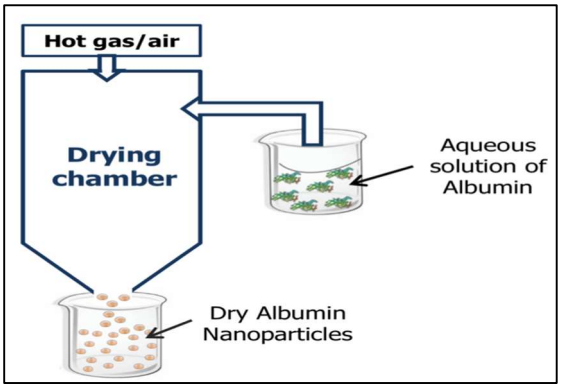

Figure 2.6. Nano spray-drying [70]

Table 2.2. Albumin Nanoparticle for cancer treatment prepared by different methods

Drug	Manufacturing Method	Cancer Type	Result	Reference
Teniposide	Emulsification	Melanoma and glioma	The compound demonstrated a reduction in systemic toxicity and exhibited enhanced antitumor activity.	[97]
Hydrophobic celastrol	Ultrasonication Emulsification followed by high pressure homogenization	Pancreatic cancer	The compound has been shown to facilitate penetration into deep tumour tissues, enhance tumour accumulation, prolong circulation and enhance tumour inhibition. Furthermore, it has been demonstrated to downregulate the immunosuppressive tumour microenvironment.	[98]
Curcumin Doxorubicin	Emulsification	Breast cancer	The simultaneous administration of a drug and the killing of cells results in a greater accumulation of the drug within the cells than would be achieved by administering the drug in a sequential manner.	[99]
Chrysin	Thermal aggregation	Lung Cancer	The potential application of thermal-induced self-	[100]

			assembled BSA nanoparticles in antitumor therapies	
Antisense oligonucleo-tide Herpes Simplex Virus	Heat denaturation	Breast cancer	The objective is to achieve efficient and targeted delivery to HER2-positive cancer cells.	[101]
Cabazitaxel	Heat denaturation	Prostate and lung cancer	The cellular internalisation process is dependent on time. There is no evidence of cytotoxicity associated with the carrier.	[102]
Curcumin	Albumin bound technology	Pancreatic cancer	The compound exhibits 300 times greater water solubility than the free drug, with a 14-fold higher accumulation in tumour tissue. It displays significantly greater antitumour activity without toxicity.	[103]

2.6 Design and Development of Albumin-Based Nanoplatforms Using Green Route

Nanocarriers are a significant development in nanotechnology, particularly in pharmaceutical and material science. These carriers, often only a few nano-meter sizes (10 – 1000 nm) offer numerous possibilities for drug delivery, enhanced imaging, and improved material properties [19]. Nanocarriers are microscopic structures that are integral to nanotechnology, primarily used in drug delivery systems. They encapsulate pharmaceutical drugs, safeguarding them from degradation and ensuring controlled release [104]. However, the use of nanocarriers presents challenges due to concerns about their stability, potential toxicity, and the body's immune response. Ongoing research aims to address these issues and improve the efficiency and safety of nanocarrier applications. Here this thesis investigated the two types of nanocarriers, namely nanoparticles and nanocapsule

Nanoparticles (NPs) are key to improving drug delivery and efficacy. Their small-sized particle improves drug solubility, stability and bioavailability, allowing drug delivery

to specific cells and minimising side effects and improving therapeutic outcomes [105]. The nanoparticles have a hydrophobic environment that is perfect for encapsulating lipophilic drugs due to the densely packed albumin molecules at their core, shown in Figure 2.7 [23,106]. The surface is composed of albumin, arranged to expose hydrophilic parts to the surrounding aqueous environment, ensuring biocompatibility and stability in biological fluids. These NPs are usually spherical and have particle size around 100 - 300 nm [107,108].

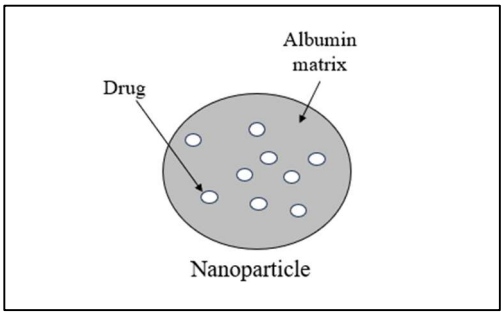

Figure 2.7. Structural representation of Albumin-based Nanoparticles (NPs)

In addition, the NPs can contain drugs by physically encapsulating them in the core or chemically binding them to the albumin membrane. The drug is released by degradation of the albumin in the target environment or by diffusion as the drug concentration gradient changes [109,110]. The NPs also improve the stability of drugs, particularly those that are unstable or rapidly degraded in the body, resulting in a more consistent therapeutic effect [111].

Nanocapsules (NCs) are a significant technological advance in the field of nanomedicine, offering a range of benefits due to their unique properties [112]. NCs can safely encapsulate various substances such as drugs, enzymes and other active ingredients. In addition, the surface of NCs can be modified with different molecules, such as ligands and antibodies, to enhance their ability to target specific biological systems, improving their interaction and effectiveness in treatments [113]. Albumin NCs with an oil core are an innovative application of nanotechnology in drug delivery and pharmaceutical treatments. These NCs consist of an oil phase core, which can be made from various biocompatible oils such as mineral or vegetable oil. This core acts

as a reservoir for lipophilic drugs, allowing for their encapsulation. The core is encapsulated within a shell made from albumin, as shown in Figure 2.8 [114].

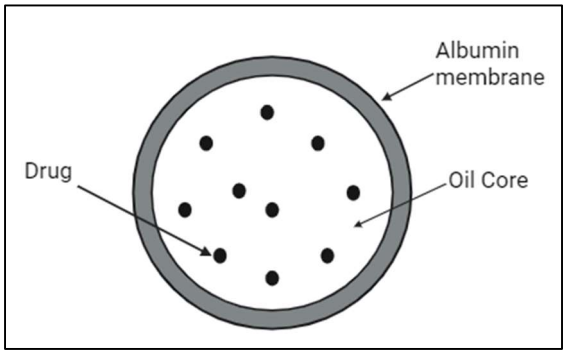

Figure 2.8. Structural representation of Albumin-based Nanocapsules (NCs)

The drugs encapsulated within these NCs are released over time, a process that can be controlled by altering the properties of the albumin shell or oil core [113]. This release typically involves the gradual breakdown of the albumin shell. A key feature is their high encapsulation efficiency, which ensures that a significant portion of the intended drug is successfully contained within the nanocapsule [115].

Chapter 3: Functionalization Approaches of albumin-based nanocarriers

Surface engineering of drug delivery systems involves modifying the formulation's physicochemical characteristics, pharmacokinetic behaviours, and pharmacological actions through the application of a range of biomaterials. This process involves the surface modification of the system, whereby it interacts with complementary coating moieties to create a thermodynamically stable, functionalised system. Surface modifications can be achieved through the coating of nanocarriers with either covalent or non-covalent bonds. Such alterations can also be achieved by depositing additional layers on the surface of the nanocarriers, which changes the properties of the drug delivery system without forming covalent bonds [116]. Conversely, surface modification can also be achieved through the formation of covalent bonds via a variety of grafting and coupling techniques [117]. This section will examine both covalent and non-covalent techniques that have been employed for the surface modification of nano-delivery systems.

3.1 Non-Covalent Surface Modifications

Surface modification of nanocarriers through non-covalent bonds has been demonstrated to result in improvements in their efficacy and enhancements in the pharmacokinetic properties of the loaded drugs. The association between the nanoparticle surface and the coating moiety can be facilitated by a number of different interactions, including hydrogen bonding, hydrophobic effects, electrostatic interactions, van der Waals forces, and a combination of these interactions as shown in Figure 3.1 [118,119].

The modification of nanosystems through electrostatic interactions involves the charge-based adsorption of various materials, such as saccharides and polyelectrolytes, onto the surface of the nanosystems, thus eliminating the need for multistep covalent conjugation chemistry [120]. Surface modification through electrostatic deposition typically involves coating a charged colloidal core, such as drug-loaded liposomes, niosomes, or nanocrystals, with oppositely charged polyelectrolytes. The electrostatic attraction between the colloidal core and the

polyelectrolytes results in the formation of an electrostatic film around the nanoparticles. This technique can be employed to enhance the stability, plasma half-life, and loading capacity of bioactive materials such as cell-penetrating peptides, as well as to introduce targeting moieties to the nanosystems [121].

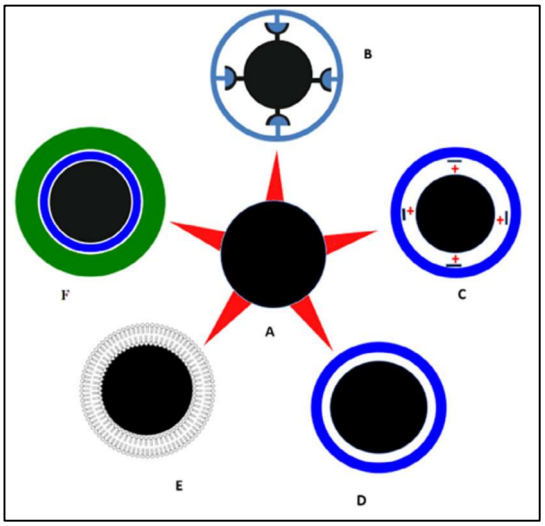

Figure 3.1 Non-Covalent Coating Techniques of Nanoparticles [122]

A number of non-covalent coating techniques are employed for nanoparticles, including (A) Uncoated nanoparticles. (B) nanoparticle surfaces are modified through supramolecular hydrogen bonding, where complementary interactions between the nanoparticle surface and the coating biomaterial form host-guest interactions. (C) nanoparticle surfaces coated via electrostatic attraction between opposite materials, forming either a single layer or multiple layers in a layer-by-layer fashion. (D) The deposition of a layer on the nanoparticle surface through hydrophobic interactions stabilises lipophilic nano systems using amphiphilic wetting agents. In this process, the lipophilic tails of the wetting agents associate with the nanosystem surface, while the hydrophilic portions interact with the aqueous environment, thus enhancing system stability. (E) The coating of nanoparticle surfaces with bilayers of human cells, such as red blood cells.

3.2 Covalent Surface Modifications

Covalent conjugation of materials on the surface of nanocarriers is a technique employed to modify the surface of nano-drug delivery systems. This method entails the attachment of biomolecules to the surface of the delivery system via

physiologically labile covalent bonds. Currently, this technique is a widely employed and valuable method, offering a powerful and versatile tool for the creation of nano-delivery systems with various covalently functionalised biomolecules [123]. The efficacy of covalent functionalisation is contingent upon the bond formed between the nanomaterial and the functional groups of the reacting molecules. This approach has facilitated the development of a wide range of nano-drug delivery systems incorporating both organic and inorganic functional groups [124]. A number of chemical techniques are employed in order to achieve the surface modification of nano-delivery systems. The most commonly utilised biodegradable bonds include amide, ester, polycyclic, disulfide, thiol, carbamate, and Schiff bases each type of covalent bond has a distinct mechanism of cleavage [125]. Functional groups, including alkoxy (OR), amino (NH2), amine (NHR), and alkyl (R), can be introduced onto the surfaces of nanomaterials, including micelles, nanoparticles, and carbon nanotubes [126]. The surface functional groups of the coating materials engage in chemical reactions with one another, forming biodegradable covalent bonds that facilitate the coating of nanoparticles.

3.3 Surface modified Albumin Nanoparticles

The well-defined primary structure of albumin provides numerous opportunities for surface modification of albumin-based nanoparticles, thanks to the presence of functional groups such as carboxylic and amino groups on their surfaces [127,128]. The surface modification of albumin nanoparticles is typically achieved through the conjugation of surface-modifying ligands via covalent bond formation between the ligands and the functional groups on the albumin surface. Alternatively, surface coating or electrostatic adsorption techniques may also be employed for nanoparticle surface modification [128].

In albumin-ligand combinations, albumin serves as a biodegradable carrier for drug delivery, while the ligands are used to modify pharmacokinetic parameters (e.g., surfactants), enhance nano system stability (e.g., Poly-L-lysine, for instance, can prolong the circulation half-life of drugs, while PEG can slow the release of drugs from nanoparticles. Cationic polymers can also be used to slow drug release. Finally,

folate, thermo-sensitive polymers and monoclonal antibodies can act as targeting agents [101,128].

3.4 Surfactant

The binding of doxorubicin to human serum albumin nanoparticles, which have a surface coating of polysorbate 80, can result in a significant reduction in the drug's haematological, cardiac, and testicular toxicities [129]. The reduced cardiotoxicity is likely due to the favourable changes in the drug's pharmacokinetics resulting from the surfactant coating. A number of studies have demonstrated that the coating of nanoparticles with polysorbate 80 results in an increase in the area under the curve (AUC) and a reduction in the volume of distribution, clearance, and cardiotoxicity of doxorubicin [130]. The reduced testicular toxicity of surfactant-coated nanoparticles may be attributed to the less efficient uptake of these particles by Sertoli cells, which have a phagocytic function. Consequently, the less opsonised surfactant-coated particles are less likely to be phagocytosed compared to uncoated particles. The uncoated particles, being more susceptible to phagocytosis, present a greater hazard to Sertoli cells. Upon entering the cells, these particles degrade and release the drug, resulting in significant cytotoxic effects and more pronounced damage to the epithelium [131].

3.5 Cationic Polymers

Albumin nanoparticles synthesized through coacervation are typically stabilized via crosslinking with glutaraldehyde. Nevertheless, the use of glutaraldehyde to enhance nanoparticle stability has been the subject of concern due to its cytotoxicity and potential adverse interactions with encapsulated therapeutic agents [132]. The coating of protein nanoparticles with biomaterials may offer a superior method for protection against enzymatic degradation. This approach, which involves the physical adsorption of a macromolecule, can obviate the necessity for the use of hazardous crosslinker agents [132]. Consequently, anionic BSA nanoparticles were surface-coated with cationic polymers like polyethyleneimine (PEI). Bone morphogenetic protein-2 (BMP-2) could be encapsulated within these PEI-coated BSA nanoparticles, with its release being regulated by the concentration of the PEI coating [133,134].

The surface charge of the particles underwent a shift from negative to neutral or slightly positive, which has the potential to reduce plasma protein adsorption on the particle surfaces and thus enhance their suitability for in vivo applications. Nevertheless, the osteoinductive activity of BMP-2 encapsulated in these nanoparticles was not effectively achieved in a rat ectopic model. This unfavourable outcome was attributed to the toxic effects of PEI on the locally present cells [133]. A study conducted by Zhang et al. demonstrated that substituting polyethylene glycol (PEG) for polyethyleneimine (PEI) significantly reduced the latter's toxicity. The BMP-2 encapsulated in BSA nanoparticles coated with PEI–PEG demonstrated more effective bone formation in a rat ectopic model compared to those coated solely with PEI. This improvement was attributed to the enhanced biocompatibility and physicochemical properties conferred by the PEG substitution [133]. Another cationic polymer, poly-L-lysine (PLL), was investigated as a potential substitute for PEI in coating BSA nanoparticles. siRNA and BMP-2 were encapsulated within PLL-coated BSA nanoparticles as model drugs [132]. The PLL coating was found to enhance proteolytic resistance, resulting in more stable nanoparticles. The stability of these nanoparticles in aqueous solutions was found to increase with higher PLL molecular weight and concentration. This was evidenced by the sustained release of FITC–BSA from BSA nanoparticles coated with 0.9 kDa PLL in phosphate buffer (pH 7.4), in contrast to the negligible release observed from nanoparticles coated with 4.2, 13.8, and 24 kDa PLL after three days. [132,135].

3.6 Chitosan

Chitin is a polymer composed of β-(1,4)-linked 2-acetamido-2-deoxy D-glucopyranose units, making it one of the most abundant organic materials and marine polysaccharides. It is readily available from natural sources, including the shells of crustaceans such as lobsters, shrimp, and crabs, as well as from industrial fungal process broths. Chitosan, a nitrogenous polysaccharide, is produced in significant quantities through the N-deacetylation of chitin as shown in the Figure 3.2. This versatile polymer exhibits a well-defined chemical structure and the capacity for chemical and enzymatic modifications. It is recognised for its physical and biological

functionality, biodegradability, and biocompatibility with various organs, tissues, and cells. Furthermore, chitosan can be processed into a diverse range of products, including flakes, fine powders, beads, membranes, sponges, cotton, and fibres. [69,136].

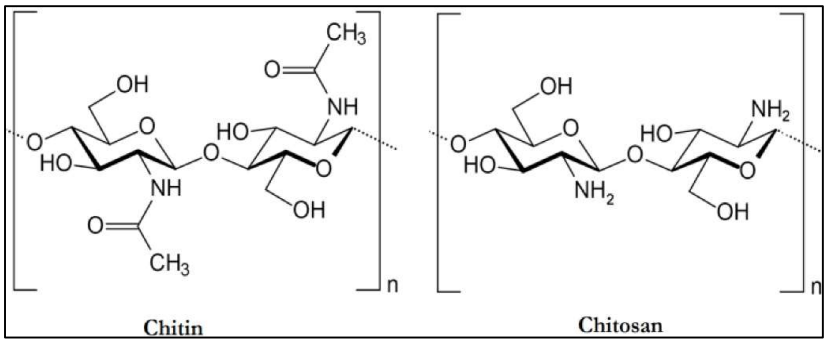

Figure 3.2. Chemical structure of Chitin and Chitosan [137]

The study of the crystalline structure of chitin/chitosan samples revealed that the partially deacetylated material was less crystalline and less anhydrous than pure chitosan. Crystallinity depends on the factors such as secondary treatment (reprecipitation, drying, and freeze-drying), origin (affects residual crystallinity), diffusion properties, and deacetylation procedures that may affect the solid-state structure of chitosan [69,138]. Chitosan obtained from deacetylation of crustacean chitin may have an MW of over 100,000 Da. The MW of chitosan depends on its source and deacetylation conditions (time, temperature, and concentration of alkali). Evaluation of the molecular weight of the polymeric chain is done using Viscometric and GPC techniques. Chitosan, being a cationic polysaccharide in neutral or basic pH conditions contains free amino groups hence, is insoluble in water. In acidic pH, amino groups can undergo protonation thus, making them soluble in water. Therefore, the solubility of chitosan depends on the distribution of free amino and *N*-acetyl groups. Chitosan is soluble in organic acids (formic, lactic, pyruvic, acetic, and oxalic acids). The extent of solubility also depends on the concentration and type of acid chosen for dissolution [139]. Higher MW chitosan often renders highly viscous solutions, which may not be desirable for industrial handling. However, lower viscosity chitosan may facilitate easy handling. The solution viscosity of chitosan

depends on its molecular size, cationic character, and concentration as well as the pH and ionic strength of the solvent [140].

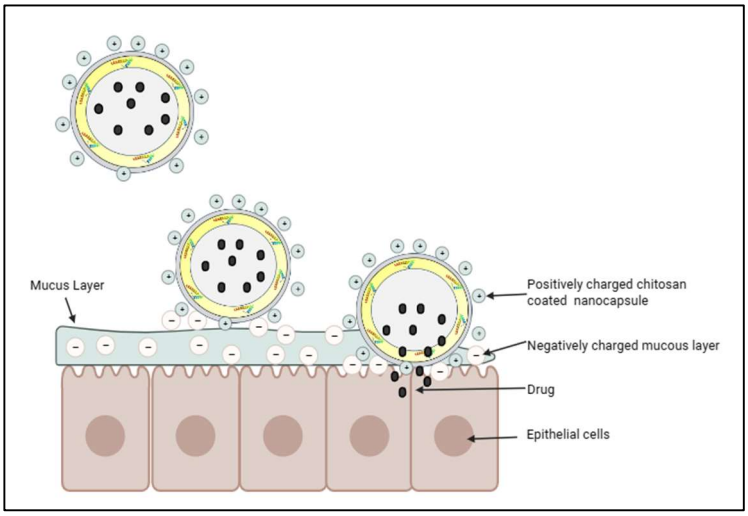

Figure 3.3. Schematic representation of Surface Modification of nanocapsule with Chitosan Coating

In order to enhance the ocular delivery of antibiotics through the eye's physiological and anatomical barriers, researchers have recently reported the utilisation of chitosan surface-modified, ciprofloxacin-loaded liposomes [141]. Doxorubicin-loaded human serum albumin (HSA) nanoparticles were stabilized by coating them with a cationic polymer, polyethyleneimine (PEI). The surface-modified HSA NPs demonstrated enhanced cellular penetration of the NPs due to the presence of a positive charge, thereby improving the cytotoxic effects of doxorubicin [142]. It has been observed that polymers capable of forming brush-like structures on the surfaces of nanoparticles can reduce van der Waals interactions among the nanoparticles, thereby enhancing their stability [76]. The objective of this study was to investigate the effect of chitosan (CS) coating on bovine serum albumin nanoparticles (BSA NPs) for ocular delivery. The presence of the CS coating was confirmed by observing changes in zeta potential (ZP). The CS coating was found to modulate drug release and enhance the mucoadhesion of the nanoparticles [143]. Chitosan is also valuable in wound healing and tissue engineering due to its ability to promote clotting and natural antibacterial properties. It is especially useful in dressings and scaffolds for new tissue growth [144,145]. Chitosan's mucoadhesive properties enable efficient transmucosal drug delivery, enhancing drug absorption

and bioavailability [146]. Additionally, its inherent antimicrobial qualities make it a suitable candidate for formulations aimed at infection control, often integrated into medical coatings and fibres [144,147].

3.7 Thermosensitive polymers

Shen et al. developed a novel thermally-targeted anti-cancer drug carrier by conjugating thermo-responsive poly (N-isopropyl acrylamide-co-acrylamide)-block-polyallylamine (PNIPAM-AAm-b-PAA) to the carboxylic groups on the surface of albumin nanospheres using the carbodiimide (EDC) coupling technique [148]. During the particle preparation process, the anti-cancer drug adriamycin was encapsulated within both unconjugated (AN) and conjugated albumin nanospheres (PAN) [77] In comparison to AN, the release rate of adriamycin from PAN in trypsin solution was found to be slower, and this further decreased with increasing amounts of conjugated PNIPAM-AAm-AA or its molecular weight. This suggests that the steric hydrophilic barrier on AN impedes its digestion. Furthermore, the release of adriamycin from PAN was accelerated above the cloud-point temperature of PNIPAM-AAm-AA due to the shrinkage of the thermo-sensitive polymer. In experiments with human hepatocellular carcinoma HepG2 cells, PAN demonstrated effective targeting of cancer cells above the cloud-point temperature of PNIPAM-AAm-AA, but not below this temperature. These findings indicate that PAN has thermal targetability, which may enable selective accumulation in solid tumours maintained above physiological temperature through local hyperthermia [77,148].

3.8 Polyethylene glycol (PEG)

The chemical coupling of polyethylene glycol (PEG) to proteins or particles, known as PEGylation, is a well-established technique that has been shown to significantly extend the circulation half-life of the coupled entities by more than 50-fold. Furthermore, PEGylation has been demonstrated to reduce immunogenicity and enhance tumour accumulation through the enhanced permeability and retention (EPR) effect [149]. mPEG-Succinimidyl Propionate (mPEG-SPA) was employed for the conjugation of polyethylene glycol (PEG) to the amino groups of bovine serum albumin (BSA) nanoparticles [149]. The release of 5-fluorouracil from PEGylated BSA

nanoparticles was found to be significantly slower than from non-PEGylated nanoparticles. This phenomenon is likely attributable to the presence of a polyethylene glycol (PEG) layer surrounding the PEGylated particles, which serves to impede the diffusion of the encapsulated drug [149]. Surface-modified human serum albumin (HSA) nanoparticles were prepared using two types of poly(ethylene glycol)–HSA conjugates: a poly(thioetheramido acid)–poly(ethylene glycol) copolymer-grafted HSA and a methoxy poly(ethylene glycol)-grafted HSA (HSA–mPEG) [150]. Rose Bengal (RB) was employed as a model drug for encapsulation into the nanoparticles. The drug loading in HSA–mPEG nanoparticles was significantly lower due to the reduced number of drugs–protein binding sites available in the HSA–mPEG molecules compared to unmodified HSA. In comparison to unmodified nanoparticles, the slower release of RB from surface-modified HSA nanoparticles in the presence of enzymes indicated that the steric hydrophilic barrier on the nanoparticle surface impeded their digestion [150].

3.9 Folic acid

Folic acid is a low-molecular-weight vitamin (441 Da) that has been observed to frequently overexpress its receptor in human cancer cells. This receptor is recognised as a tumour marker, particularly in ovarian carcinomas, and is minimally expressed in most normal tissues. [151,152]. Folic acid offers several advantages as a targeting agent for tumor cells. Firstly, it is stable, cost-effective, nonimmunogenic, and compatible with organic solvents used in the preparation process, unlike proteins such as monoclonal antibodies. Secondly, folic acid binds with high affinity to folate receptors on cell surfaces and is internalized via receptor-mediated endocytosis [153]. The carboxylic group of folic acid was covalently conjugated to the amino groups on the surface of albumin nanoparticles using the 1-ethyl-3-(3-dimethylaminopropyl) carbodiimide (EDC) coupling technique [77]. The enhanced uptake of nanoparticles by cancer cells indicates that folate-conjugated albumin nanoparticles provide a drug delivery system with specificity for cancer cells [128]. Consequently, numerous anticancer drugs have been loaded into folate-conjugated albumin nanoparticles, including doxorubicin, [77] paclitaxel, [154] cisplatin, [155]

vinblastine sulfate, [156] mitoxantrone [157]. Folic acid (FA) is employed as a selective targeting ligand to target the overexpressed folate receptor alpha (FRα) on the surface of tumour cells. Bexarotene-loaded BSA NPs modified with folic acid demonstrated enhanced tumour cell growth inhibition in comparison to non-targeted NPs. (Qi et al., 2014). Nosrati et al. demonstrated that conjugating chrysin-loaded BSA NPs with FA had the superior potential to overcome the poor solubility of chrysin, with improved targeting. (Nosrati et al., 2018). The incorporation of ginsenoside Rg5 into folate-decorated bovine serum albumin nanoparticles (FA-BSA NPs) resulted in enhanced cytotoxic activity and the accumulation of Rg5 at the tumour sites. (Dong et al., 2019). Folic acid-modified baicalein-loaded BSA NPs exhibited extensive accumulation in the breast tumour microenvironment with a prolonged circulation time, thereby enhancing the therapeutic efficiency of baicalein. (F. Meng et al., 2021). Fluorescein isothiocyanate-labelled folate-conjugated BSA nanoparticles were internalised by SKOV3 cells, a human ovarian cancer cell line. This uptake was inhibited by an excess of folic acid, indicating that the binding and/or uptake were mediated by the folate receptor [158]. Similarly, folate-decorated paclitaxel-loaded BSA nanoparticles were observed to effectively target a human prostate cancer cell line [159] Shen et al. reported that folate-conjugated doxorubicin-loaded BSA nanospheres were incorporated into HeLa tumour cells after only 2 hours of incubation, whereas HeLa cells did not incorporate the unconjugated nanospheres even after 4 hours of incubation [77]. Furthermore, aortic smooth muscle cells (AoSMC) exhibited higher viability compared to HeLa cells when treated with folate-conjugated doxorubicin-loaded BSA nanoparticles, suggesting that these nanoparticles were selective for HeLa cells (which express folate receptor alpha, FRα) and non-selective for AoSMC cells (which do not express FRα). The results demonstrated that folate-conjugated magnetic HSA nanoparticles loaded with cisplatin exhibited a significant sustained-release effect, with the half-release time (t1/2) of cisplatin being 65 minutes from solution and 24 hours from nanoparticles [128,155,160].

3.10 Peptides

The PEGylated human serum albumin (HSA) nano micelles were formed by self-assembly and subsequently surface-conjugated with cyclic RGD peptides. This was done in order to facilitate the selective delivery of doxorubicin to cells expressing the αvβ3 integrin. The cyclic RGD peptide was conjugated to the micelles' PEG chains [161]. When incubated with human melanoma cells (M21+) that express the αvβ3 integrin, there was a higher uptake and longer retention of doxorubicin. Upon entering the cells, both covalently linked and noncovalently absorbed doxorubicin were effectively released from the albumin carrier. This release was facilitated by the reduction of disulfide bonds by intracellular thiols and proteolytic processes within endosomes and lysosomes [162]

In the study by Karmali et al., tumour-homing peptides, specifically CREKA (a pentapeptide consisting of cysteine, arginine, glutamic acid, lysine, and alanine) and LyP-1 (a cyclic nine-amino acid peptide), were employed to target Abraxane (nab-paclitaxel) to tumors in mice [163]. Peptide Abraxane conjugates were prepared by coupling peptides to Abraxane via their cysteine sulfhydryl groups using a sulfo-SMCC (sulfosuccinimidyl 4-[N-maleimidomethyl] cyclohexane-1-carboxylate) cross-linker. Upon intravenous injection of CREKA-Abraxane into mice bearing MDA-MB-435 human cancer xenografts, the conjugate accumulated in tumour blood vessels, forming aggregates that included red blood cells and fibrin. The self-assembled mixed micelles, which carried the homing peptide on different subunits, accumulated in the same tumour regions as LyP-1-abraxane. This demonstrated that LyP-1 can deliver intact nanoparticles to extravascular sites. The results demonstrated that LyP-1-Abraxane resulted in a statistically significant inhibition of tumour growth compared to untargeted Abraxane [163].

3.11 Monoclonal antibodies

Monoclonal antibodies (mAbs) have emerged as a promising group of ligands for specific tumour targeting. The human epidermal growth factor receptor-2 (HER2) is a tumour-targeting marker that is employed in the treatment of metastatic breast cancer. To exploit this, the surface of HSA nanoparticles was modified with the humanised anti-HER2 antibody trastuzumab (Herceptin®) using an avidin-biotin

complex formation. This entailed the attachment of NeutrAvidin, a biotin-binding protein, to the nanoparticles, followed by the conjugation of the biotinylated antibody [164]. The attachment of trastuzumab-conjugated HSA nanoparticles to the surface of HER2-overexpressing cell lines (BT474, MCF7, and SK-BR-3) was found to be both time and dose dependent. This process facilitated the effective internalisation of the nanoparticles by these cells through receptor-mediated endocytosis [164].

Steinhauser et al. employed trastuzumab-modified human serum albumin (HSA) nanoparticles for the cell-specific targeting of antisense oligonucleotides (ASOs) to human epidermal growth factor receptor 2 (HER2)-overexpressing breast cancer cells. The antisense oligonucleotides (ASOs), which were directed against polo-like kinase 1 (Plk1), demonstrated a significant downregulation of Plk1 mRNA and Plk1 protein following incubation with the nanoparticle formulations [101]. BSA-Nps with Another ligand, cholesterol, was conjugated with tamoxifen-loaded BSA NPs in order to develop an indirect tumour-targeting strategy. The NPs demonstrated enhanced cytotoxicity and specificity on cancer cells overexpressing low-density lipoprotein (LDL) receptors, compared to non-targeted NPs. (Gharbavi et al., 2020). In another study, docetaxel-loaded human serum albumin (HSA) conjugates were developed utilising folate and biotin targeting ligands. The drug-albumin conjugates demonstrated superiority in terms of cellular uptake and antitumor activity compared to free docetaxel [165]. Luteinizing hormone-releasing hormone (LHRH) conjugated methotrexate-loaded human serum albumin (HSA) nanoparticles (NPs) were developed as active targeting nanocarriers, exhibiting a significant delay in tumour growth of 4T1 cells compared to non-targeted HSA NPs and free methotrexate formulations (Taheri et al., 2012). A number of malignant tumours, including those of the colon, head and neck, non-small cell lung, ovary, breast and prostate, as well as glioma, display overexpression of the epidermal growth factor receptor (EGFR) on their surfaces. In 2004, the FDA approved cetuximab, a humanized IgG1 monoclonal antibody targeting EGFR, for the treatment of colorectal cancer [166]. Consequently, cetuximab-modified HSA nanoparticles represent a promising carrier system for drug delivery. It has been demonstrated that EGFR-expressing colon carcinoma cells accumulate in a specific manner when exposed to

cetuximab [166]. DI17E6, a monoclonal antibody directed against αv-integrins, was covalently coupled to human serum albumin (HSA) nanoparticles loaded with doxorubicin. The thiolated antibody was linked to the nanoparticles via a sulfhydryl-reactive nanoparticle suspension, thereby establishing a covalent bond between the antibody and the nanoparticle system [167]. The target-specific nanoparticles demonstrated selective targeting of αvβ3 integrin-positive melanoma cells, with increased cytotoxic activity compared to the free drug [167].

3.12 Inducible T-Cell Costimulator (ICOS)

It is a crucial component of the immune system, molecular weight of approximately 55∼60 kD, specifically in regulating T-cell function [168]. It belongs to the CD28 family of immune costimulatory receptors, which includes CD28, CTLA-4, and PD-1. ICOS improves all fundamental T cell responses to foreign antigens, such as proliferation, lymphokine secretion, upregulation of molecules that mediate cell-cell interactions, and effective support of antibody secretion by B cells [169]. Additionally, it prevents apoptosis of pre-activated T cells and plays a critical role in CD40-mediated class switching of immunoglobulin isotypes. CD278/ICOS is a transmembrane protein that plays a critical role in the adaptive immune response [170]. It is predominantly expressed on the surface of T cells and is inducible rather than constant. Upon T cell activation, triggered by recognition of an antigen, ICOS expression is upregulated. Up-regulation is crucial for fine-tuning the immune system to amplify the T-cell response when necessary. ICOS primarily functions by binding to its ligand, ICOSL, which is found on other immune cells, such as antigen-presenting cells (APCs) [171]. This interaction provides an essential co-stimulatory signal for the full activation of T cells, increasing their proliferation, survival, and efficacy. ICOS plays a central role in T cell activation and survival, influencing cytokine production and shaping the nature and intensity of the immune response. As such, it is an important target in immunotherapies, including cancer immunotherapy [172,173].

To improve its therapeutic potential, ICOS is often fused with the Fc region of an antibody, a process known as Fc Fusion. The Fc region, which is the constant part of an antibody, is known for its stability and prolonged circulation in the blood. This

fusion aims enhance in the stability and half-life of ICOS, allowing for prolonged circulation time and potentially increased efficacy in modulating immune responses. [171,174]. Manipulations like Fc Fusion are particularly relevant in developing treatments for conditions where modulating the immune response is crucial, such as certain cancers or autoimmune diseases. The manipulation of ICOS through techniques like Fc Fusion opens new avenues in immunotherapy [175].

The conjugation of the Fc region of an antibody with ICOS, a member of the CD28 family of T-cell co-stimulators, results in the creation of an ICOS-Fc hybrid molecule with specific targeting capabilities. This approach has numerous applications in targeted drug delivery. Drugs conjugated to ICOS-Fc can selectively impact cells expressing the ICOS ligand, enhancing efficacy while minimizing side effect Nanoparticles are frequently used in drug delivery the encapsulation of NPs with ICOS-Fc behaves as an effective antitumor agent by triggering an anticancer immune response, inhibiting tumor angiogenesis, and possibly altering the behaviour of the tumor cells [109]. Conjugating them with ICOS-Fc enables precise targeting of immune cells, which is particularly useful in cancer therapy for targeting the tumor microenvironment (as shown in Figure 3.4). This technology can also be applied to other therapeutic agents, such as small molecule inhibitors or genetic material like siRNA, by conjugating them with ICOS-Fc to direct them specifically to desired immune cells [176].

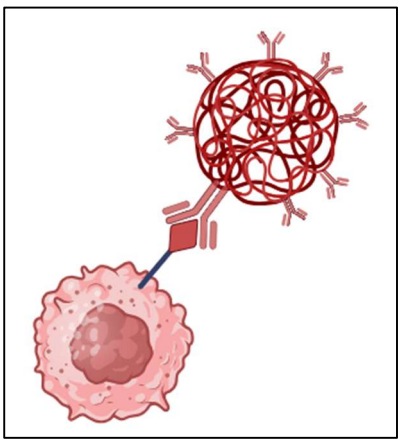

Figure 3.4. Schematic Representation of ICOS-Fc conjugated with Nanoparticles

Chapter 4: Development of nanomedicine as per ICH Q8 Guidelines

The ICH Q8 guideline, titled 'Pharmaceutical Development', is part of a set of International Council for Harmonisation of Technical Requirements for Pharmaceuticals for Human Use (ICH) guidelines. These guidelines aim to harmonise regulatory requirements for pharmaceuticals in Europe, Japan, and the United States. The key aspects of the ICH Q8 guideline include the development of a pharmaceutical product's identification of critical quality attributes (CQAs), critical material attributes (CMAs) and critical process parameters (CPPs) [177,178].

4.1 Critical Quality Attributes (CQA)

Critical Quality Attributes refer to the physical, chemical, biological, and microbiological properties or characteristics of an ingredient or product that must be controlled within predefined limits to ensure the desired product quality. These attributes are considered critical because they have an impact on the efficacy, safety, and stability of the drug product [179].

CQAs start with comprehending the correlation between the drug substance's attributes, ingredients, and the drug product. This requires an examination of the drug's therapeutic context, route of administration, dosage form, and the characteristics of the active pharmaceutical ingredient (API).

CQAs are directly linked to the quality of the drug product. They can influence important factors such as the drug's bioavailability, stability, and patient acceptability. Parameters such as particle size, polymorphism, purity, and strength.

CQAs are closely linked to Critical Process Parameters (CPPs). CPPs are the key variables that affect the production process and must be monitored or controlled to ensure that the product meets its CQAs. It is essential to comprehend the relationship between CPPs and CQAs for effective process control [180].

4.2 Critical Material Attributes (CMAs)

CMAs are defined in the ICH Q8 (R2) guideline on pharmaceutical development. They are crucial for ensuring that the raw materials used in pharmaceutical products

contribute to the final product's quality, safety, and efficacy. The process usually requires a comprehensive understanding of the effects of material properties on both the process and the product. This can be achieved through experimental investigation and prior knowledge [181–184].

CMAs are essential characteristics of materials used in pharmaceutical manufacturing and they are typically classified into several types…

Physical Attributes

These are the measurable physical characteristics of materials: particle size, shape, and distribution. These aspects can significantly impact the material's performance in a formulation.

Chemical Attributes

These relate to the composition and chemical properties of the material. The primary concern is purity, ensuring that the material is free from unwanted contaminants. Potency, which measures the strength or effectiveness of the material, is also critical, especially in pharmaceuticals where dosage accuracy is crucial. It is important to identify and control specific impurities or contaminants as they can affect the safety and efficacy of the final product.

Biological Attributes

This category is especially important for materials sourced from biology, such as cell lines, enzymes, and other bioactive substances. Essential factors include biological activity, which measures how effectively a material performs its intended biological function, and immunogenicity, which refers to the potential of the material to provoke an immune response.

Microbiological Attributes

These aspects are essential for materials used in sterile pharmaceutical products. Bioburden, which refers to the amount of microbial contamination, must be controlled to ensure safety and stability. Endotoxin levels, toxins released by bacteria, are a significant concern in injectable drugs. Sterility is also a critical attribute, ensuring that no viable microorganisms are present in the final product.

Understanding CMAs is essential for designing robust manufacturing processes and control strategies. This knowledge is crucial in mitigating risks associated with variability in material attributes.

4.3 Critical Process Parameters (CPPs)

CPPs are process parameters whose variability impacts a Critical Quality Attribute (CQA) and must be monitored or controlled to ensure the desired quality of the process. They are crucial in process design and control in pharmaceutical manufacturing. The parameters required for the manufacturing process can vary widely but usually include temperature, pressure, pH level, stirring speed, and reaction time [180,181,185].

4.4 Development of Nanomedicine

The development of a pharmaceutical product typically involves a comprehensive and meticulous process, usually divided into two main steps: Formulation Development and Process Development.

I. Formulation Development

This is the first stage in developing the composition of the albumin-based nanomedicine. The types of albumins to be used, along with other additives and stabilisers that may be required, are determined.

a) Optimization of Blank Formulations

In this stage, the focus is on developing the albumin-based carrier system without the active pharmaceutical ingredient (API). The aim is to optimize the formulation's properties, such as solubility, stability, and biocompatibility. Key factors that are taken into consideration include the concentration of albumin, pH levels, ionic strength, and isoelectric point and the presence of any additives or stabilizers [186].

b) Optimization of Drug-Loaded Formulation

Once the blank formulation is optimized, the next step involves incorporating the hydrophilic and lipophilic drugs into the albumin-based system. This stage requires careful consideration of the drug's molecular interaction with albumin [187]. The

critical factors to consider are the drug loading capacity, encapsulation efficiency, release profile, and stability of the drug-albumin formulation [188,189]. Techniques such as high-performance liquid chromatography (HPLC) can be used to analyse the formulation and ensure that the drug is properly incorporated and maintained within the albumin carrier.

II. Process Development

Once the formulation is established, attention turns to scaling up the production process. This involves establishing manufacturing processes that are consistent, reliable, and scalable.

a) Optimization of Process Parameters

Optimising process parameters for the production of albumin-based nanomedicine is a critical aspect of pharmaceutical manufacturing. It requires a careful balance of various factors to ensure the efficacy and quality of the final formulation. Temperature is a key parameter because the stability of albumin, a protein, is highly temperature-sensitive. Therefore, maintaining an optimal temperature is essential to preserve the albumin's structure and function. The pH level is important for the structure and functionality of albumin, as it affects its binding properties and stability. This is crucial for targeted drug delivery. The mixing speed during formulation affects the size and uniformity of nanomedicine. Precise control is necessary to ensure consistent quality of nanomedicine [190].

In addition, it is important to optimize the reaction time duration for each manufacturing step to ensure that albumin is exposed to ideal conditions for an appropriate amount of time. This will have an impact on drug loading efficiency and release profiles. It is important to consider the interactions between these parameters, as optimal pH may vary with temperature changes and mixing speed may need to be adjusted based on process duration [191].

b) Physico-chemical Characterization

In this final step, the physico-chemical properties of the albumin-based formulation are comprehensively characterised. This involves determining the particle size, zeta potential, morphology, and thermal stability of the formulation [192]. Techniques

such as dynamic light scattering (DLS), scanning electron microscopy (SEM), and differential scanning calorimetry (DSC) and Fourier-transform infrared spectroscopy (FTIR) are commonly employed [193,194]. This characterisation is crucial for predicting how the formulation will behave in biological systems and for regulatory approval processes.

Chapter 5: Aim of the work

The aim of the study is to develop new albumin-based nanoformulation tuning advanced manufacturing technologies, including surfactant-mediated coacervation, ultrasonication technology (US), microwave-assisted (MW), and a combination of microwave and ultrasonication (MW/US). The surfactant-mediated coacervation method uses organic solvents to denature albumin. This process creates a coacervate of albumin that can encapsulate drug molecules, but the use of solvents and the need for cross-linking agents are limitations. As a consequence, the thesis will be evaluated as greener and sustainable. The formulation design and development will follow the ICH Q8 guidelines for manufacturing methods, such as ultrasonication, microwave and combined microwave and ultrasonication.

The primary objective will be to achieve the quality target attributes, including particle size, polydispersity index (PDI), zeta potential, encapsulation efficiency, *in vitro* drug release profiles, and shelf life. These attributes are of paramount importance for ensuring the stability, bioavailability and safety. The research will begin by optimizing the formulation of BSA nanoparticles and nanocapsules. Various approaches will be evaluated to achieve the desired quality target attributes. The optimization of the preparation methods will be adjusting the concentration of albumin, and the parameters of the manufacturing processes. After extensive experimentation and analysis, the optimal conditions for producing high-quality BSA nanomedicine will be tuned.

Once the optimal formulation will be identified with the BSA as a component, HSA will be used to obtain the nanocarriers. A comparison will be carried out between the findings and the preparation of HSA nanomedicine. A comprehensive analysis will be conducted to ensure that the optimal conditions for BSA will be appropriately adapted for HSA.

The final stage of the PhD research will concern the development of optimised BSA and HSA nanoparticles and nanocapsules, incorporating a hydrophilic drug, doxorubicin hydrochloride. This drug is a common therapeutic agent in the treatment of cancer, serving as a model drug for our study. The objective will be to achieve

targeted delivery of the Doxorubicin to cancer cells, by modifying the surface of the albumin nanomedicine with specific coatings and ligands. These modifications will enhance the targeting capability by recognizing and binding to receptors overexpressed on cancer cells, thereby improving the therapeutic efficacy and reducing side effects.

Chapter 6: Preparation and Optimization of Blank Bovine Serum Albumin-Based Nanomedicine by Approaching Advanced Manufacturing Technologies

In this chapter, the development of various advanced manufacturing technologies for the optimization and preparation of blank bovine serum albumin-based nanomedicine delivery systems, with a particular focus on nanoparticles (BSA-NPs) and nanocapsules (BSA-NCs) formation by using the Coacervation Method, Ultrasonication Technology (US), Microwave Technology (MW) and Combined Microwave and Ultrasonication (MW/US). Our objective was to achieve specific quality target attributes to ensure the effectiveness and physical stability of these nanomedicines as per the ICH Q8 guidelines for the quality target attributes, which included particle size, polydispersity index (PDI), zeta potential, encapsulation efficiency, in-vitro drug release, and physical stability as shown in Table 6.1. These parameters were essential in guiding the optimization process.

Table 6.1. Parameters of Quality Target Critical Attributes

Critical Attribute	Specifications
Particle Size	≤ 200 nm
Polydispersity (PDI)	≤ 0.25
Zeta Potential Value (mV)	≥ -20 mV
Encapsulation Efficiency (EE %)	≥ 50 %
In-Vitro Drug Release	Prolonged release profile
Stability (Shelf Life)	6 months minimum

Here is a detailed explanation of each quality target attribute listed below [195–197].

Particle Size

The particle size must be equal to or less than 200 nm. Smaller particles can enhance the bioavailability of the incorporated drug, improve its distribution in the body, and potentially allow for vascular targeted delivery to specific sites.

Polydispersity Index (PDI)

The Polydispersity Index (PDI) measurement determines the range of particle sizes present in the nanoparticle population. A PDI less than 0.25 represent a narrow size distribution, that can affect the stability of the system.

Zeta Potential

The zeta potential of nanoparticles indicates their surface charge. A negative charge of greater than -20 mV or higher suggests that there is enough surface charge to prevent nanoparticle aggregation, which improves their physically stability. Additionally, the surface charge can affect the cellular uptake and distribution of the nanomedicine in the body.

Encapsulation Efficiency

This parameter indicates the percentage of drug that is successfully encapsulated within the nanomedicine, in respect to amount used. It is important to achieve an encapsulation efficiency of at least 50% to ensure effective manufacturing process drug incorporation.

In-Vitro Drug Release

A prolonged release profile refers to the controlled and constant release of the drug over an extended period of time. This release profile is designed to maintain therapeutic drug levels within the body's system, reducing the need for frequent dosing and thereby enhancing patient compliance.

Physical Stability

The critical attributes of the nanomedicine should remain stable for at least six months without any significant changes of physicochemical parameter. Physical stability encompasses maintaining nanoparticle size, polydispersity index, zeta potential, and encapsulation efficiency over this period. This ensures the efficacy and safety of the product throughout its intended shelf life.

6.1 Formulation Components of BSA NPs and NCs

In the manufacturing and optimization of bovine serum albumin nanoparticles (BSA-NPs), Bovine Serum albumin was bought by Sigma-Aldrich as the key component of the formulation. This ensures that the formulation is biocompatible and biodegradable. The non-ionic surfactant Polyoxyl 15 hydroxy stearate (Kolliphor® HS15) from BASF Chemical Company is another essential component to keep the

stability of BSA-NPs. Sodium phosphate buffer, (Sigma Aldrich), plays a role in maintaining the pH and ionic balance strength. Ethanol serves as the organic solvent bought (Sigma Aldrich) and used to denaturated the BSA nanoparticle. Lecithin, phosphatidylcholine (Epikuron® 200) kind gift from Cargill Company. Finally, a 0.9% NaCl solution is used in the dialysis step to adjust the solution's osmolarity and facilitate the removal of excess BSA molecules thus purifying the formulation. A dialysis membrane with a 14,000 k Dalton cutoff bought from Carl Roth. In the manufacturing process of bovine serum albumin nanocapsules (BSA-NCs), the component is used Caprylic/Capric Triglyceride (Miglyol® 829). However, the incorporation of Miglyol 829, a neutral lipid-based additive from IOI Oleochemical, is used to form the oily core nanocapsules. Sorbitan Sesquioleate (Span® 83) is a non-ionic surfactant from (Sigma Aldrich) was used to solubilise the hydrophilic drug.

Kolliphor® HS15 (polyoxyl 15 hydroxy stearate, HS15) is an innovative non-ionic surfactant. It is composed of polyglycerol esters of 12-hydroxystearic acid (70%) and free polyethylene glycol (30%) as shown in the Figure 6.1. This surfactant is also known by other names, including Solutol HS® 15, macrogol 15-hydroxystearate, and polyoxyethylated 12-hydroxystearic acid. It is recognised in the European, US, and Japanese Pharmacopoeias. It should also be noted here that Kolliphor® HS15 possesses a hydrophilic-lipophilic balance (HLB) value of 16 and exhibits a critical micelle concentration (CMC) ranging from 0.005% to 0.02% [198–200]

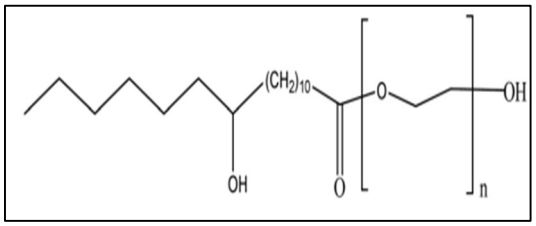

Figure 6.1. Chemical Structure of Kolliphor HS15

The chemical structure of lecithin phosphatidylcholine, (Epikuron® 200) shown in the Figure 6.2 consists of a central glycerol backbone with three carbon atoms. The first carbon is attached to an unsaturated fatty acid chain, the second carbon is attached to a saturated fatty acid chain and the third carbon is attached to a phosphate group.

This phosphate group is further linked to a choline group containing a positively charged nitrogen atom. Lecithin is used in pharmaceutical preparations as an emulsifier, solubilizer and stabiliser to improve the delivery and bioavailability of drugs [201,202].

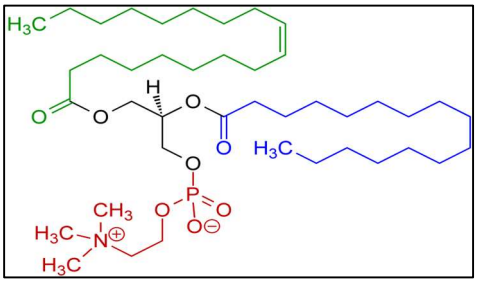

Figure 6.2. Chemical Structure of Lecithin Phosphatidylcholine (Epikuron® 200)

Caprylic/Capric Triglyceride, more commonly referred to as Miglyol® 829, is a mixed triester of glycerin and caprylic (C8) and capric (C10) acids. Figure 6.3 illustrates the chemical structure of a triglyceride molecule, which is composed of a glycerol backbone esterified with three fatty acid chains. The central portion of the molecule is glycerol, a three-carbon alcohol with hydroxyl groups (-OH) on each carbon, each of which is esterified with a fatty acid. The acyl groups attached to the glycerol backbone are caprylic acid (C8H16O2), an 8-carbon fatty acid, and capric acid (C10H20O2), a 10-carbon fatty acid. Caprylic acid is an oily liquid, insoluble in water, due to its hydrophobic nature and having a slightly unpleasant rancid-like smell. Caprylic acid exhibits excellent shelf life characteristics due to its high stability and resistance to oxidation [203,204].

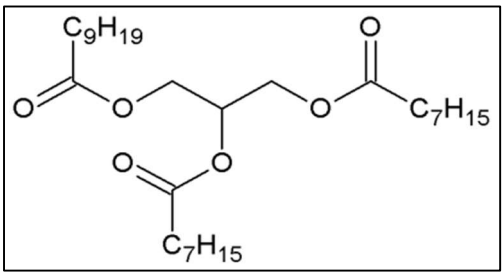

Figure 6.3. Chemical Structure of Caprylic /Capric Triglyceride (Miglyol® 829)

Sorbitan sesquioleate (Span® 83) is a chemical compound consisting of sorbitan, a derivative of sorbitol, esterified with oleic acid. Its structure includes a sorbitan moiety which is a tetrahydrofuran (THF) ring with hydroxyl groups attached to the

second, third and fourth carbon atoms and an additional hydroxyl group attached to the first carbon outside the ring. The oleic acid moiety is an 18-carbon fatty acid with a cis double bond between the 9th and 10th carbon atoms and a terminal carboxyl group (COOH) as shown in Figure 6.4. It can play a role in the solubilisation of hydrophilic drugs in formulations. As an emulsifier, it helps to disperse and stabilise hydrophilic drugs in oil-based formulations or emulsions, improving their bioavailability and efficacy.

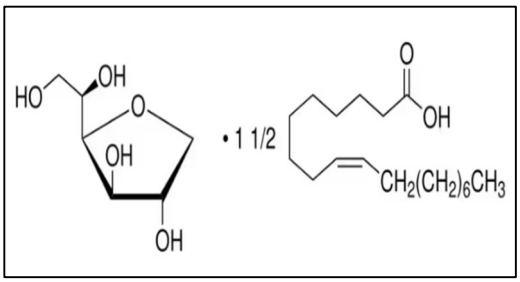

Figure 6.4. Chemical Structure of Sorbitan Sesquioleate (Span® 83)

6.2 Preparation of BSA-NPs Using Surfactant-mediated Coacervation Method

To prepare BSA-NPs, the Bovine Serum Albumin (BSA) 8 mg/mL containing Kolliphor HS15 (0.1% w/v) in sodium phosphate buffer (0.1M) at pH 8.0. The next step is to induce denaturation of the albumin solution by adding either ethanol or ethanolic Epikuron® solution 200 (1 % w/v) drop-by-drop under magnetic stirring conditions at room temperature. Observations revealed that the addition of ethanol alone leads to the precipitation of big BSA particle sizes, whereas using ethanolic Epikuron® 200 solution results in the successful formation of BSA-NPs. Subsequently, the ethanol was evaporated using nitrogen purge. Once the ethanol has evaporated, the resulting BSA-NPs are purified by dialysis against a NaCl 0.9% solution. a schematic representation is shown in Figure 6.5.

Kolliphor HS15 is selected to stabilize albumin nanoparticle. Several experiments were conducted using surfactant-mediated coacervation methods to form albumin nanoparticle without using Kolliphor HS15 in formulations utilizing either ethanol or ethanolic Epikuron® 200, there is no formation of nanoparticle occurred in both cases. The incorporation of Kolliphor HS15 has been observed to play a significant role in the formulation and stabilization of BSA-NPs within drug delivery systems.

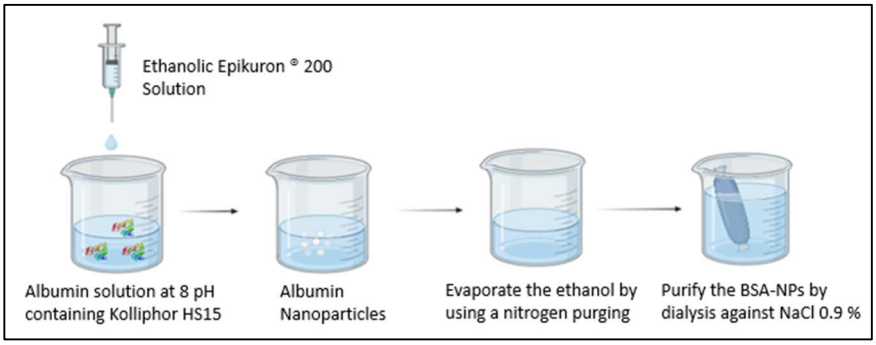

Figure 6.5. Schematic representation of the preparation of BSA-NPs By the Optimized Surfactant-mediated Coacervation Method

6.3 Optimization of BSA-NPs Preparation by Surfactant-mediated Coacervation Method

I. Size Optimization of BSA-NPs

The relationship between the concentration of BSA against the size of the BSA-NPs was investigated. Based on the experimental results of the present work, the size of the BSA-NPs increases as the BSA concentration in the solution increases from 6 to 16 mg/mL, as shown in Figure 6.6. This indicates that adjusting the BSA concentration in the preparation process can control the size of BSA-NPs.

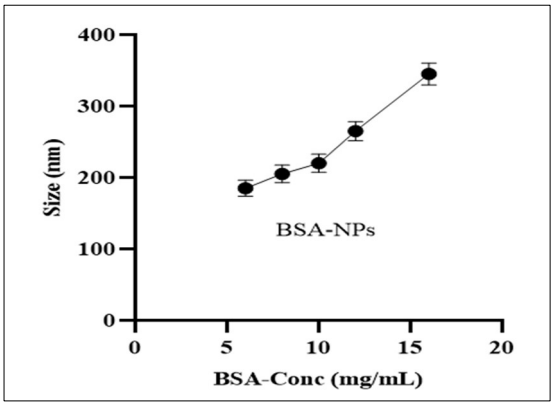

Figure 6.6. Size of BSA-NPs against the BSA Concentration.

II. Zeta Potential Value Optimization

The zeta potential of the BSA-NPs is dependent on the concentration of BSA in the solution. All zeta potential values are negative due to the negative charge of BSA at pH 8.0. The zeta potential values decrease as the concentration of BSA increases,

ranging from approximately -15 mV to below -30 mV as the concentration of BSA increases from 6 to 16 mg/mL as shown in Figure 6.7. The nanoparticles are likely to be stable due to electrostatic repulsion, as indicated by the high zeta potential values. Additionally, the value of the zeta potential decreases with increasing BSA concentration.

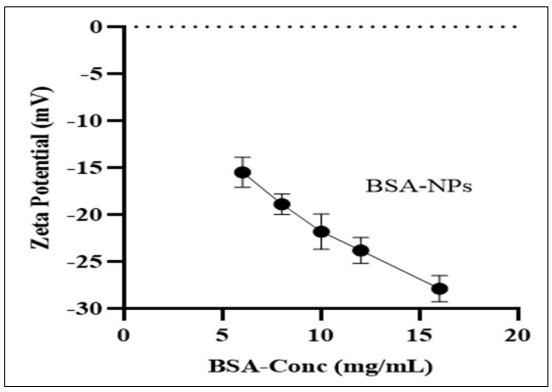

Figure 6.7. Zeta Potential of BSA-NPs against the BSA Concentration

Bovine serum albumin-based nanoparticles (BSA-NPs) were prepared by using the surfactant-mediated coacervation method. To stabilise the BSA-NPs Kolliphor HS15 was used, which helps to reduce aggregation and ensure a uniform size distribution. Furthermore, Ethanolic Epikuron® 200 solution is used to denaturated the albumin to facilitate in the formation of stable and uniform BSA-NPs, without the addition of a crosslinking agent. While this method is suitable for lipophilic molecules, it presents challenges for hydrophilic molecules.

Limitations of the surfactant-mediated coacervation method are as follows.

Limited Control Over Particle Size Distribution

The ability to precisely control the size of nanoparticles is crucial for their effectiveness and safety in pharmaceutical applications. However, current methods often result in a wide range of nanoparticle sizes within a single batch. This variability can compromise the performance and reliability of the nanoparticles, especially when uniform size is critical for their intended use.

Challenges in Scale-Up

Scaling the production of nanoparticles from a laboratory setting to industrial-scale manufacturing presents several challenges. Maintaining the quality and efficiency of the nanoparticles when produced in large quantities is a key issue. This is due to the complexity of managing factors such as temperature, mixing speed, and reactant concentration at an industrial scale, which are easily controlled in a small-scale laboratory environment.

Difficulty in Achieving High Drug Loading

Another challenge is achieving high drug loading. Incorporating a sufficient amount of a therapeutic agent into BSA-NPs is a crucial aspect of drug delivery. However, there are limitations to the amount of drug that can be loaded into nanoparticles without compromising their stability, size, and other physical properties. This poses a significant challenge in developing effective nanoparticle-based drug delivery systems by surfactant-mediated coacervation.

Potential for Burst Release

Controlled release of the therapeutic agent is often essential in drug delivery. However, nanoparticles may release the encapsulated drug too quickly, a phenomenon known as 'burst release.' This is particularly problematic when a sustained, gradual release is required for therapeutic effectiveness.

Risk of Batch-to-Batch Variability

Consistency in albumin nanoparticle production is critical to avoid batch-to-batch variability. Minor variations in production parameters, such as temperature, pH, or stirring speed, can lead to significant differences in the final product's characteristics. This batch-to-batch variability can affect particle size, drug loading capacity, and release properties, which can impact the overall efficacy and safety of the nanoparticles.

6.4 Preparation of BSA-NPs Using Ultrasonication Technology (US)

Ultrasonication is a process whereby ultrasound waves, typically in the frequency range of 20 kHz to 100 kHz, are applied to a liquid medium. US technology uses high-frequency sound waves to induce cavitation, which involves the formation, growth,

and collapse of bubbles in a medium. These bubbles, created by alternating pressure waves, generate intense thermal effects that lead to the denaturation of albumin.

The manufacturing of the BSA-NP requires the preparation of a solution of BSA at a concentration of 8 mg/mL, which contains Kolliphor HS15 (0.1% w/v) in sodium phosphate buffer (0.1M) at a pH of 8.0. Subsequently, to induce the thermal denaturation of albumin, was employed ultrasonication technology at a frequency of 100 kHz for 90 seconds to form BSA-NPs.

However, our observations indicated that the use of ultrasonication technology did not result in the formation of BSA-NPs. A schematic representation is shown in Figure 6.8.

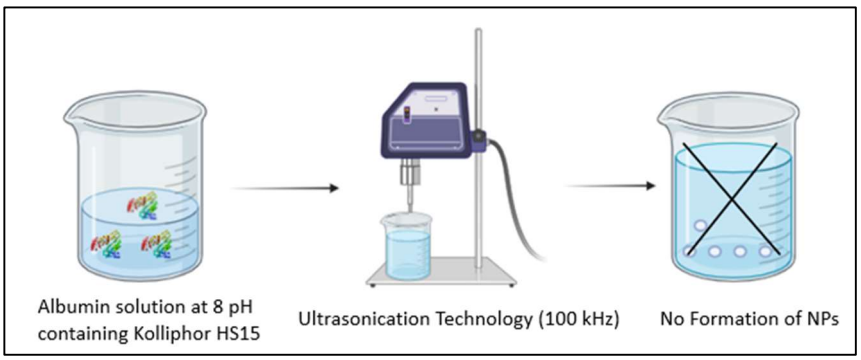

Figure 6.8. Schematic representation of the preparation of BSA-NPs by using Ultrasonication Technology

6.5 Microwave Assisted Technology (MW)

Instrumentation

The Microwave-assisted technology is a sophisticated device designed for conducting controlled chemical reactions using microwave energy. The detailed instrumentation of an microwave technology typically includes the following components [205].

Microwave Generator

This is the core component that produces microwave radiation. The generator is usually a magnetron that creates microwaves at a specific frequency, commonly 2.45 GHz.

Reaction Chamber

The chamber is made of microwave-transparent materials, like quartz and is designed to contain the reaction mixture. It is where the actual chemical reaction occurs under the influence of microwave radiation.

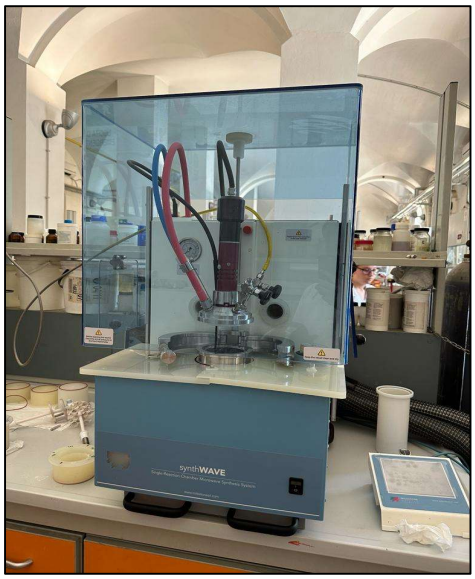

Figure 6.9. Microwave Single Reaction Chamber

Temperature Control System

This system monitors and regulates the temperature within the chamber. It often includes sensors like thermocouples sensor and may have a cooling system to prevent overheating.

Pressure Control System

Many microwave-assisted reactions occur under pressure. This system includes pressure sensors and a relief mechanism to maintain a safe pressure level inside the chamber.

Stirring Mechanism

To ensure uniform heating and reaction consistency, a magnetic stirrer or mechanical agitator is often included.

Control Unit

This is the interface for the operator, consisting of a display and input controls. It allows for the programming of microwave power, preparation time, temperature, and other parameters.

Safety Features

These include interlocks to prevent operation when the chamber is open, and shielding to prevent microwave leakage.

Gas Inlet/Outlet Ports

For reactions involving gases, the SRC includes ports for gas introduction and exhaust.

Cooling System

SRCs are equipped with a cooling system to manage the heat generated during reactions, which can be crucial for temperature-sensitive processes.

6.6 Mechanisms of Microwave-Assisted Technology

Microwave-assisted technology for the formulation of albumin-based nanoparticles employs a number of mechanisms to enhance the formation of nanoparticles. Firstly, microwaves generate heat by interacting with polar molecules such as water and functional groups present in albumin, ensuring rapidly and uniform heating throughout the reaction mixture. The introduction of stabilisers into the reaction mixture results in accelerated reactions due to microwave temperature, which in turn leads to the efficient formation of stable nanoparticles. Furthermore, the controlled heating permits precise control over preparation kinetics, thereby facilitating the design of nanoparticles with tailored properties. This encompasses the adjustment of power, irradiation time, and composition in order to regulate the processes of nucleation, growth, and stabilization. Furthermore, the efficient heat transfer and rapid kinetics associated with microwave-assisted technology can facilitate good drug loading and encapsulation within albumin-based nanoparticles [206,207].

6.7 Microwave Process Design

The process steps involved in operating a microwave single reaction chamber are as follows:

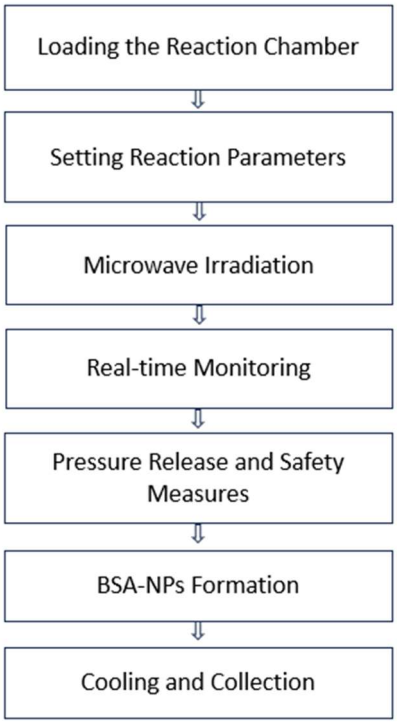

Figure 6.10. Process Steps Involved in Microwave Technology

The first step in the process is to load the albumin solution into the reaction chamber, which is commonly known as 'Loading the Reaction Chamber.' Following this, the reaction parameters are set, which involves programming specific conditions such as temperature, pressure, preparation time, and stirring potency, cooling temperature based on the process requirements. The chamber is then subjected to 'microwave irradiation'. Microwaves provide the energy to drive the preparation, resulting in faster preparation times and higher yields compared to conventional heating methods. The next step is 'Real-time Monitoring,' which is crucial for observing the progress of the preparation to ensure that it proceeds as expected. This monitoring may involve measuring temperature, ramp time, pressure, and preparation time. During the final stages of the process, safety measures are taken into account, including the release of excess pressure and the implementation of various safety protocols to prevent potential hazards. Finally, the BSA-NPs was

formed then the process concludes with 'Cooling and Collection of the formulation is cooled to a at room temperature, and the desired BSA-NPs are collected. Purification steps were carried out. This systematic approach ensures safe and efficient preparation of BSA-NPs.

The use of a microwave technology for the manufacture of BSA-NPs offers several significant advantages that improve the production process. Microwave heating temperature helps to denaturation of albumin and the rapid preparation times are a result of the direct interaction of the microwaves with the molecular components, which accelerates the kinetic energy of the molecules and speeds up the preparation of BSA-NPs [207]. Additionally, the precision of microwave-assisted technology enables controlled temperature settings, which is critical ensuring the formulation of the BSA-NPs [208].

6.8 Preparation of BSA-NPs Using Microwave-Assisted Technology

The tuned manufacturing process to obtain, BSA-NPs involves the preparation of a solution of BSA 8 mg/mL with Kolliphor HS15 (0.1% w/v) in a sodium phosphate buffer (0.1M) at a pH of 8.0, The thermal denaturation of albumin by employing a microwave technology is used under optimized conditions. The preparation of BSA-NPs was identified as maintaining a temperature of 80 °C, setting the ramp time 90 seconds to reach the set temperature and the preparation time was 12 minutes with 100 % the stirring potency. The microwave step facilitates the thermal denaturation of albumin and reduction of particle size of albumin nanoparticles. Finally, the BSA-NPs are purified by dialysis against 0.9% NaCl. A schematic representation is shown in Figure 6.11.

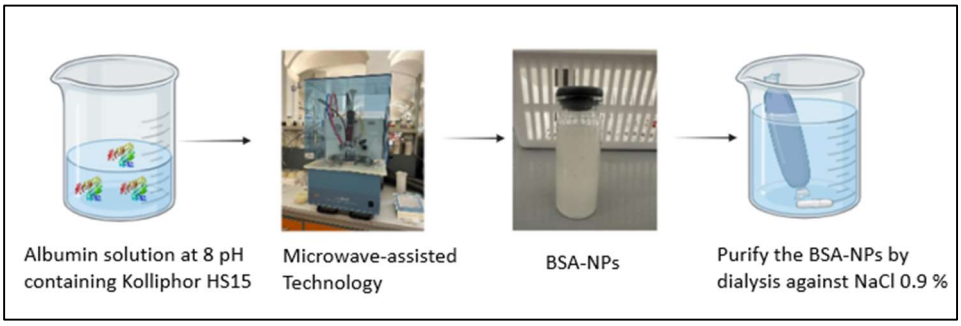

Figure 6.11. Schematic representation of the tuned preparation of BSA-NPs By Microwave-assisted Technology

6.9 Optimization of BSA-NPs Prepare by Microwave-Assisted Technology

I. Optimization of Ramp time

The ramp time is a vital parameter in the microwave technology, this parameter determines the time required to reach a set temperature. During process optimization, the relationship between ramp time (in seconds) and temperature is investigated. As shown in Figure 6.12, it is necessary to set an appropriate ramp time to reach the optimum temperature. In simple terms, increasing the ramp time will increase the temperature. It is important to carefully note the desired temperature and the corresponding ramp time set to achieve it.

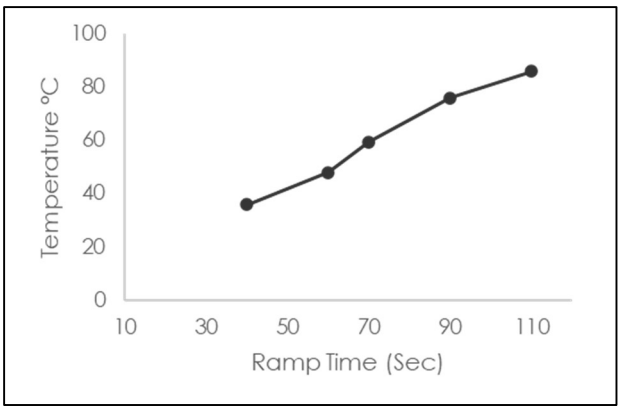

Figure 6.12. Optimization of Temperature (°C) against the Ramp Time (Sec)

II. Optimization Condition of Microwave Technology according to BSA Concentration

The optimization of microwave technology was started by varying the concentration of BSA. Two concentrations were chosen: 8 and 10 mg/ml. These concentrations were tested at three different temperatures: 60, 70 and 80 °C. The process was done for the different preparations 2, 5, 7, 10, 12 and 16 minutes. The aim was to prepare the formation of BSA-NPs, with good physical stability. This approach was designed to identify the optimal conditions of microwave technology for bovine serum albumin.

The experimental data indicates that at 60°C, BSA concentrations of 8 and 10 mg/mL in a sodium phosphate buffer (0.1 M) at pH 8.0 did not result in the formation of stable BSA nanoparticles (BSA-NPs) throughout the entire preparation time. It was observed that the thermal denaturation of albumin necessitates a higher

temperature for the formation of BSA-NPs. Consequently, the temperature was elevated to 70°C for both BSA concentrations in the PBS buffer. It was demonstrated that increasing both the temperature and the preparation time resulted in the formation of BSA-NPs. At 10 and 12 minutes of preparation time, the formation of BSA-NPs was observed. Further increasing the temperature to 80°C for both BSA concentrations demonstrated a similar pattern to that observed at 70°C. The size of the BSA-NPs was found to range from 50 to 60 nm. At 16 minutes of preparation time, was found that the particles were sediment after the colling of the formulation. In addition, the zeta potential was found to be consistently stable at a range of -28 to -32 mV for both BSA concentrations (8 and 10 mg/mL) and preparation times as shown in Figure 6.13. This indicates that the BSA-NPs are stable under these conditions. In conclusion the 70 °C and 80 °C at preparation times of 10 and 12 minutes show the stable BSA-NPs and are less likely to aggregate due to sufficient electrostatic repulsion between them, resulting in a stable colloidal system.

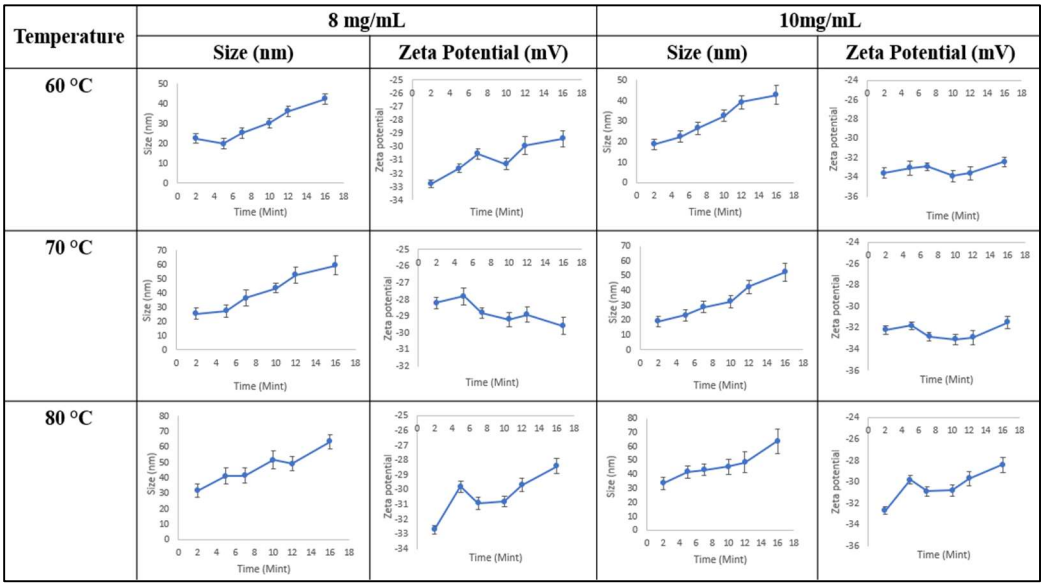

Figure 6.13. BSA Concentration Across Various Temperatures and Preparation Times

III. Optimization Condition of Microwave according to BSA Concentration containing Kolliphor HS15

Kolliphor HS15 is a crucial excipient in pharmaceutical formulations, particularly when combined with bovine serum albumin (BSA). It functions as a non-ionic

surfactant and emulsifier, enhancing the solubility of lipophilic drugs and increasing their bioavailability. Bovine serum albumin (BSA) acts as a carrier protein, stabilising the formulation by preventing drug aggregation and degradation. The combination of Kolliphor HS15 and bovine serum albumin (BSA) improves the stability of formulations. To optimise the BSA concentration with Kolliphor HS15 at 0.1% w/v as a stabilising agent was followed a methodology similar to that shown in Figure 6.11. Our aim was to study the formation of spherical BSA-Kolliphor nanoparticles, to assess of their surface charge and denaturation of the BSA structure.

The objective of this study was to investigate the stability of bovine serum albumin (BSA) in the presence of Kolliphor (0.1 w/v) in phosphate-buffered saline (PBS) buffer (0.1 M) at pH 8.0. The same methodology was employed as in the previous study. Two different concentrations of BSA (8 and 10 mg/mL) were employed to assess the thermal denaturation of BSA at various preparation times and temperatures. The study found that BSA-Kolliphor began forming nanoparticles at 70 °C, with the BSA-NPs exhibiting a size range of 60 to 70 nm after 10 and 12 minutes of preparation time. At 80 °C, after 10 and 12 minutes, the size of the BSA-NPs ranged from 85 to 95 nm. At both temperatures of 70 °C and 80 °C, with a preparation time of 16 minutes, the average particle size of the BSA-NPs exceeded 100 nm. In this instance, the nanoparticles exhibited sedimentation behaviour upon cooling. Furthermore, the zeta potential of BSA-Kolliphor NPs at a concentration of 8 and 10 mg/mL of BSA at various preparation times is shown in Figure 6.10. It can be observed that the zeta potential values remain relatively constant within the range of -28 to -32 mV.

The final conclusion of the optimisation process for developing a BSA-NPs formulation by microwave technology has been established. The results of the optimisation process indicate that the preparation time of 10 and 12 minutes at temperatures of 70 °C and 80 °C, respectively, resulted in the formation of BSA-NPs with good stability. In this instance, the thermal denaturation of albumin is employed to facilitate the formation of BSA-NPs. The results demonstrate that an 80 °C temperature at a 12-minute preparation time yields a more stable formulation over an extended period.

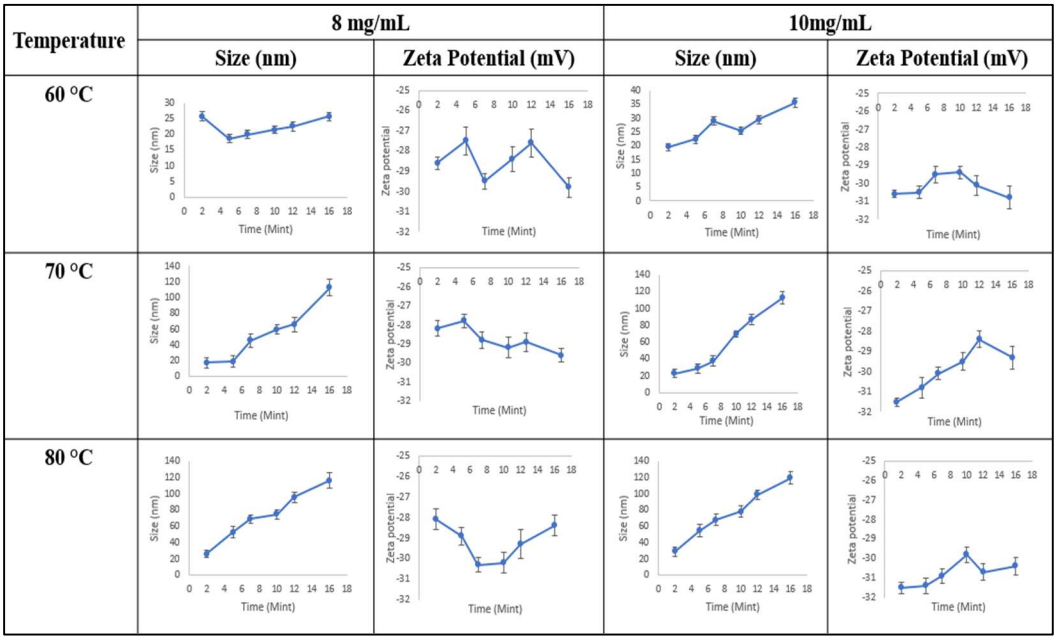

Figure 6.14. BSA Containing Kolliphor HS15 Across Various Temperatures and Preparation Times

It can be concluded that the optimal conditions for the preparation of BSA-NPs have been identified as maintaining a temperature of 80 °C, setting the ramp time to 90 seconds to reach the set temperature, and the optimised preparation time is 12 minutes with 100% stirring potency, as shown in Table 6.2.

Table 6.2. Optimise the Process Parameters of BSA-NPs Obtained by MW Technology

Process Parameters	Condition
Temperature	80 °C
Ramp Time	90 Second
Sample volume	10 mL
Preparation Time	12 Minutes
Stirring Potency	100

6.10 Preparation of BSA-NPs Using Combined Microwave and Ultrasonication Technology

The manufacturing of the BSA-NP involves the preparation of a solution of BSA 8 mg/mL containing Kolliphor HS15 (0.1% w/v) in sodium phosphate buffer (0.1M) at a pH of 8.0. Subsequently, to induce the thermal denaturation of albumin temperature is necessary. Begin by employing microwave technology with a ramp time of 90 seconds to heat the mixture to 76°C. Simultaneously, apply ultrasonication technology at 20.52 KHz with a power of 15W for 12 minutes.

However, our observations indicated that the use of combined microwave and ultrasonication technology did not result in the formation of BSA-NPs. A schematic representation is shown in Figure 6.15

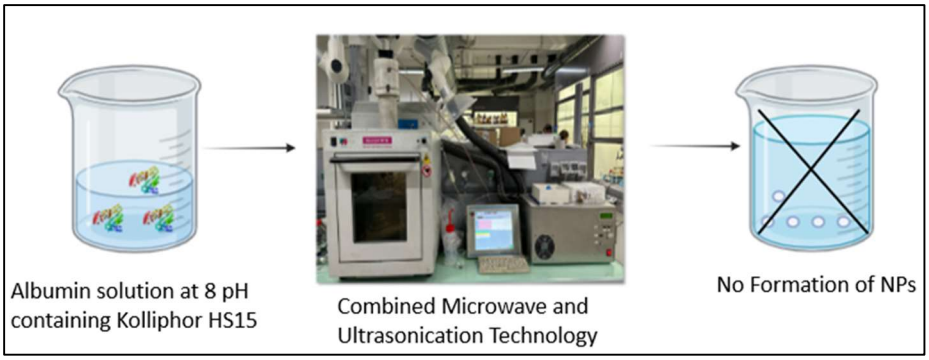

Figure 6.15. Schematic representation of the preparation of BSA-NPs by using Combined Microwave and Ultrasonication Technology (MW/US)

6.11 Physicochemical characterization of BSA-NPs

In our research, investigated the optimisation of blank albumin-based nanoparticles (BSA-NPs) using various manufacturing process. Initially, was employed the surfactant-mediated coacervation method, ultrasonication (US) technology, and microwave-assisted technology (MW) and combined microwave and ultrasonication technology (MW/US) to produce BSA-NPs. In the surfactant-mediated coacervation method, albumin is undergoing solvent denaturation using ethanolic Epikuron® 200 solution. Our observations indicated that the addition ethanolic Epikuron® 200 resulted in the formation of stable BSA-NPs, which were stabilized by the interface between the aqueous phase and albumin nanoparticles. The thermal denaturation of albumin is achieved through the ultrasonication (US), which induces temperature

and high-pressure changes within the solution, resulting in the formation of particles. Nevertheless, our observations indicated that this method did not result in the formation of BSA-NPs with small size. Microwave technology was employed to denature the albumin at a constant temperature and other parameter of microwave. This method was found to be effective for the formation of stable BSA-NPs. When the MW/US technology were combined to prepare BSA-NPs, the resulting particles precipitated, indicating no formation of BSA-NPs but only aggregates. In conclusion, the combination of the surfactant-mediated coacervation method, denaturation with organic solvent, and microwave technology by temperature denaturation provides an optimal approach for the preparation of BSA nanoparticles (BSA-NPs).

To determine the average diameter and polydispersity index of NPs formulations, the photon correlation spectroscopy was used in conjunction with the measurement of zeta potential through electrophoretic mobility. The analyses were conducted using the 90 Plus instrument (Brookhaven, NY, USA) with a fixed angle of 90 degrees and a temperature of 25°C. Before analysis, the samples were diluted with filtered water. The diluted samples were then placed into an electrophoretic cell, and a rounded 15 V/cm electric field was applied to determine the zeta potential.

In the surfactant-mediated coacervation method BSA is denaturated with ethanolic Epikuron® 200 (1% w/v) solution for the formation of BSA-NPs was optimized the BSA concentration of 8 mg/mL containing Kolliphor HS15 (0.1% w/v). The Blank-BSA NPs prepared using the surfactant-mediated coacervation method have a size of 180 nm. When prepared using microwave technology, they exhibit a size in between 85 to 95 nm, with a polydispersity index ranging from 0.26 to 0.28. Additionally, they show a negative zeta potential between -18 and -30, as presented in Table 6.3.

Table 6.3. Physicochemical Characteristics of BSA-NPs Obtained by Different Manufacturing Technologies

Methods	Average Diameter ± SD (nm)	PDI	Zeta Potential ± SD (mv)
Surfactant-mediated Coacervation Method	180.90 ± 6.85	0.28 ± 0.02	-18.80 ± 5.53
Ultrasonication (US)	No Formation of nanoparticles		
Microwave technology (MW)	92.69 ± 2.54	0.26 ± 0.01	-30.56 ± 3.91
Combined Microwave and Ultrasonication Technology (MW/US)	No Formation of nanoparticles		

Both the surfactant-mediated coacervation method and microwave technology effectively achieve the quality target attributes for the preparation of BSA-NPs.

6.12 Yield of Bovine Serum Albumin Nanoparticles (BSA-NPs)

To accurately calculate the yield of BSA NPs each empty vial was weight using an analytical balance and record the weights. Add exactly 1 mL of the BSA-NPs into each pre-weighed vial, ensuring precise measurement with a calibrated pipette. Seal the vials with parafin to prevent contamination. Freeze the vials overnight at -20°C or use liquid nitrogen for instant freezing. After freezing, transfer the vials to a lyophilizer and freeze-dried the samples until all water content is removed, resulting in a dry powder of BSA NPs.

Weigh the vials containing the dried powder using an analytical balance and record the weights. Determine the exact weight of the BSA-NPs powder by subtracting the weight of the empty vial from the weight of the vial with the dried powder. Calculate the initial weight of BSA used in the nanoparticle formulation process, which should

be calculated during the preparation stage. Finally, calculate the yield percentage of BSA-NPs was calculated using the formula:

Yield (%) = (Weight of BSA NPs Powder / Initial Weight of BSA Used) X 100

Table 6.4. Yield of BSA NPs Obtained by Different Manufacturing Technology

Manufacturing Technologies	BSA-NPs Powder weight after dialysis (mg)	Theoretical weight of BSA-NPs (mg)	Yield %
Surfactant-mediated Coacervation Method	13.2	14	94.28
Microwave-assisted Technology	7.7	8.8	83.50

The percentage yield of BSA-NPs using the surfactant-mediated coacervation method was found to be 94.28 %, while the yield using the MW technology was found to be 83.50 %.

6.13 Anova test of BSA-NPs

An ordinary two-way ANOVA test was used in Graph Pad Prism to assess the effect of two different preparation techniques surfactant-coacervation (CO) and microwave (MW) on the physicochemical properties of BSA NPs, including size, polydispersity index (PDI) and zeta potential (mV).

The results, as illustrated in Figure 6.16, use asterisks to indicate statistical significance levels.

Four asterisks ("****") represent a p-value less than 0.0001, which is considered to be extremely high statistical significance. Three asterisks ("***") indicate a p-value less than 0.01, which is indicative of very significant results.

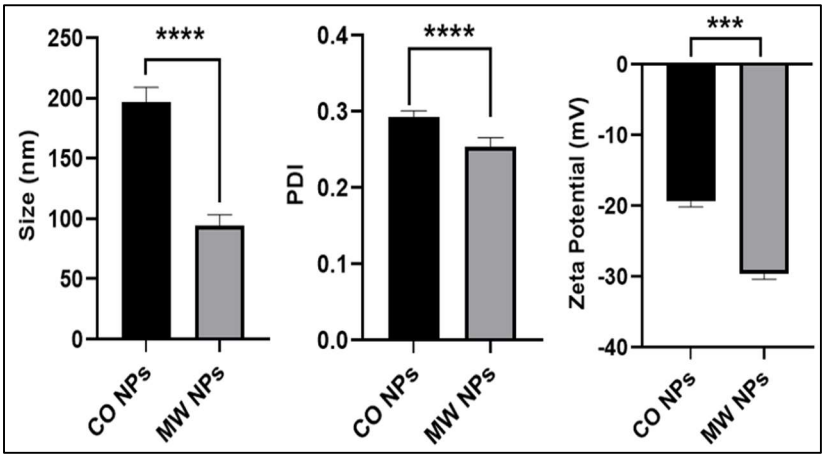

Figure 6.16. Physicochemical Characteristics Variation of BSA-NPs Obtained by Surfactant-mediated Coacervation Method (CO) and Microwave Technology (MW)

Particle Size

The surfactant-mediated coacervation method (CO) results in significantly larger albumin nanoparticles compared to the MW method. The mean particle size for CO NPs is approximately 200 nm, whereas for Microwave (MW) NPs it is about 92 nm. This difference is highly significant (****, $p < 0.0001$).

Polydispersity Index (PDI)

The CO method albumin nanoparticles with a higher PDI compared to the MW method. The PDI for CO NPs is around 0.29, while for MW NPs it is approximately 0.26. This difference is also highly significant (****, $p < 0.0001$).

Zeta Potential

The CO method results in nanoparticles with a more negative zeta potential compared to the MW method. The zeta potential for CO NPs is about -30 mV, whereas for MW NPs it is around -22 mV. This difference is significant (***, $p < 0.001$).

6.14 Scanning Electron Microscopy of BSA-NPs

Scanning Electron Microscopy (SEM) is a powerful imaging technique used to view the surface of samples at high magnifications. A focused beam of electrons is scanned across the specimen's surface, producing signals that contain information

about the sample's surface topography and composition. Here are the main components of SEM [209].

A SEM uses an electron gun to generate electrons that scan a sample, producing highly detailed images of its surface structure and composition. The core components that facilitate this process include electron lenses, a scanning system, detectors, and a display/computer system. The electron lenses are responsible for focusing the electron beam onto the sample with precision. The quality of the image resolution is significantly influenced by the lenses' ability to narrow the electrons into a fine beam. The focused beam is then systematically swept across the sample in a raster pattern by the scanning system, similar to the electron scanning method of a television screen, covering the sample's surface systematically. When the sample is exposed to the electron beam, it produces secondary electrons, backscattered electrons, and X-rays. These signals are essential for mapping the sample's topography, determining its atomic composition, and conducting elemental analysis. The SEM detectors are optimized to capture these signals effectively. Finally, the display and computer system play a crucial role in converting the detected signals into a clear image. This image clearly shows the surface structure and composition of the sample, allowing researchers and scientists to analyse materials with exceptional detail and accuracy. SEMs are powerful tools in material science, biology, and beyond. They offer microscopic views that are fundamental for scientific and industrial applications. The integrated operation of these components makes SEMs highly effective.

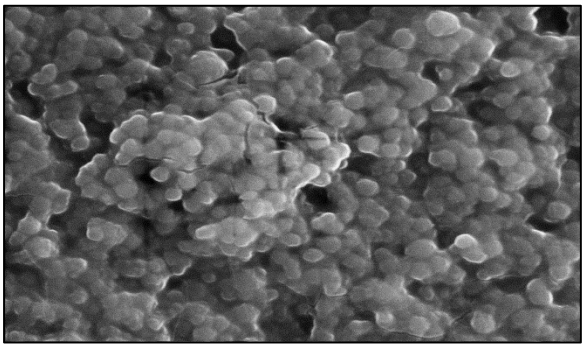

Figure 6.17. BSA-NPs Shape Determination by SEM

6.15 Fourier-Transform Infrared Spectroscopy of BSA-NPs

Fourier-Transform Infrared Spectroscopy is a technique used to obtain an infrared absorption or emission spectrum of a solid, liquid, or gas. It identifies chemical bonds in a molecule. Infrared (IR) spectroscopy is an analytical technique that uses light absorption to identify and quantify substances. The method involves passing light emitted from an infrared source through a sample to be analysed. The interaction between the light and the sample provides valuable information about the sample's chemical composition and structure [210].

The Michelson interferometer is a vital component of modern IR spectroscopy, especially in FTIR spectroscopy. It comprises a fixed mirror and a moving mirror that modify the path lengths of beams of IR radiation, resulting in an interference pattern. The pattern of light and dark bands, or fringes, encodes the spectral information of the light after it interacts with the sample. The Michelson interferometer generates an interference pattern that is recorded by a detector as the path difference between the two beams changes. This recorded signal does not immediately appear as a spectrum, but instead represents the interaction of light with the sample at different path differences. To convert this interference pattern into a usable absorption spectrum, a mathematical operation called the Fourier Transform is used. The process of transformation involves extracting spectral information, which reveals peaks corresponding to the vibrational frequencies of the molecules in the sample [211].

To achieve this, the sample is placed in a holder that is positioned in the path of the IR light, allowing the light to pass through the sample. The interaction between the sample and the IR light results in absorption at specific wavelengths, which is related to the molecular structure of the sample. Finally, the operation of FTIR spectroscopy is reliant on a computer. The computer controls the instrument, ensuring precise movement of the moving mirror and accurate collection of data by the detector. Additionally, it performs the complex Fourier Transform calculations required to interpret the interference pattern. The outcome is a detailed absorption spectrum that can be analysed to deduce the molecular composition and structure of the sample [210].

Bovine serum albumin: The spectrum shows a peak at around 3300 cm-1, which is indicative of an amide bond stretch. There are also peaks at around 1650 cm-1 and 1550 cm-1, which are indicative of carbonyl and amide groups, respectively.

The characteristic peaks of DPPC at 2857 and 2919 cm-1 corresponding to the CH2 symmetric and asymmetric stretching vibrations respectively, and at 1735 cm-1 attributed to C-O stretching are clearly detected in the spectrum of albumin nanoparticles, indicating the presence of phospholipids on the outer surface as shown in the Figure 6.18.

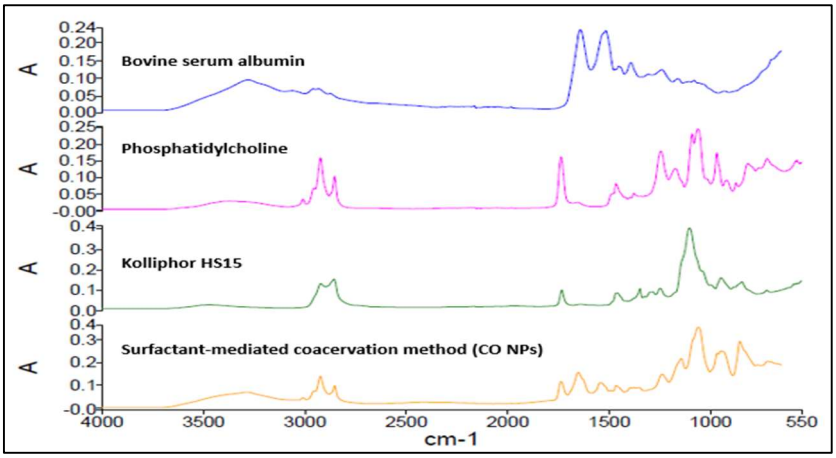

Figure 6.18 FTIR Spectra of BSA-NPs with Surfactant-mediated coacervation method

The characteristic peaks of Kolliphor HS15 spectrum shows a broad peak at around 2800 cm^{-1}, which is indicative of an O-H stretch. There is also a peak at around 1740 cm-1, which is indicative of a C=O stretch. The FTIR spectra for the nanoparticles prepared using microwave technology (MW-BSA NPs) demonstrate the successful interactions between BSA, Kolliphor HS15 as shown in the Figure 6.19.

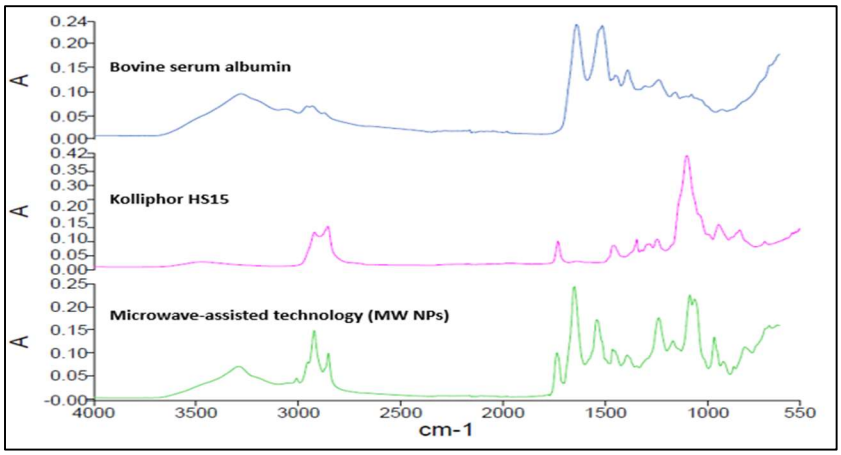

Figure 6.19 FTIR Spectra of BSA-NPs with Microwave-assisted technology

6.16 Release study of BSA fragments from Nanoparticles

In order to gain insight into the fragments of albumin within nanoparticle formulations was conducted release studies utilising the BCA Protein Assay Kit from Thermo Scientific and prepared an all type of BSA-NPs and placed them in a multi-compartment system designed for release studies. This system consisted of two phases: the donor phase and the receiving phase, separated by a dialysis membrane with a molecular weight cut-off of 14 kDa. In the donor phase, 1 mL of the blank nanoparticle formulation was added, while the receiving phase contained 1 mL of 0.1 M sodium phosphate buffer at 7.4 pH, at specific time intervals (0.5, 1, 1.5, 2, 3, 4, 5, and 6 hours), 1 mL of the receiving phase was withdrawn and replaced with fresh buffer.

All collected samples were initially treating by using the BCA Protein Assay Kit in order to quantify the released albumin. Subsequently, UV analysis was performed at 562 nm in order to further assess the extent of albumin fragments. The preparation of BSA standards should be initiated by diluting the standard solution into clean vials. It is recommended that the same diluent be used as that employed for the samples. The table below provides a guide to the creation of a series of BSA standards. Each 1 mL of BSA standard is sufficient to prepare a set of diluted standards for the range of concentrations indicated in the Table 6.5.

Table 6.5. BSA standard dilution scheme for the solution preparation

Vials	Volume of diluent	Volume and source of BSA	Final BSA concentration
A	700 µL	100 µL of stock	250 µg/mL
B	400 µL	400 µL of vial A dilution	125 µg/mL
C	450 µL	300 µL of vial B dilution	50 µg/mL
D	400 µL	400 µL of vial C dilution	25 µg/mL
E	400 µL	100 µL of vial D dilution	5 µg/mL

F	400 µL	0	0 = Blank

To Prepare BCA working reagent (WR), The total volume of WR required for the assay can be determined by applying the following formula

(standards + unknowns) × (replicates) × (volume of WR per sample) = total volume
The preparation of WR requires the mixing of 50 parts of BCA reagent A with one part of BCA reagent B (50:1, Reagent A: B). In the aforementioned example, a solution comprising 50 mL of reagent A and 1 mL of reagent B should be prepared.

It should be noted that upon the initial addition of reagent B to reagent A, a turbidity is observed that Surfactant mediately dissipates upon mixing, yielding a clear, green WR. It is recommended that a sufficient volume of the WR be prepared based on the number of samples to be assayed. The WR is stable for several days when stored in a closed container at room temperature.

100 µL of each standard added in the 1 ml of the reagent and vortex for 2 minutes and incubation for at 37 °C for 30 minutes this reaction takes place in the dark environment (light protection) and analysis the samples on UV at 562 nm and sample F used as blank. Analysis of the all-release sample with the same procedure.
The release of BSA fragments from the nanoparticle's formulation was analysed. It was found that the surfactant-mediated coacervation method nanoparticles (CO-NPs) and microwave-assisted nanoparticles (MW-NPs) had small release of BSA fragments. The release of BSA was observed to be below 4% over a six-hour period, as shown in Figure 6.20.

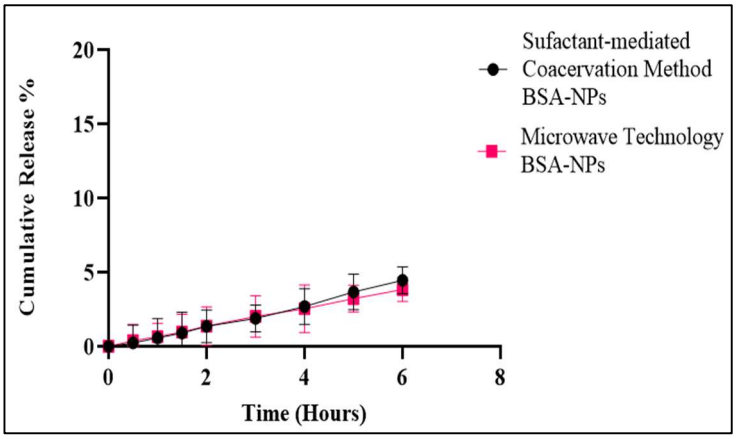

Figure 6.20 Release study of BSA Fragments from Surfactant-mediated Coacervation and Microwave Nanoparticles

6.17 Stability Study of BSA-NPs

The stability study results of BSA NPs prepared by the Surfactant-mediated Coacervation Method and Microwave Technology over a period of 90 days show significant differences. BSA-NPs prepared by the surfactant-mediated Coacervation Method start at a particle size of around 180 nm and gradually increase to around 205 nm, (12%) whereas those prepared by the Microwave Technology start at around 90 nm and remain stable around 110 nm in change of (18%).

In terms of Polydispersity Index (PDI), the surfactant-mediated Coacervation Method shows a slight decrease from 0.29 to 0.27, whereas the Microwave Technology maintains a more consistent PDI around 0.26, indicating a uniform particle size distribution.

In addition, the zeta potential for particles from the Surfactant-mediated Coacervation Method decreases slightly from -18 mV to -20 mV, while those from the Microwave Technology remain stable around -29 mV. Overall, BSA NPs prepared by surfactant-mediated coacervation method exhibit stability, lower PDI and stable zeta potential compared to those prepared by the microwave technology.

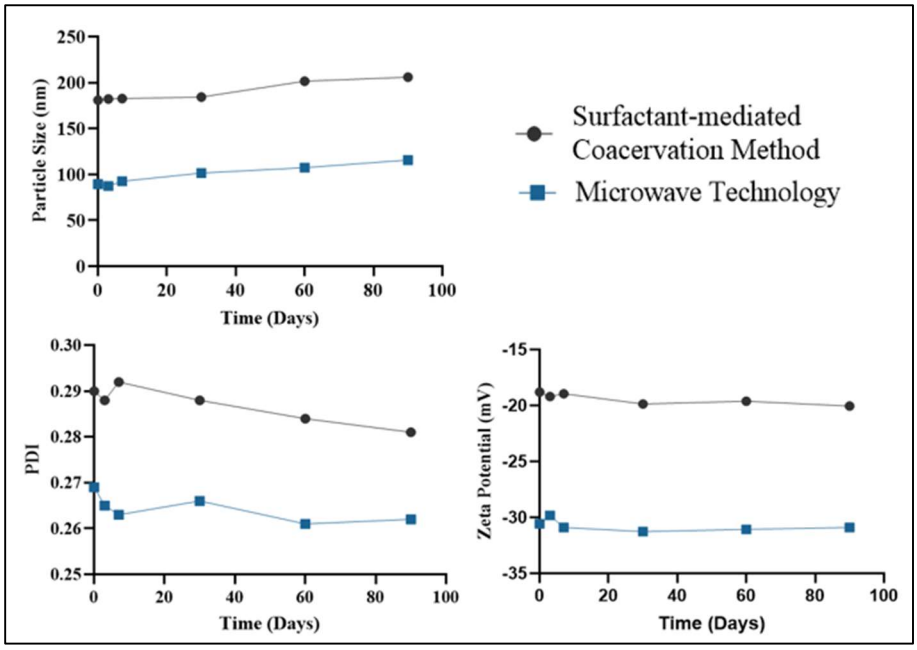

Figure 6.21. BSA-NPs Stability Study in Two Different Methods up to 90 Days at 4 °C

6.18 Preparation of Bovine serum albumin Nanocapsules (BSA-NCs)

Taking into the account challenge of loading hydrophilic molecules in albumin-based nanoparticles, the surfactant-mediated coacervation method and microwave-assisted technology, manufacturing methods are effective in encapsulating and stabilising lipophilic molecules, but it has limitations when dealing with hydrophilic molecules. To address this issue, a novel approach involving the use of Nanocapsules (NCs) has been developed. The NCs are designed to improve the encapsulation and stability of both lipophilic and hydrophilic molecules, overcoming the challenges of the surfactant-mediated coacervation method in handling such molecules.

In the manufacturing and optimization of bovine serum albumin nanocapsules, surfactant-mediated coacervation is not suitable for obtaining nanocapsules. Consequently, our research has focused on investigating advanced, green and sustainable manufacturing technologies namely the Ultrasonication technology (US), Microwave technology (MW) and Combined Microwave and Ultrasonication technology (MW/US). Our target is to prepare BSA-NCs and achieve the quality target attributes as discussed in Table 6.1.

6.19 Ultrasonication Technology (US)

The instrumentation of an ultrasonication technology involves several key components. Herein, they present a brief overview of the components of an ultrasound-based technology [212,213]

Figure 6.22. Instrument of Ultrasonication technology

Ultrasonic Generator/Power Supply

This component converts AC power from the mains to high-frequency electrical energy, typically in the ultrasonic range (20 kHz to 1 MHz), providing the electrical energy required for ultrasonication.

Transducer

The transducer is a crucial component that converts electrical energy into mechanical vibrations. It typically contains piezoelectric materials that vibrate at ultrasonic frequencies when an electric current is passed through them.

Horn or Sonotrode

The transducer is attached to the horn, also known as a sonotrode. produced by the transducer. It is designed to resonate at a specific frequency and can be made from various materials depending on the application's needs. The shape of the horn is often tapered to focus the ultrasonic energy.

Probe or Tip

The probe or tip is the component of the instrument that makes direct contact with the sample. It transmits ultrasonic energy into the material being processed. The design of the probe can vary depending on the application.

Control System

This includes the user interface and controls for adjusting the ultrasonic parameters like power, frequency, and duration of sonication.

Safety Features

This includes the equipment used to hold the ultrasound unit and ensure safety during operation, such as acoustic enclosures to reduce noise levels.

6.20 Process Characterization of Ultrasonication Technology

The technique of ultrasonic cavitation is widely used to reduce microscale emulsions to nano-size particles. Nanosized particles are produced using an ultrasonicator equipped with a piezoelectric probe. The probe emits high-frequency ultrasonic waves into the liquid, forming cavitation bubbles that grow until they become unstable and implode. This implosion generates intense local heat and pressure, creating jet streams of liquid that produce shear forces. These forces break down the larger particles in the emulsion into nanosized particles. Figure 6.23 depicts the sequence of events from bubble formation to implosion and subsequent particle size reduction.

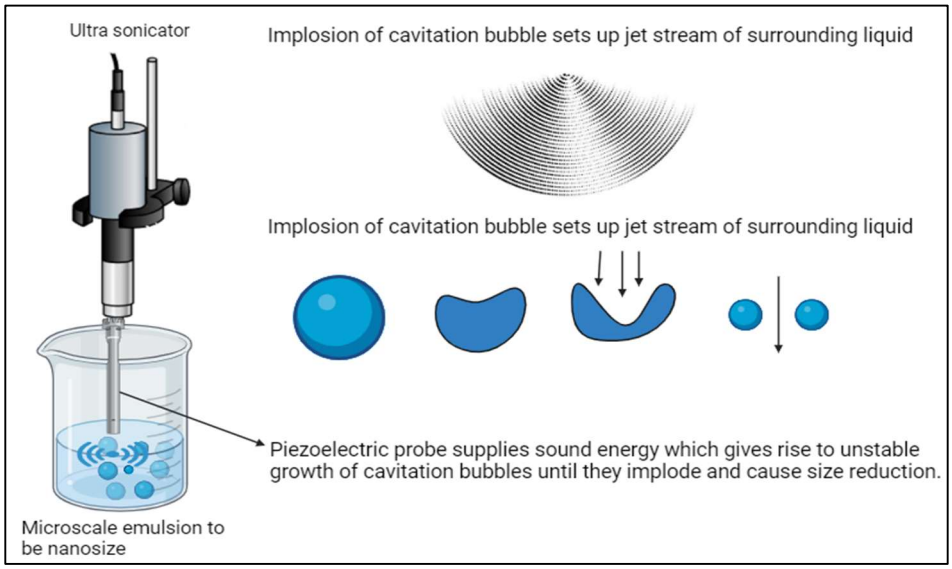

Figure 6.23. Schematic representation of the US technology

6.21 Mechanisms of Ultrasonication Technology

The utilisation of ultrasonication technology is of vital importance in the formation of oil-in-water (o/w) emulsification albumin nanocapsules. This is achieved by the

generation of high-intensity acoustic fields through the application of ultrasonic waves, which induces cavitation. This process results in the formation of microbubbles that implode, thereby producing high temperatures and pressures. This, in turn, gives rise to intense shear forces and microturbulence. These shear forces disrupt the oil phase into fine droplets, which are dispersed into the water phase. This process reduces droplet size to the nanoscale and promotes the formation of stable albumin nanocapsules. The introduction of microturbulence serves to enhance the mixing and homogenisation of the oil and water phases, thereby ensuring an even distribution of surfactants or stabilisers, which are responsible for stabilising the nanodroplets and preventing coalescence. The elevated temperatures and pressures facilitate the interaction between the oil phase and surfactants, enhancing their adsorption at the oil-water interface and stabilising the emulsified droplets, thereby enabling the formation of albumin nanocapsules with a well-defined core-shell structure.

Ultrasonication technology is used to prepare BSA-NCs, that offers several advantages for applications requiring precise nanocapsules manufacturing, such as drug delivery systems [214]. One of its primary benefits is the production of a homogeneous particle size distribution. This feature ensures that particles are consistently sized throughout a sample, which is critical for applications where uniformity directly impacts effectiveness, such as targeted pharmaceutical delivery. Furthermore, US enables precise control over particle size. This accuracy in determining particle dimensions is crucial in situations where BSA-NCs size can greatly affect the behaviour and effectiveness of the material, particularly in drug delivery systems. In the administration US technology can reduce agglomeration and it can be effective for drug loading, as it can encapsulate drugs within carrier [215]. In addition US technology enhances the physical stability and performance of colloidal suspensions by preventing particle agglomeration, making it particularly advantageous for designing more efficient in drug delivery systems [216]. This is a crucial aspect in maintaining the quality and consistency of pharmaceutical preparations. The process also offers significant scalability benefits. Its ability to be easily scaled up from small-scale laboratory settings to large-scale industrial production makes it an ideal technique for commercial applications, ensuring that

the benefits of precise particle measuring can be widely applied in the pharmaceutical industry [217,218].

Ultrasonication is a process that uses high-frequency sound waves to agitate BSA-NCs in a medium. However, it poses several challenges. Firstly, it requires a significant amount of energy, which can make the process costly and less energy-efficient. Additionally, the high energy input, combined with the heat generated. Achieving the desired results with US requires careful optimization of parameters such as frequency and duration, which adds to the complexity and time consumption [214].

6.22 Preparation of BSA-NCs by using Ultrasonication Technology

The process of BSA-NCs formulation begins with the preparation of BSA 8mg/mL in a sodium phosphate-buffer solution 0.1M at pH 8.0 containing Kolliphor HS15 (0.1% w/v). 500 µL of Miglyol 829 is added dropwise to this solution under magnetic stirring to form an oil-in-water (o/w) nanoemulsion. The o/w nanoemulsion was then subjected to ultrasonication at 100 kHz for 90 seconds facilitating the reduction of droplet size. NCs formulation was dialysis against the NaCl 0.9 % w/v to obtain purified BSA-NCs as shown below in Figure 6.24.

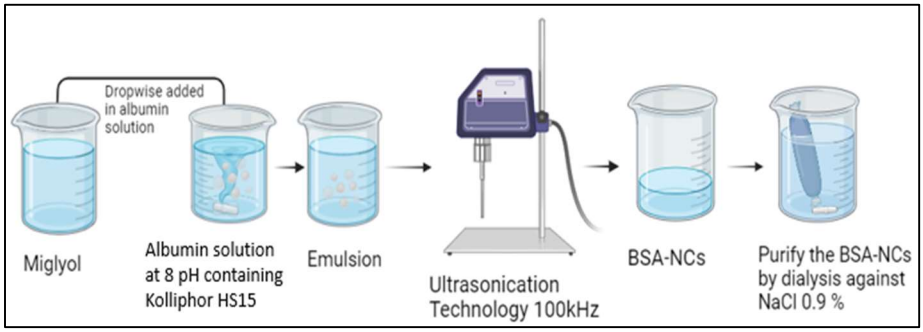

Figure 6.24. Schematic representation of the involved steps in BSA-NCs preparation by using Ultrasonication Technology

6.23 Condition Optimization of Ultrasonication Technology (US)

I. Optimization of Frequency Against BSA-NCs Size

The relationship between ultrasonication frequency (kHz) and the size of BSA-NCs (nm) is shown in Figure 6.25. It suggests that increasing the frequency of

ultrasonication from 10 kHz to 100 kHz results in a decrease in the average particle size of BSA-NCs. This indicates that higher frequencies of ultrasonication may be more effective at producing smaller nanocapsules. However, at 100 kHz, the average particle size is below 250 nm. Observed that when the frequency exceeds 100 kHz and the temperature rises above 80 °C, it is not suitable for the formation of BSA-NCs.

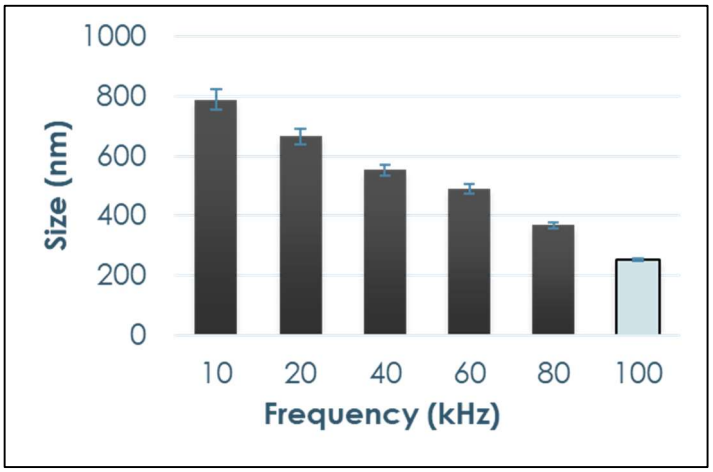

Figure 6.25. BSA-NCs Size *versus* the used US Technology Frequency

II. Optimization of Time Against Temperature

The thermal dynamics of the ultrasonication technology are mainly related to the rise in temperature as a function of time. In Figure 6.26 x-axis displays the independent variable, time, measured in seconds with intervals of 20, 30, 40, 60, 80, and 100 seconds. The y-axis represents the dependent variable, temperature (°C). To maintain the integrity of the BSA-NCs, it is crucial to keep the temperature within a specific threshold between 60°C to 85°C. This will favour the denaturation of albumin by temperature within the formulation. According to the optimal duration of ultrasonication, up to 90 seconds is recommended to maintain a temperature for albumin. For the albumin, caution must be taken when using ultrasonication beyond this time to avoid exceeding the critical temperature of 80°C.

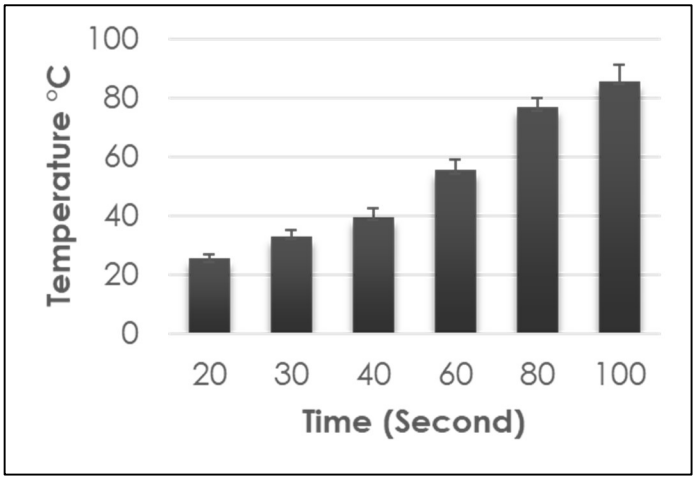

Figure 6.26. Changes In the Real Temperature During Time

II. Optimization of BSA-NCs Size by using Ultrasonication Technology

The relationship between the concentration of bovine serum albumin (BSA) and the size of BSA-NCs is investigated. As the concentration of BSA increases from 6 to 16 mg/mL, the size of the BSA-NCs also increases, indicating a direct correlation between BSA concentration and BSA-NC size. The use of a BSA concentration of 6 mg/mL in the nanocapsules formulation resulted in a size below 230 nm with a polydispersity index (PDI) of 0.21. At concentrations of 8 mg/mL, the BSA-NCs exhibited a size below 250 nm with 0.22 PDI. At 10 mg/mL, the BSA-NCs approached a size of 300 nm with 0.22 PDI. As the concentration increases to 12 mg/mL and 16 mg/mL, the size of the BSA-NCs approaches 320 to 420 nm with 0.20 PDI, indicating that they are large-size nanocapsules as shown in Figure 6.27. It was observed that for applications requiring smaller BSA-NCs in drug delivery systems, where a size below 260 nm might be desirable for improved cellular uptake and biodistribution, the optimal BSA concentration was 8 mg/mL. The optimal BSA concentrations were found to be 8 mg/mL, achieved through the use of ultrasonication technology. The concentrations of BSA-NCs produced by this method are consistently in the range of 240 to 260 nm with a 0.22 PDI.

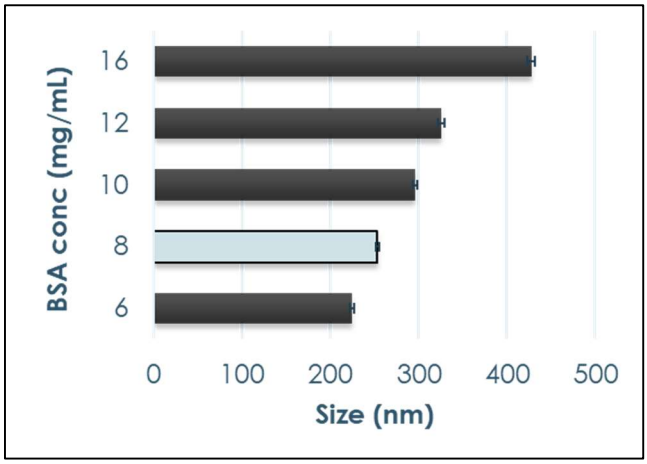

Figure 6.27. Size of BSA-NCs against the BSA Concentration

III. Zeta potential values

In this study, was employed a systematic approach to optimise the BSA concentration with respect to the zeta potential of the BSA-NCs. The observations indicate a clear trend: as the BSA concentration increases from 6 mg/mL to 16 mg/mL, there is a corresponding shift in the zeta potential towards more negative values. A corresponding change in zeta potential is observed, with values becoming increasingly negative, reaching -18 to -38 mV as illustrated in Figure 6.28. This correlation indicates that elevated BSA concentrations result in increased negative charge on nanocapsule surfaces. The hypothesis is that the enhanced negative charge leads to improved stability of the BSA-NCs due to increased electrostatic repulsion among the nanocapsules.

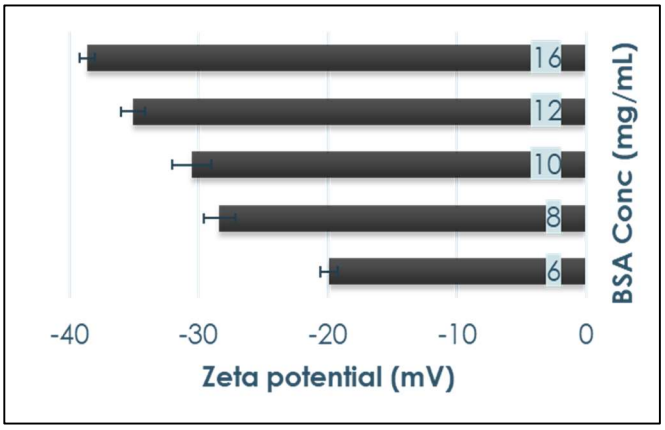

Figure 6.28. Changes in the Zeta Potential of BSA-NCs against the BSA Concentration

In conclusion, at a BSA concentration of 6 mg/mL, the formulation exhibits smaller nanocapsules in comparison to concentrations of 8 and 10 mg/mL. Nevertheless, the formulation with a BSA concentration of 6 mg/mL exhibited a lower zeta potential and was found to be unstable over an extended period. To address this issue, opted to use a concentration of 8 mg/mL, which provides greater physical stability for the formulation over time. The final optimization of the process for manufacturing BSA-NCs using the US technology has been established as shown in Table 6.6.

Table 6.6. Optimise Process Parameters of BSA-NCs Obtained by US technology

Process Parameters	Condition
Temperature	80 °C
Preparation time	90 Second
Sample volume	4.5 mL
Frequency	100 kHz

The US technology has been shown to be effective for the preparation of BSA-NCs under the optimized conditions was successfully achieved a desirable BSA-NC size of 253 nm at 8 mg/mL concentration accompanied by a low polydispersity index of 0.22 and the BSA-NCs exhibited an excellent zeta potential of -29 mV. The use of the US technology for manufacturing drug delivery systems is reliable for the BSA-NCs formulation but it does not meet our quality targets attributes as shown in Table 6.1. As a result, were continue to explore alternative manufacturing methods, with a focus on microwave technology (MW) to thermally denaturated the albumin by constant temperature.

6.24 Preparation of BSA-NCs by using Microwave Technology (MW)

Prepare a solution of BSA 8 mg/mL in a phosphate buffer 0.1M at pH 8.0 containing Kolliphor HS15 (0.1% w/v) to stabilize the BSA. Subsequently, Miglyol 829 is added dropwise under magnetic stirring condition to BSA solution to form an oil-in-water

emulsion. Then use of microwave technology with a proper optimized condition was identified as maintain a temperature 80 °C, setting the ramp time 90 second to reaching the set temperature and the preparation time was 12 minutes with 100 % the stirring potency. The addition of the microwave step facilitates the reduction of albumin nanoparticle size.

In our observations, the preparation of BSA-NC by using microwave technology, was found that an oil layer formed in the formulation. Based on our practical observation, was concluded that microwave technology is not suitable for the manufacturing of BSA-NCs.

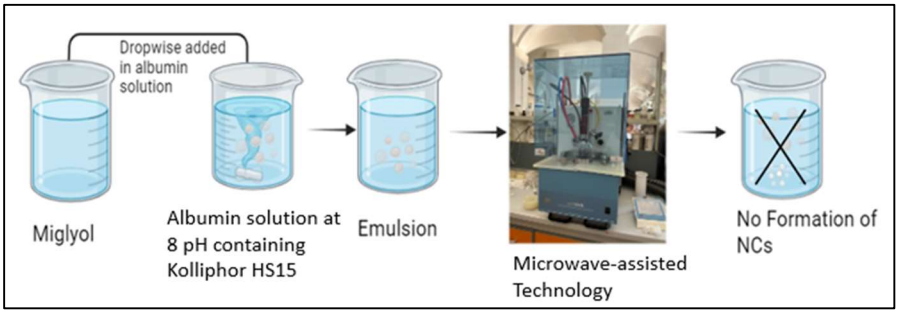

Figure 6.29. Schematic representation of the involved steps in BSA-NCs preparation by using Microwave-assisted Technology

As a results of microwave technology, the exploration of manufacturing technology that combined microwave and ultrasonication (MW/US) technology. This combined MW/US approach is a novel tool in drug manufacturing processes. Its application is expected to improve particle size control, efficiency and uniformity of BSA NCs. This strategy is not only beneficial for improving manufacturing processes, but also plays a crucial role in the continuous advancement of drug delivery methods.

6.25 Combined Microwave and Ultrasonication Technology (MW/US) Instrumentation

The combined microwave and ultrasonication (MW/US) technology are a challenging instrumentation setup typically used for advanced materials processing [219]. This setup integrates two key components as shown in Figure 6.30.

Microwave (MW) technology

Microwave technology generates microwave radiation to heat materials. It consists of a magnetron to generate the microwaves, a waveguide to direct the microwaves, and

a microwave cavity or chamber in which the sample is placed. The system is designed to provide controlled and uniform heating.

Ultrasonication (US) technology

The US technology involves an ultrasonic generator that produces an electrical signal, a transducer that converts the electrical signal into mechanical vibrations, and sometimes an ultrasound chamber or probe to deliver ultrasonic waves to the sample. US is a highly effective technology that utilizes high frequency sound waves (ultrasound) to achieve various processes such as emulsification, dispersion, and cell disruption.

Figure 6.30. Combined Microwave and Ultrasonication Technology (MW/US)

The combination of microwaves and ultrasound provides enhanced processing capabilities to prepare albumin nanocapsules. Microwaves uniformly and volumetrically heat the sample, while ultrasound improves mass transfer, mixing and homogenizing. In a combined MW/US, these components are integrated to allow simultaneous or sequential application of microwaves and ultrasonication. To achieve this, use a chamber specifically designed to accommodate both microwave irradiation and ultrasound waves. The chamber must have controls that allow for the independent or combined adjustment of the parameters of each technology [220].

The principles and effects of two distinct technologies used to enhance preparation processes: MW and US. Microwave technology utilizes electromagnetic radiation with frequencies up to 300 GHz, which affects microwave-absorbing materials,

typically polar molecules or those in solvent-free preparation, through dielectric heating and specific thermal effects [221]. Ultrasonication employs sound waves in the frequency range of 20-500 kHz in aqueous media to facilitate preparation of BSA-NCs through cavitation and mechanical effects [222]. The flowchart below converges to show in Figure 6.31, that both technologies result in multiple beneficial effects such as increased reaction rates, improved conversions, and enhanced heat and mass transfer, making them valuable in various applications for their efficiency and effectiveness.

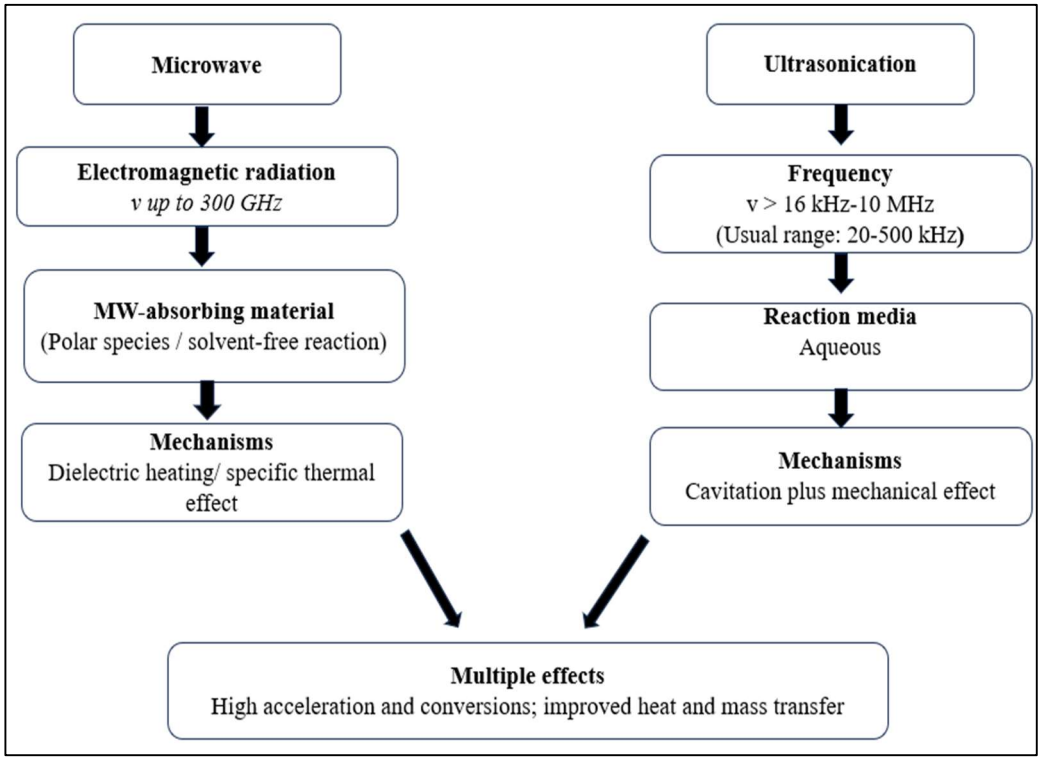

Figure 6.31. Flow Chart of Main Properties of MWUS

6.26 Process of Combined MW/US technology

The process steps involved in operating a MWUS are as per the Figure 6.32.

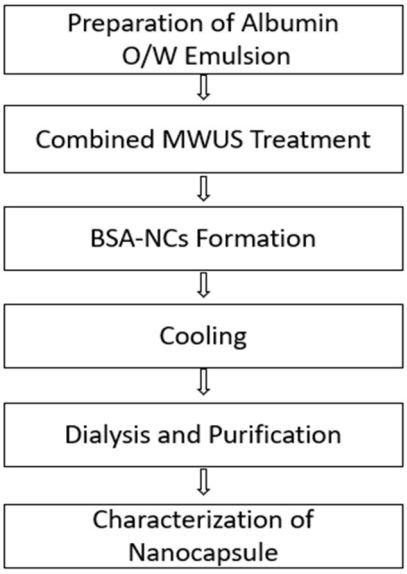

Figure 6.32. Process Steps involved in combined MW/US

The manufacture of BSA-NCs is a multi-step process. First, a BSA in a PBS buffer solution containing Kolliphor HS15 is prepared, then add Miglyol 829 to form an o/w emulsion under magnetic stirring condition. The emulsion is then simultaneously treated with a combined microwave and ultrasonication (MWUS) technology to form the formation of BSA-NC. Exploring thermal denaturation of albumin to form Nanocapsules. After this treatment, the BSA-NCs are cooled to allow to stabilise. The next step involved dialysis and purification, by using a dialysis membrane to remove any unencapsulated substances and impurities to ensure the purity of the Nanocapsules. Finally, the BSA-NCs are characterised by various analyses to determine their physical properties, such as size, surface charge and encapsulation efficiency. This comprehensive process is critical to the successful manufacturing of high quality BSA-NCs.

The use of the combined MW/US for preparing BSA-NCs offers several advantages. that improve pharmaceutical manufacturing processes. This innovative approach enhances production efficiency, ensuring effective encapsulation of drug within the BSA-NCs. One of the main advantages of this method is the precise control over nanocapsules size, which is crucial for the consistent delivery of therapeutics. The

controlled temperature during preparation process to thermally denaturated of BSA and contributes to the improved homogeneity of the final product, ensuring uniform distribution of the active ingredients. Additionally, the combine MW/US technology enables the scalability and its application to large-scale manufacturing without compromising quality, making it a practical option for commercial pharmaceutical applications.

The preparation of BSA-NCs using a combined MW/US presents several key limitations.

Complexity of Equipment

The preparation of BSA-NCs using a combined microwave-ultrasound (MW/US) system necessitates the utilisation of highly specialised equipment. The complexity of the process arises from the integration of microwave and ultrasonication technology.

Optimization Challenges

The process of optimising the parameters for the formation of BSA-NCs represents a significant challenge. The process entails the adjustment of a multitude of variables, including microwave power, ultrasound frequency, temperature, and preparation time, in order to achieve the desired characteristics of BSA-NCs. It is evident that each parameter can influence the outcome, and thus, the identification of the optimal combination necessitates a profound comprehension of the underlying process and a multitude of trial-and-error experiments. The intricate and time-consuming nature of this optimisation process represents a substantial barrier to practical implementation.

Non-Uniform Heating

A significant technical challenge associated with the combined MW/US process is the non-uniform heating of the system, which can result in an uneven temperature distribution within the BSA-NC formulation. This inconsistency can result in the formation of BSA-NCs with variable sizes and shapes, which may subsequently affect their quality, efficacy, and physical stability.

Design and Cost Equipment

The equipment required for the combined MW/US process is often custom built or involves sophisticated components, which drives up the initial investment and ongoing maintenance costs. Such financial constraints can potentially restrict the

accessibility of this technology, particularly for smaller research institutions with limited budgets. The high cost of the equipment, in addition to the necessity for specialised facilities to operate it, can be a significant barrier to the widespread adoption of the technique.

6.27 Preparation of BSA-NCs by using combined MW/US Technology

Prepare a solution of a BSA 8 mg/mL containing Kolliphor HS15 (0.1% w/v) in phosphate buffer (0.1M) at pH 8.0. Subsequently, add Miglyol 829 dropwise to the BSA solution under stirring conditions to form an oil-in-water nanoemulsion. To denaturation of albumin by thermal, begin by employing microwave technology with a ramp time of 90 seconds to heat the mixture to 76°C. Simultaneously, apply ultrasonication technology at 20.52 KHz with a power of 15W. Allow the preparation to proceed for 12 minutes to obtain BSA-NCs. Finally, purify the BSA-NCs by dialysis against 0.9% NaCl for 1 hour.

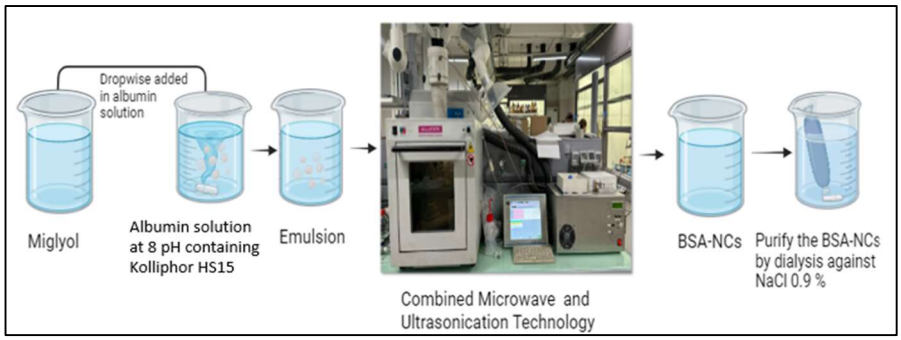

Figure 6.33. Schematic representation of the involved steps in BSA-NCs preparation by using MW/US

6.28 Condition Optimization of MW/US

I. Optimization of Ramp Time

The ramp time is a crucial factor in the combined MW/US as it specifies the duration needed to attain a set temperature. Optimization processes require a thorough examination of the correlation between ramp time and temperature. The ramp time optimization is similar to the MW as previously discussed in Figure 6.12.

II. Optimization of Nanocapsule Size by using MW/US

A direct correlation can be observed between the concentration of BSA and the size of BSA-NCs. As the concentration of BSA is increased from 6 to 20 mg/mL, there is a corresponding increase in the size of the BSA-NCs. Specifically, at concentrations between 6 and 10 mg/mL, the BSA-NCs are relatively small nanocapsules, with sizes under 200 nm and a PDI of 0.21. However, as the concentration reaches 12 mg/mL, the size increases to approximately 220 nm with 0.20 PDI. It is noteworthy that at higher concentrations of BSA 16 to 20 mg/mL, the BSA-NCs exhibit a size range of 380 to 450 nm with a 0.21 PDI. This trend indicates that higher BSA concentrations result in the formation of larger-sized BSA-NCs, as illustrated in Figure 6.34.

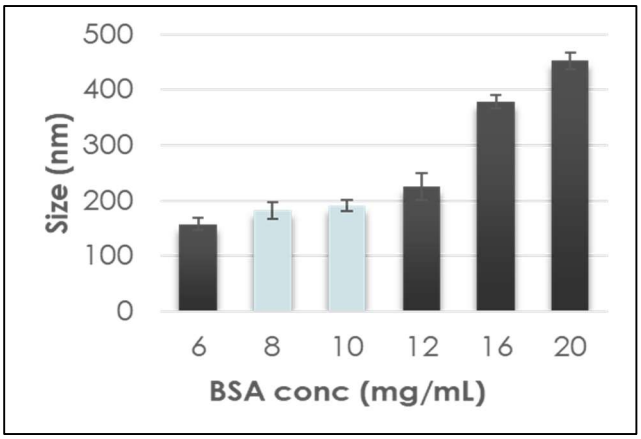

Figure 6.34. Size of BSA-NCs against the BSA Concentration

III. Optimization of Zeta Potential Values

This study systematically optimised the concentration of BSA to determine its effect on the zeta potential of BSA-NCs. The results show a clear trend, as the BSA concentration increases from 6 mg/mL to 20 mg/mL, the zeta potential becomes more negative, ranging from -18 to -40 mV. This correlation suggests that higher BSA concentrations lead to an increased negative charge on the nanocapsule surfaces. It is hypothesized that the enhanced negative charge contributes to the improved stability of the BSA-NCs. This is due to increased electrostatic repulsion between particles. This finding is significant as it provides insights into the mechanisms that govern in the stability of these systems. It can guide the development of more

efficient and stable BSA-NCs. It is concluded that a BSA concentration between 8 and 10 mg/mL is optimal for the preparation of BSA-NCs, as demonstrated in Figure 6.35.

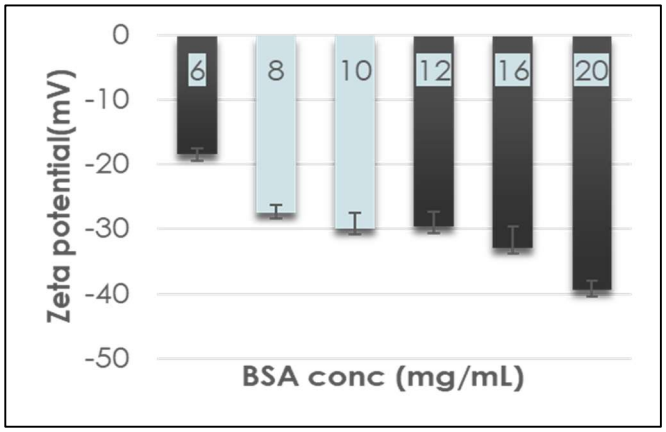

Figure 6.35. Changes in the Zeta Potential of BSA-NCs against the BSA Concentration

In conclusion, at 8 and 10 mg/mL, the BSA-NCs exhibited sizes below 200 nm and demonstrated stable zeta potentials greater than -27 mV. Conversely, while a concentration of 6 mg/mL also resulted in sizes below 200 nm, the zeta potential is below -18 mV and it's not achieved our quality target attributes.

IV. Optimization of Preparation Time

The relationship between the preparation time are two key properties of BSA-NCs, size and zeta potential. The graph was discussed such as into two distinct segments. The size of the BSA-NCs is plotted on the left y-axis as a function of the preparation time, indicated in minutes (min), on the x-axis. The right-hand part of the graph shows the zeta potential of these BSA-NCs, expressed in millivolts (mV), also plotted against preparation time. This clear and concise dual-part of figure 6.36, effectively demonstrates the changes in both size and zeta potential of the BSA-NCs over time. Optimal conditions for the formation of stable BSA-NCs are achieved when the preparation time is increased from 2, 5, 8, 10 and 12 minutes, the observed that the 12 minutes preparation time is decreases the BSA-NCs size below 200 nm and a more negative zeta potential -28 mV. Preparation time shorter than 12 minutes lead to larger nanocapsule size and lower negative zeta potential, which may not be optimal for the desired application of these BSA-NCs. At 16 minutes of preparation time of BSA-NCs shows the precipitation. Indicating an overtime preparation condition that

leads to nanocapsule aggregation. The size and zeta potential value of BSA-NCs can have a critical impact on their behaviour in biological systems, including their stability, distribution, and interaction with target cells or tissues.

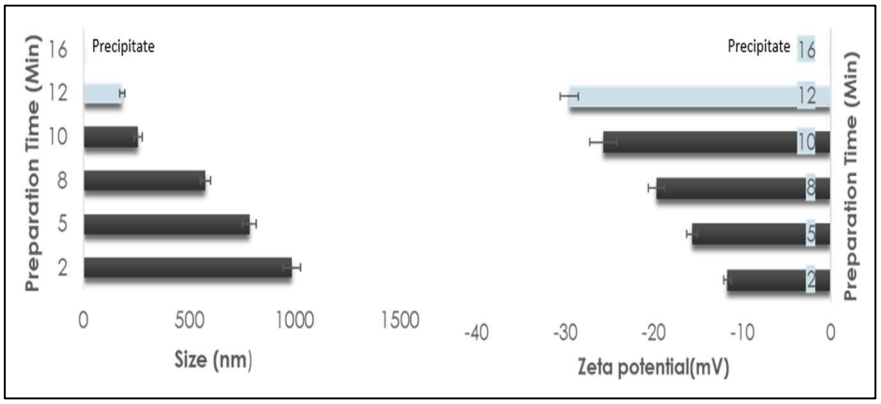

Figure 6.36. Size and Zeta Potential of BSA-NCs against the Preparation Time

The final optimized process for the manufacturing of BSA-NCs using the combined microwave and ultrasonication (MW/US) technology has been successfully developed. Through this process, the optimal conditions for the preparation of BSA-NCs have been precisely identified. These conditions include maintaining a temperature of 76°C, a ramp time of 90 seconds is to reach the set temperature in the MW. While simultaneously applying an US. The specific settings for ultrasound are a frequency of 20.52 kHz and a power of 15 watts. In addition, the optimised preparation time for this process was also determined to be 12 minutes. The parameters as shown in the Table 6.6. This careful maintaining of temperature, US frequency and power, ramp time and preparation time ensures the efficient and effective formation of BSA-NCs using the MW/US method.

Table 6.6. Optimize Process Parameters of BSA-NCs Obtained by Combined MW/US

Parameters	Condition
Temperature	76 °C
Ramp Time	90 Second
Sample volume	30 mL

Preparation Time	12 Minutes
Ultrasound frequency	20.52 kHz
Watts	15 W

The combined MW/US technology has proven to be highly effective in the preparation of BSA-NCs particularly under the optimized conditions outlined in this study. The BSA-NCs with a desirable size of 182 nm. Additionally, these NCs exhibited a good polydispersity index of 0.23, indicating a narrow size distribution and uniformity in the size of the NCs. Notation, the zeta potential of these BSA-NCs was -27 mV value also indicates a good degree of stability in the NCs formulation. The combination of MW/US technology provides a synergistic effect, resulting in improved control over the formation process of BSA-NCs. This method is highly reliable and suitable to prepare nanocapsules stable over an extended period, offering optimal characteristics in terms of particle size, polydispersity (PDI), zeta potential (mv), and stability. These attributes are critical for manufacturing an efficient drug delivery system. The MW/US technology meets our quality target attributes successfully. The integration of MW/US technologies has significantly improved the precision and effectiveness of preparing BSA-NCs. This combination allows for a more controlled and efficient manufacturing process.

In our investigation of various manufacturing technologies for the preparation of bovine serum albumin nanocapsules (BSA-NCs), was initially employed a surfactant-mediated coacervation method that is not suitable for the BSA-NCs. The results demonstrated that both US technology and the combined MW/US technology manufactured the stable and well-formed BSA-NCs over time. In contrast, MW technology was found to be ineffective, as it resulted in the formation of an oily layer. This discussion will present the results and insights gained from these experiments, as detailed below.

6.29 Physicochemical Characterization of BSA-NCs

Based on our experimental data, the optimization of various manufacturing processes of albumin nanocapsule, as illustrated in Table 6.7. Our findings indicate that ultrasonication is a relatively reliable method for preparing BSA-NCs. This technique shows excellent polydispersity, consistently below 0.22 and maintains a stable zeta potential -29 mV over time. The particle size produced by this method ranges from 220 to 250 nm. Although these dimensions did not meet our initial quality target attributes. Consequently, exploration of a combined technology of MW/US. This technology demonstrated significant potential and reliability for drug delivery systems. It consistently produced particles smaller than 200 nm, exhibited good polydispersity 0.23, and maintained a negative zeta potential -27 mV. Therefore, that the MW/US technology successfully meets our quality target attributes.

Table 6.7. Physicochemical Characterization Of BSA-NCs Obtained by Different Manufacturing Process

Manufacturing Process of BSA-NCs	Average Diameter ± SD (nm)	PDI	Zeta Potential ± SD (mv)
Ultrasonication Technology (US)	238.20 ± 4.12	0.22 ± 0.02	-29.32 ± 2.85
Combined Microwave and Ultrasonication (MWUS)	182.51 ± 2.80	0.23 ± 0.01	-27.85 ± 5.41

6.30 Yield of Bovine Serum Albumin Nanocapsule (BSA-NCs)

To accurately calculate the yield of BSA NCs begin by weighing each empty vial using an analytical balance and record the weights. For the preparation of BSA-NCs in vials, add 10 mg of trehalose to the vials before lyophilization to protect and stabilize the BSA-NCs. Due to the oil content in the NCs formulation, a cryoprotectant is needed for effective lyophilization. Add exactly 1 mL of the BSA-NCs into each pre-weighed

vial, ensuring precise measurement with a calibrated pipette. Seal the vials with paraffin to prevent contamination. Freeze the vials overnight at -20°C or use liquid nitrogen for instant freezing. After freezing, transfer the vials to a lyophilizer and freeze-dried the samples until all water content is removed, resulting in a dry powder of BSA NCs, The Procedure as already discussed in section 6.11

Table 6.8. Yield of BSA NCs Obtained by Different Manufacturing Technologies

Manufacturing Technologies	Final Powder weight after dialysis (mg)	Theoretical weight of BSA-NPs (mg)	Yield %
Ultrasonication Technology	15.8	19.11	82.67
Combined Microwave and Ultrasonication Technology	18.0	19.11	95.18

The percentage yield of BSA-NCs using the ultrasonication (US) technology was found to be 82.67 %, while the yield using the combined microwave and ultrasonication (MW/US) technology was found to be 96.18 %.

6.31 ANOVA Test of BSA-NCs

An ordinary two-way ANOVA test performed by Graph Pad Prism to comparing the effects of two different manufacturing methods (Ultrasonication, Combined MWUS) on the physicochemical characteristics of BSA-NCs. These characteristics are Size, Polydispersity Index (PDI), and Zeta Potential(mV). The statistical significance is indicated by asterisks as indicated in the Figure 6.37.

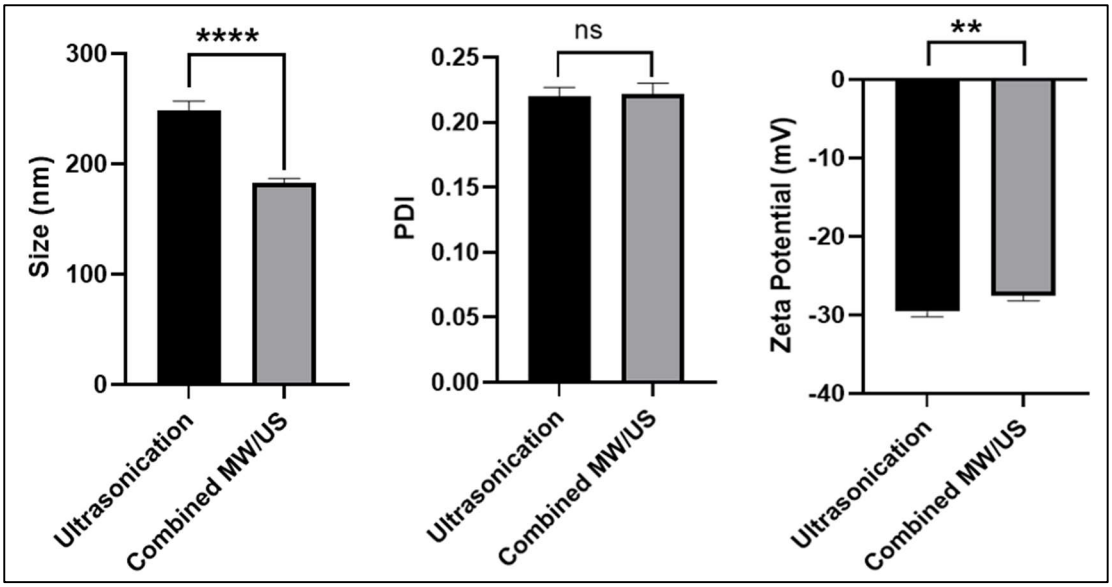

Figure 6.37. Physicochemical Characteristics Variation of BSA-NCs Obtained by Using the Different Manufacturing Methods

Particle Size

All comparisons between the manufacturing methods (US vs. Combined MW/US) show extremely statistically significant differences with $p < 0.0001$.

Polydispersity (PDI)

The comparison between US technology and Combined MW/US methods shows an extremely statistically significant difference not significant. (ns)

Zeta Potential value

The comparison between US technology and MW/US methods shows a very statistically significant difference with $p < 0.0069$.

6.32 Scanning Electron Microscopy (SEM) of BSA NCs

The scanning electron microscopy (SEM) analysis shows that the BSA-NCs have a spherical shape and it can be manufactured at the nanoscale to improve delivery efficiency and targeting. Figure 6.38 includes annotations indicating particle size measurements in nanometre.

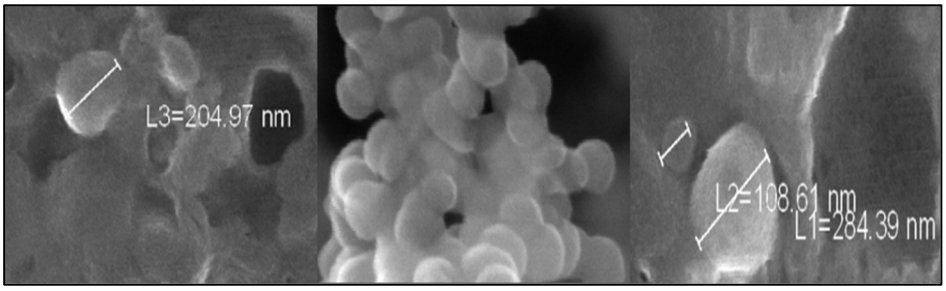

Figure 6.38. BSA-NCs Particle Shape Determination by SEM

The ultrasonication nanocapsules (US NCs) and combined microwave and ultrasonication nanocapsule (MW/US NCs) are analysis by scanning electron microscopy (SEM), elucidated specific dimensional parameters, with a notable dimension measured at 204 and 284 nm, which serves to emphasise the nanoscale magnitude of the particles. The SEM image provides essential insights into the physical characteristics of the BSA-NCs, which are crucial for understanding their interactions within biological environments and for ensuring in-process quality control measures throughout their manufacturing.

6.33 Fourier-Transform Infrared Spectroscopy (FTIR) of BSA-NCs

The Fourier transform infrared (FTIR) spectra display the absorption spectra of bovine serum albumin (BSA), Kolliphor HS15, and BSA nanocapsules (BSA-NCs) prepared using ultrasonication technology (US-BSA NCs) and combined microwave and ultrasonication (MW/US-BSA NCs). The characteristic peaks of Kolliphor HS15 spectrum shows a broad peak at around 2800 cm-1, which is indicative of an O-H stretch. There is also a peak at around 1740 cm-1, which is indicative of a C=O stretch. The FTIR spectra for the nanocapsules prepared using both technologies demonstrate the successful detection of the BSA and Kolliphor HS15 as shown in the Figure 6.39.

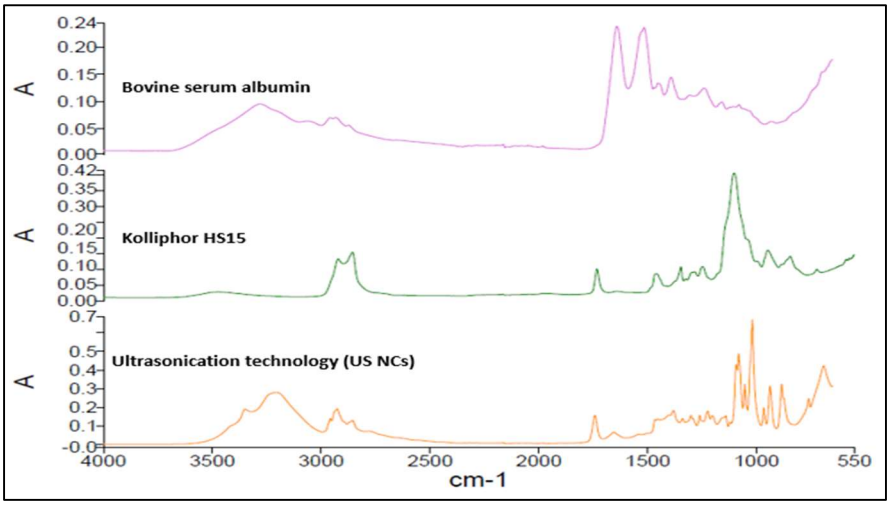

Figure 6.39. FTIR Spectra of BSA-NCs with Ultrasonication Technology (US)

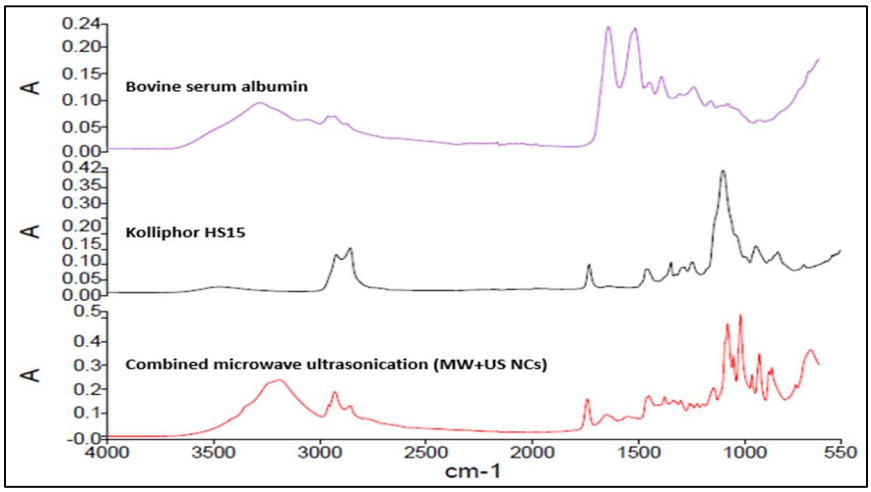

Figure 6.40. FTIR Spectra of BSA-NCs with Combined Microwave Ultrasonication (MW/US)

6.34 Release study of BSA Fragments from Nanocapsule

The release of BSA fragments from the nanocapsule was analysed, and it was found that both the Ultrasonication technology nanoparticle (US-NC) and combined microwave and ultrasound nanocapsule (MW/US) had a release of BSA fragment. The release of BSA fragment was release to be below 2.60% over a six-hour period, as illustrated in Figure 6.41.

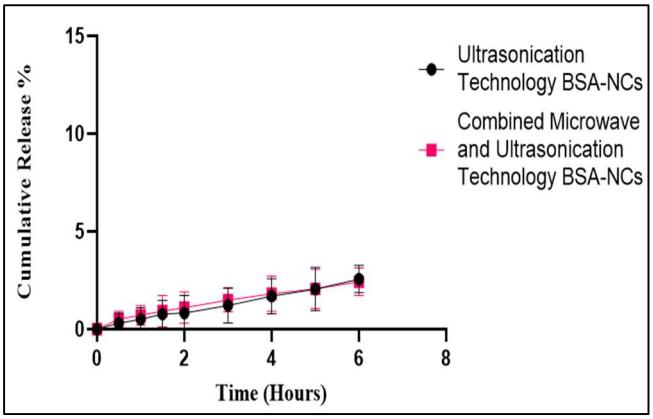

Figure 6.41 Release study of albumin from different types of Nanocapsules

6.35 Stability Study

This study integrates two methods to prepare BSA-NCs. Ultrasonication technology and combined MW/US, Over a period of 90 days. In contrast, BSA-NCs produced through US technology showed a negligible increase in size, while those prepared using a combined MW/US method demonstrated almost no change in particle size, indicating stability up to 90 days.

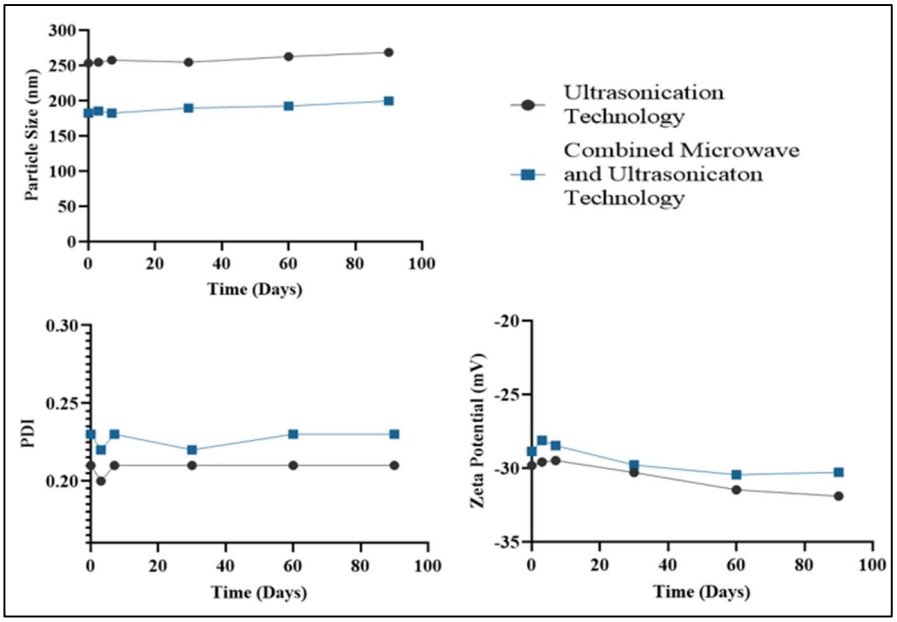

Figure 6.42. BSA-NCs Stability Study in Two Different Methods up to 90 Days at 4 °C

In term of polydispersity index, the US technology shows a 0.20 to 0.21, whereas the Combined MW/US technology maintains the PDI around 0.22 to 0.23. In addition,

the zeta potential for particle from US technology decreases slightly -29 to -31 and also in Combined MW/US technology more negative zeta potential value -28 to -30 up to 90 days. However, the persistent negative charge indicates that the nanocarriers remain stable against aggregation. It was observed that the BSA-NCs maintain stability for up to 90 days when stored at 4 °C as shown in Figure 6.42.

6.36 Chitosan Coating of Bovine Serum Albumin Nanoparticles and Nanocapsules

In this chapter, was prepared the formulation of bovine serum albumin (BSA) nanoparticles (NPs) and nanocapsules (NCs) with different manufacturing technologies such as surfactant-mediated Coacervation method BSA-NPs, Microwave Technology BSA-NPs, Ultrasonication Technique BSA-NCs and Combined Microwave and Ultrasonication BSA-NCs. To enhance their targeting capabilities, these BSA-based nanomedicines are further coated with chitosan (2.2 % w/v), a natural polysaccharide renowned for its biocompatibility and bio adhesive properties. The combination of chitosan's mucoadhesive properties with the biocompatibility of BSA results in a robust delivery system.

In our experimental investigations, the optimised various manufacturing processes,

In the surfactant-mediated coacervation method BSA-NPs coated with chitosan (2.2% w/v) shows the particle size in the range to 195 to 205 nm with 0.27 PDI and +18 mV zeta potential.

In the microwave technology BSA-NPs has been shown to produce chitosan (2.2 % w/v) coatings with a size range of 150 to 170 nm, a PDI of 0.26, and a zeta potential of +19 mV.

In Ultrasonication technology BSA-NCs was observed that subsequent coating with chitosan (2.2% w/v) resulted in an increase in the size of the BSA-NCs to dimensions exceeding 300 nm. his enlargement is due to the high concentration of the nanocapsules. Despite the increase in size, the method consistently yields a good polydispersity index, registering below 0.22. Additionally, it ensures a stable and positive zeta potential over time.

Additionally, was explored a combined technique of MW/US followed by coating with chitosan (2.2% w/v). In particular, it consistently produced BSA-CS-NCs with particle was 200 nm, exhibited good 0.22 PDI and maintained a stable and positive zeta potential +21 as shown in Table 6.10.

Table 6.10. Physicochemical Characterization of BSA NPs and NCs Coated with Chitosan Obtained by Different Manufacturing Technologies

Manufacturing Process	Average Diameter ± SD (nm)	PDI	Zeta Potential ± SD (mv)
Surfactant-mediated Coacervation Method (BSA-CS NPs)	203.6 ± 4.11	0.27 ± 0.02	+18.78 ± 4.91
Microwave Technology (BSA-CS NPs)	168.2 ± 2.81	0.26 ± 0.01	+19.64 ± 3.71
Ultrasonication Technique (BSA-CS NCs)	323.5 ± 6.31	0.20 ± 0.02	+21.85 ± 5.81
Combined Microwave and Ultrasonication (BSA-CS NCs)	200.6 ± 6.7	0.22 ± 0.012	+24.85 ± 5.4

6.37 Conclusion

In conclusion, the surfactant-mediated coacervation method, utilising ethanolic Epikuron® 200, was found to be an effective approach for the formation of BSA-NPs with desirable properties. The organic solvent ethanol is employed for the denaturation of albumin. The size and zeta potential of the BSA-NPs were optimised by varying the concentration of BSA, resulting in BSA-NPs with sizes below 200 nm and stable zeta potentials.

Despite initial attempts, ultrasonication (US) did not result in the formation of BSA-NPs. Nevertheless, it proved to be an effective method for preparing BSA-NCs. The

optimization process involved adjusting the ultrasonication frequency, time, and BSA concentration while maintaining the temperature, resulting in BSA-NCs with sizes below 250 nm, 0.21 polydispersity index (PDI) and negative zeta potential values -29. Microwave-assisted technology was employed to thermal denaturation of albumin, resulting in the successful fabrication of stable BSA nanoparticles (BSA-NPs) with a size distribution of 85 to 95 nm, with a 0.26 PDI, and a highly negative zeta potential -30 mV. The optimal conditions were identified as a temperature of 80°C, a ramp time of 90 seconds, and a preparation time of 12 minutes. Nevertheless, several experimental trials indicated that the preparation of BSA-NCs by using microwave technology resulted in the formation of an oil layer on the surface of the formulation. The combination of microwave and ultrasonication technologies did not result in the formation of BSA-NPs, but was effective for the preparation of BSA-NCs. The optimization process involved the setting of specific parameters for temperature, ramp time, ultrasonication frequency, and preparation time, with the objective of inducing the thermal albumin denaturation. This resulted in the formation of BSA-NCs with an average diameter of approximately 182 nm, a polydispersity index (PDI) within an acceptable range, and a stable zeta potential.

The physicochemical characterization of BSA-NPs demonstrated that the surfactant-mediated coacervation method and microwave technology produced stable nanoparticles below 200 nm. BSA-NCs produced by the combined MW/US method met our quality targets attributes. The combined MW/US technology was particularly effective, offering a synergistic approach that enhanced control over particle formation, stability, and drug encapsulation efficiency. The ultrasonication technology achieved all quality target parameters except size. The ANOVA test confirmed significant differences in particle size, PDI, and zeta potential between the different manufacturing technologies. Scanning Electron Microscopy (SEM) and Fourier-Transform Infrared Spectroscopy (FTIR) provided further insights into the structural integrity and successful formulation of the nanoparticles and nanocapsules. Stability studies demonstrated that BSA-NPs produced by the surfactant-mediated coacervation method and microwave technology, as well as BSA-NCs produced by ultrasonication and combined MW/US technology, retained

their physicochemical properties for a period of 90 days. This indicates their suitability for long-term storage at 4°C and utilisation.

The chitosan coating, added at a concentration of 2.2% w/v to the BSA nanoparticles (NPs) and nanocapsules (NCs) produced via optimised manufacturing processes, produced notable effects on their physicochemical properties. The coating resulted in a consistent increase in zeta potential, indicative of enhanced stability and reduced aggregation potential. Furthermore, the chitosan coating conferred mucoadhesive properties, rendering the BSA-NPs and NCs more suitable for pharmaceutical applications, particularly those requiring targeted delivery and prolonged circulation times.

Chapter 7: Preparation of Blank Human Serum Albumin-based Nanomedicine by Approaching Advanced Manufacturing Technologies

In this chapter, was employed human serum albumin (HSA) in the development of two nanomedicine: nanoparticles (NPs) and nanocapsules (NCs) already studied with BSA. The methods investigated include the coacervation method, ultrasonication technology (US), microwave technology (MW), and a combination of microwave and ultrasonication (MWUS) to achieve specific quality target attributes to ensure the effectiveness and physical stability of these nanomedicines as shown in Chapter 6 Table 6.1. For the manufacturing of the HSA formulations, the components previously employed to obtain BSA nanomedicine.

7.1 Preparation of HSA-NPs Using Surfactant-mediated Coacervation Method

To prepare HSA-NPs, a Human Serum Albumin (HSA) solution of 8 mg/mL containing Kolliphor HS15 (0.1% w/v) in sodium phosphate buffer (0.1M) at pH 8.0 was prepared to Induce denaturation of the albumin solution by ethanolic Epikuron® solution 200 (1% w/v) was added drop-by-drop under magnetic stirring conditions at room temperature. Subsequently, the ethanol was evaporated using nitrogen purge. Once the ethanol has evaporated, the resulting HSA-NPs are purified by dialysis against a NaCl 0.9% solution.

7.2 Preparation of HSA-NPs Using Microwave-Assisted Technology

The tuned manufacturing process to obtain, BSA nanoparticles was used. A solution of HSA 8 mg/mL with Kolliphor HS15 (0.1% w/v) in a sodium phosphate buffer (0.1M) at a pH of 8.0 was prepared. Microwave-assisted technology was employed. For the preparation of HSA-NPs was identified maintaining a temperature 80 °C, setting the ramp time to 90 seconds to reach the set temperature and the preparation time was 12 minutes with 100 % stirring potency. The microwave step facilitates the thermal denaturation of albumin and the reduction of particle size of albumin nanoparticles. Finally, the HSA-NPs are purified by dialysis against 0.9% NaCl.

7.3 Preparation of HSA-NCs by using Ultrasonication Technology (US)

The manufacturing process to obtain HSA-NCs formulation begins with the preparation of HSA solution 8 mg/mL in a sodium phosphate-buffer solution 0.1M at pH 8.0 containing Kolliphor HS15 (0.1% w/v). Miglyol 829 is added dropwise to this solution under magnetic stirring to form an oil-in-water (o/w) nanoemulsion. The o/w nanoemulsion was then subjected to ultrasonication at 100 kHz for 90 seconds facilitating the reduction of droplet size. NCs formulation was dialysis against the NaCl 0.9 % w/v to obtain purified HSA-NCs.

7.4 Preparation of HSA-NCs by using combined MW/US Technology

To obtain nanocapsules a solution of HSA 8 mg/mL containing Kolliphor HS15 (0.1% w/v) in phosphate buffer (0.1M) at pH 8.0 was prepared. Miglyol 829 was dropwise added to the HSA solution under stirring conditions to form an oil-in-water nanoemulsion. To obtain thermal denaturation of albumin the microwave technology with a ramp time of 90 seconds to heat the mixture to 76°C was employed. Simultaneously, apply ultrasound at 20.52 KHz with a power of 15W. The process was for 12 minutes to obtain HSA-NCs. Finally, the HSA-NCs were purified by dialysis against 0.9% NaCl for 1 hour.

7.5 Physicochemical characterisation of HSA NPs and NCs

The results demonstrate that it is possible to produce nanomedicine with HSA. The average diameter, polydispersity index (PDI), and zeta potential of the HSA nanoparticles and nanocapsules exhibited variability dependent on the manufacturing technologies. The nanoparticles prepared using the surfactant-mediated coacervation method exhibited an average diameter of about 192 nm, with a polydispersity index (PDI) of 0.29 and a zeta potential of -16 mV. Therefore, did not meet the quality attribute because of high PDI and zeta potential is lower than -20 mV. In contrast, the formulation developed with microwave-assisted technology exhibited the smallest nanoparticle size of 95 nm, with a PDI of 0.27 and more negative zeta potential of -27 mV, which did not meet our quality target attribute due to high PDI as shown in the Table 7.1.

Table 7.1. Physicochemical Characteristics of Blank-HSA NPs Obtained by Surfactant-mediated Coacervation Method and Microwave-assisted Technology

Manufacturing Methods	Average Diameter ± SD (nm)	PDI	Zeta Potential ± SD (mv)
Surfactant-mediated Coacervation Method	192.5 ± 2.62	0.29 ± 0.01	-16.35 ± 4.50
Microwave-assisted technology	98.6 ± 5.11	0.27 ± 0.02	-27.54 ± 3.22

The nanocapsules developed through ultrasonication technology exhibited a diameter of 228 nm, yet exhibited the most negative zeta potential of -29 mV with a PDI of 0.22. These NCs are good but the size is more than 200 nm. The combination of microwave and ultrasonication technology resulted in the smallest HSA nanocapsules 173 nm with the lowest polydispersity index of 0.21 and a highly negative zeta potential of -29 mV, indicating a more uniform and stable colloidal formulation. The HSA-NCs manufactured by a combined MW/US manufacturing process meet our targeted quality attributes as per Table 7.2.

Table 7.2. Physicochemical Characteristics of Blank-HSA NCs Obtained by Ultrasonication Technology and Combined Microwave and Ultrasonication Technology

Methods	Average Diameter ± SD (nm)	PDI	Zeta Potential ± SD (mv)
Ultrasonication Technology	228.5 ± 3.26	0.22 ± 0.02	-29.88 ± 4.64
Combined Microwave and Ultrasonication Technology	173.1 ± 6.41	0.21 ± 0.01	-28.54 ± 4.62

The Blank human serum albumin nanocapsules prepared using, combined microwave and ultrasonication technology meet our targeted quality attributes.

7.6 Yield of HSA Nanoparticles and Nanocapsules

To accurately calculate the yield of HSA NPs and NCs begin by weighing each empty vial using an analytical balance and record the weights. Add exactly 1 mL of the HSA-NPs into each pre-weighed vial, ensuring precise measurement with a calibrated pipette. Seal the vials with parafin to prevent contamination. Freeze the vials overnight at -20°C or use liquid nitrogen for instant freezing. After freezing, transfer the vials to a lyophilizer and freeze-dried the samples until all water content is removed, resulting in a dry powder of HSA nanoparticles.

For the preparation of HSA-NCs in vials, add 1 % w/v of trehalose to the vials before lyophilization to protect and stabilize the HSA-NCs. Due to the oil content in the NCs formulation, a cryoprotectant is needed for effective lyophilization. Weigh the vials containing the dried powder using an analytical balance and record the weights. Determine the exact weight of the HSA nanoparticles/nanocapsules powder by subtracting the weight of the empty vial from the weight of the vial with the dried powder. Calculate the initial weight of HSA used in the nanoparticle/nanocapsule formulation process, which should be calculated during the preparation stage.

Finally, calculate the yield percentage of HSA nanoparticles/nanocapsules using the formula: Yield (%) = (Weight of HSA NPs/NCs Powder / Initial Weight of HSA Used) X 100.

Table 7.3. Yield of HSA NPs Obtained by Surfactant-mediated Coacervation Method and Microwave-assisted Technology

Manufacturing Technologies	HSA NPs Powder weight after dialysis (mg)	Theoretical weight of HSA-NPs (mg)	Yield %
Surfactant-mediated Coacervation Method (HSA-NPs)	13.3	14	95.0
MW technology (HSA-NPs)	7.2	8.8	81.8

The percentage yield of HSA-NPs using the surfactant-mediated coacervation method was found to be 95 %, while the percentage yield using the MW technology was found to be 81.80 %.

Table 7.4. Yield of HSA-NCs Obtained by Ultrasonication Technology and Combined Microwave and Ultrasonication Technology

Manufacturing Technologies	HSA NCs Powder weight after dialysis (mg)	Theoretical weight of HSA-NCs (mg)	Yield %
Ultrasonication Technology (HSA-NCs)	17.5	19.1	91.6
Combined Microwave and Ultrasonication Technology (HSA-NCs)	17.9	19.1	93.6

The percentage yield of HSA-NCs using the ultrasonication technology was found to be 91.6 %, and by using the combined MW/US technology was found to be 93.6 %.

7.7 Comparison of ANOVA test of Bovine Serum Albumin (BSA) and Human Serum Albumin (HSA) Nanoparticles and Nanocapsules

A two-way ANOVA test was employed in GraphPad Prism to assess the comparative analysis of BSA and HSA nanomedicine manufactured by different preparation technologies on the physicochemical properties, including size, polydispersity index (PDI), and zeta potential (mV). The following manufacturing technologies were employed: surfactant-mediated coacervation (CO), microwave-assisted technology (MW NPs), ultrasonication (US NCs) and combined microwave and ultrasonication (MW+US NCs).

The comparison of BSA and HSA nanoparticles and nanocapsules prepared by different manufacturing technologies revealed that the formulations were not statistically significant ($p > 0.05$). Therefore, it can be concluded that if the optimised formulations are prepared with either BSA or HSA, the outcomes will be similar. This demonstrates the suitability of our formulations for both BSA and HSA as shown in Figures 7.1, 7.2, 7.3 and 7.4.

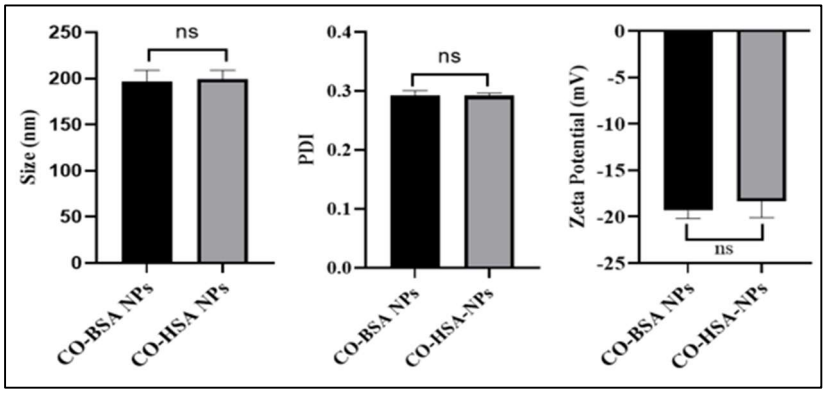

Figure 7.1. Comparison of Physicochemical Characteristics Variation of Surfactant-mediated Coacervation BSA and HSA Nanoparticles

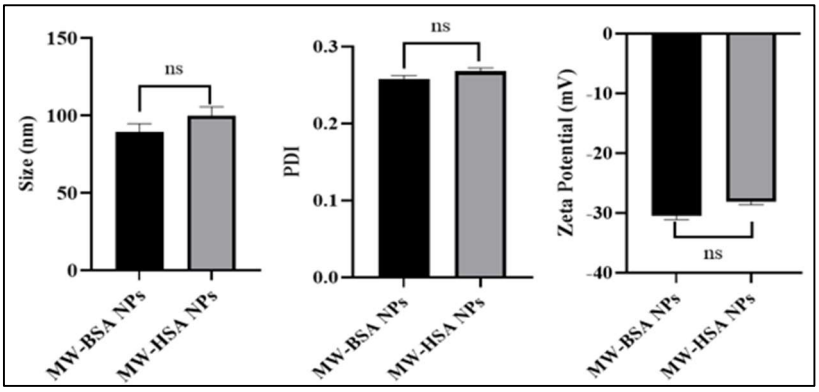

Figure 7.2. Comparison of Physicochemical Characteristics Variation of Microwave-assisted Technology BSA and HSA Nanoparticles

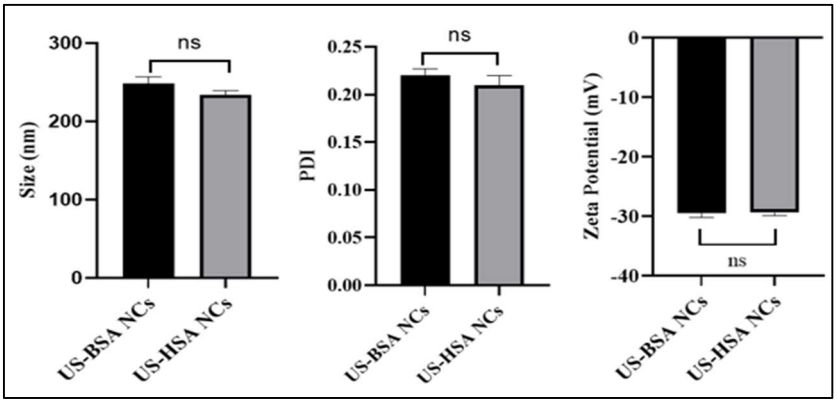

Figure 7.3. Comparison of Physicochemical Characteristics Variation of Ultrasonication BSA and HSA Nanocapsules

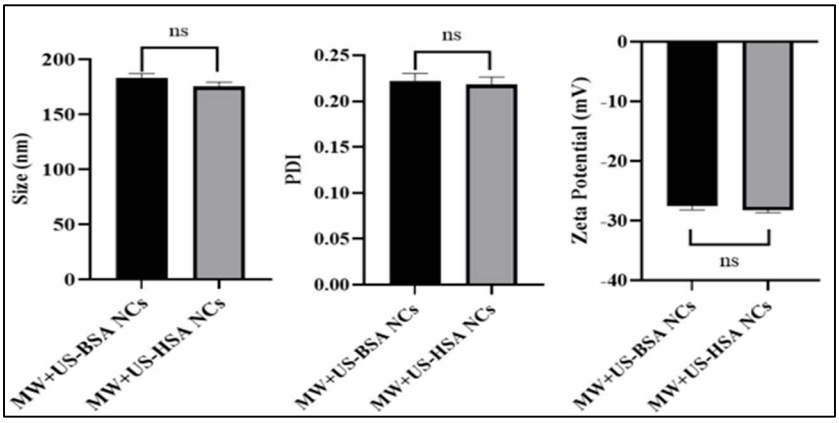

Figure 7.4. Comparison of Physicochemical Characteristics Variation of Combined Microwave and Ultrasonication BSA and HSA Nanocapsules

7.8 Comparison of Release Study of HSA Fragments and BSA Fragments from NPs and NCs

The preparation of the standard working solution and the BCA working reagent (WR) was discussed in Chapter 6.

The release of BSA and HSA fragments from nanoparticles and nanocapsules formulation was analysed using the bicinchoninic acid (BCA) protein assay. It was observed that both the surfactant-mediated coacervation nanoparticles (CO-NPs) and microwave-assisted technology (MW NPs) exhibited a BSA and HSA fragment release of 5 to 7% within 6 hours as shown in Figure 7.5.

In contrast, the ultrasonication nanocapsules (US-NCs) and the nanocapsules formed by combining microwave and ultrasonication (MW/US-NCs) demonstrated a low release of BSA and HSA fragments. The nanocapsules released 1.5 to 2.8 % of BSA and HSA over the six hours, as illustrated in Figure 7.6. It can be concluded that the comparisons of the formulations prepared by using both BSA and HSA have good stability in the nanoparticles and nanocapsules.

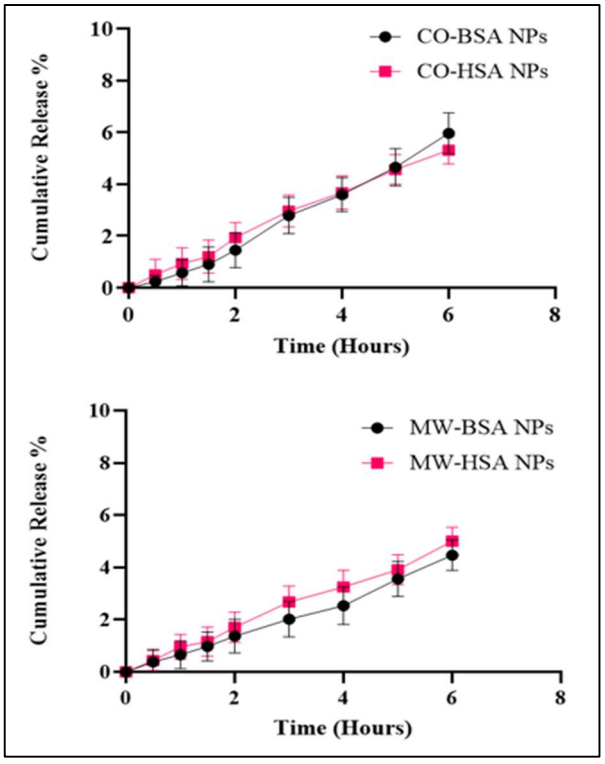

Figure 7.5. Comparison of Release study of BSA and HSA Fragment from different types of Nanoparticles

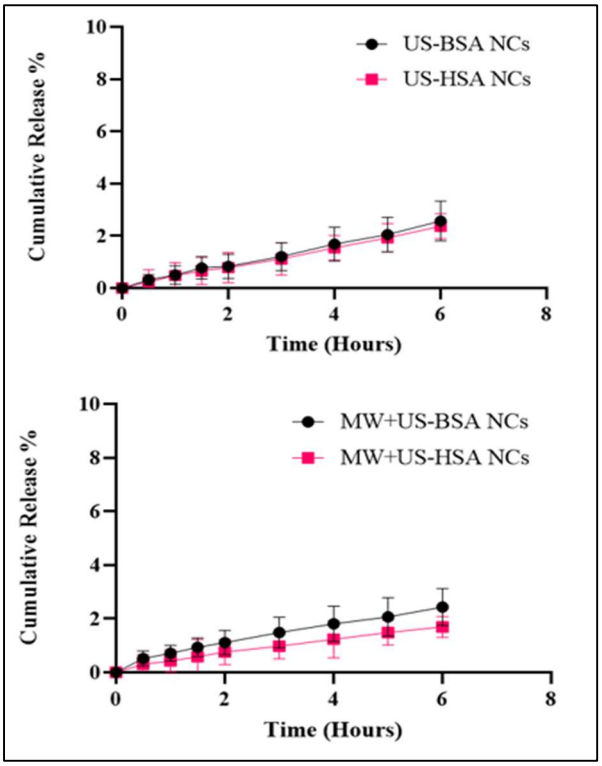

Figure 7.6. Comparison of Release study of BSA and HSA Fragment from different types of Nanocapsules

The comparisons of development between human serum albumin (HSA) and bovine serum albumin (BSA) nanoparticles and nanocapsule using different manufacturing technologies. Based on the physicochemical characterization, percentage yield, and BSA and HSA fragments release from both BSA and HSA nanoparticles and nanocapsules formulations found that the similar result were concluded that the HSA-NCs manufactured by combined MW/US technology achieved our quality target attributes and provides better physical stability, and reliability for targeted drug delivery, with smaller nanocapsule size for both lipophilic and hydrophilic drugs.

Chapter 8: Development and Optimization of Doxorubicin Albumin-based Nanocapsules by Approaching Advanced Manufacturing Technologies

In this chapter, the development and the optimization of doxorubicin-loaded albumin nanocapsules by using ultrasonication technology (US) and a combination of microwave and ultrasonication (MW/US), taking into account the results obtained for blank BSA and HSA-based formulations. Indeed, the formation of nanocapsules was achieved with both technologies reaching our quality target attributes.

Doxorubicin hydrochloride (DOX-HCl) is a chemotherapeutic agent used in the treatment of various cancers, including breast cancer, ovarian cancer, bladder cancer, lymphoma, and leukaemia. It belongs to the anthracycline class of drugs, the chemical structure of Dox-HCl is characterized by the core structure consisting of four fused rings, with various functional groups attached to it, including a daunosamine (a sugar moiety) linked through a glycosidic bond as shown in Figure 8.1 [223].

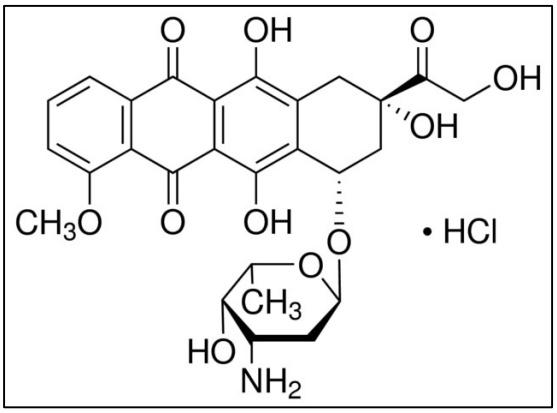

Figure 8.1. Chemical Structure of Doxorubicin Hydrochloride (DOX-HCl) [223]

The hydrochloride salt form of DOX increases its solubility in water, thus facilitating its administration as an injectable solution. The molecular formula of DOX-HCl is C27H29NO11•HCl, which reflects the complex structure of the molecule and the various functional groups that contribute to its mechanism of action and pharmacological properties [224]. DOX-HCL is originally derived from the bacterium Streptomyces peucetius. This bacterium produces DOX as part of its secondary

metabolism, a process common among various species of the Streptomyces genus. The discovery of DOX was part of a broader search for new anticancer agents from natural sources during the mid-20th century [225,226].

Doxorubicin acts primarily through intercalating into DNA, which disrupts the normal function of the nucleic acids. This intercalation prevents the replication of DNA and the transcription of RNA, leading to the inhibition of protein synthesis, which is crucial for cell growth and division [227]. Additionally, doxorubicin has the capacity to Inhibit Topoisomerase II, The stabilisation of the cleavable complex between topoisomerase II and DNA by doxorubicin induces DNA damage, resulting in the apoptosis of cancer cells [228]. The generation of free radicals is a process that occurs naturally within the body. DOX undergoes redox cycling, resulting in the production of free radicals that damage cellular membranes, DNA, and proteins, thereby contributing to the process of cell death [229].

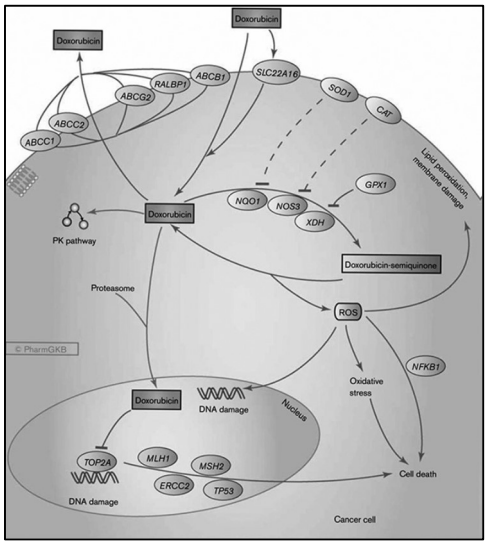

Figure 8.2. Mechanism of action of doxorubicin [228]

The doxorubicin is administered intravenously, it bypasses the gastrointestinal tract, resulting in almost complete bioavailability. This means that almost the entire dose of the drug enters the systemic circulation, making it highly effective for the cancer treatment. The distribution of DOX is extensive upon entering the systemic circulation, reaching various tissues. This characteristic is advantageous for targeting cancer cells throughout the body, but it also poses a risk of toxicity to non-target

tissues. In the metabolism of DOX in the liver, where cytochrome P450 enzymes metabolize it. The major metabolite, doxorubicin, retains anticancer activity but has a different toxicity profile. This metabolic process is crucial for the drug's pharmacokinetics, affecting its duration of action and side effects. Doxorubicin has a biphasic elimination pattern with an initial rapid distribution phase followed by a slower elimination phase. This pattern reflects the drug's extensive tissue distribution followed by gradual clearance from the body [230–232].

The doxorubicin major side effect is cardiotoxicity, one of the most serious adverse effects, can manifest in two ways: acutely or chronically. In the former case, it results in heart muscle damage, which may potentially culminate in congestive heart failure due to oxidative stress and apoptosis of cardiac cells. Myelosuppression is another significant side effect, characterised by a reduction in the production of blood cells, thereby increasing the risk of infections, bleeding, and fatigue. This condition arises from the drug’s impact on DNA synthesis in rapidly dividing bone marrow cells. Other adverse effects include alopecia, where patients experience temporary hair loss due to the drug targeting rapidly dividing cells in hair follicles, and mucositis, an inflammatory condition of the digestive tract mucous membranes causing painful ulcers and gastrointestinal discomfort. Furthermore, nausea and vomiting are frequently observed, resulting from the stimulation of the brain’s chemoreceptor trigger zone. The management of these side effects necessitates rigorous monitoring, the use of protective agents such as dexrazoxane, scalp cooling caps, antiemetic drugs, and the implementation of supportive care measures to enhance the quality of life of patients undergoing treatment [232–235].

8.1 Preparation and Optimization of DOX-BSA Nanocapsules using Ultrasonication Technology

At the suitable concentration of Doxorubicin HCL, was initiated the preparation of the drug solution with concentrations DOX-HCl 40, 60 and 70 mg/0.5mL was dissolving in a mixture of 500 µL of 1% aqueous Span 83 and N-methyl-2-pyrrolidone, maintaining a volume ratio of 70:30. This mixture was then thoroughly vortexed and

subsequently subjected to sonication in US bath for 10 minutes. The 80 mg/0.5mL of doxorubicin HCl was try to solubilize, but it resulted in a saturated solution.

Then a double emulsion was intentionally tuned to obtain doxorubicin-loaded BSA-NCs. For this process 100 µl of DOX-HCL solution at each concentration was added to 2 mL of Miglyol 829 individually. The solution was sonicated using ultrasonication technology (US) for 60 seconds to form a water-in-oil emulsion. Simultaneously a 4 mL solution of BSA at a concentration of 8 mg/mL in PBS 0.1M at pH 8.0 containing Kolliphor HS15 (0.1% w/v) was prepared. Then add the 500 µl water-in-oil emulsion dropwise to the BSA solution. The mixture was sonicated for 90 seconds to obtain DOX-BSA-NCs. Finally, the DOX-BSA-NCs was purified by dialysing them against NaCl 0.9% for 1 hour.

8.2 Physicochemical Characterization of Doxorubicin loaded nanocapsules

In order to ascertain the average diameter and polydispersity index of NCs formulation, was employed photon correlation spectroscopy in conjunction with the measurement of zeta potential through electrophoretic mobility. Prior to analysis, the samples were diluted with filtered water. The diluted samples were then placed into an electrophoretic cell, where a rounded 15 V/cm electric field was applied to determine the zeta potential.

The DOX-BSA NCs encapsulation efficiency was evaluated by using a centrifugal filter system, A portion of the formulation was put into an Amicon Ultra-0.5 centrifugal filter device and spun on a Beckman Coulter 64R centrifuge for 15 minutes at 12,000 rpm. High-performance liquid chromatography (HPLC) was then used to analyze the filtered solution with proper dilution with mobile phase. On a sample of freeze-dried NCs, the drug loading capacity was assessed. A weighted portion of each formulation freeze-dried powder was separately suspended in 10 mL of filtered water. After sonication and centrifugation, the supernatant was diluted with a mobile phase and analysed with HPLC.

The method was performed using a Shimadzu system consisting of a fluorescence detector, a solvent delivery module (RF-10A XL) with a Rheodyne injection valve and a 20 L loop attached, isocratic chromatographic separation (250 mm x 4.6 mm i.d., 5 m particle size), and a stainless-steel Kinetex EVO C18 column, at 25 ºC, with a mobile phase of Potassium dihydrogen phosphate (KH2PO4): acetonitrile: methanol (65:25:10 v/v) and a flow rate of 1.0 mL/min. The mobile phase was degassed after being filtered through a 0.45 µm Millipore membrane filter. Fluorescence was used to measure drug concentration, with excitation and emission adjusted to 480-590 nm. A linear calibration curve was created in the concentration range of 0.02-0.10 µg/mL, with a high regression coefficient of 0.999.

An *in vitro* release study of doxorubicin from BSA NCs was conducted using a multi-compartment system comprising a donor phase and a receiving phase, separated by a dialysis membrane with a molecular weight cutoff of 14 kDa. In the donor phase, 1 mL of the DOX-BSA NC formulation was introduced. The receiving phase consisted of 1 mL of a 0.1 M phosphate buffer with a pH of 7.4. At predetermined time intervals (0.25, 0.50, 0.75, 1, 1.5, 2, 3, 4, 5, 6, 22, 24, 48, and 50 hours), 1 mL samples were withdrawn from the receiving phase and immediately replaced with 1 mL of fresh phosphate buffer of the same concentration and pH. Subsequently, all collected samples were subjected to HPLC analysis following appropriate dilution.

Doxorubicin-loaded bovine serum albumin nanocapsules obtained employing ultrasonication technology and a theoretical concentration was 0.44, 0.66 and 0.77 mg/mL respectively. The average particle size in the range between 260 to 270 nm. The formulation shows a negative zeta potential with a value of -31 mV, which is attributed to the presence of carboxyl groups on the albumin nanocapsules. The encapsulation efficiency was evaluated utilising a centrifugal filter system, The encapsulation efficiency of all the nanocapsule formulation was found to be in the range of 91 to 95%, with good drug loading as shown in Table 8.1.

Table 8.1. Physicochemical Characterization, Encapsulation efficiency (EE%) and Drug loading (DL%) of Different concentrations of DOX-BSA NCs obtained by Ultrasonication Technology

Theoretical Concentration of DOX-HCl in mg/mL	Average Diameter ± SD (nm)	PDI	Zeta Potential ± SD (mv)	DL %	EE %
0.44	264.2 ± 2.6	0.21 ± 0.02	-31.95 ± 4.13	4.11 ± 0.22	91.3 ± 1.54
0.66	269.1 ± 3.8	0.21 ± 0.01	-30.73 ± 3.56	4.32 ± 0.24	93.7 ± 2.30
0.77	270.8 ± 4.9	0.20 ± 0.02	-31.54 ± 3.83	5.43 ± 0.12	94.9 ± 1.08

± SD (n=5)

This *in vitro* study examines the release profile of Doxorubicin encapsulated within albumin nanocapsules at varying theoretical concentrations (0.44, 0.66, and 0.77 mg/mL). The objective of the study is to assess the sustained release capabilities of these nanocarriers for the drug delivery. The cumulative percentage of DOX released is plotted against time over 50 hours, illustrating a controlled release dynamic for all three formulations. Over time, the drug is released gradually and consistently from the encapsulated nanocapsules without any sudden spikes, indicating the ability of the nanocapsules to prolong the presence of the drug in the simulated environment as shown in Figure 8.3.

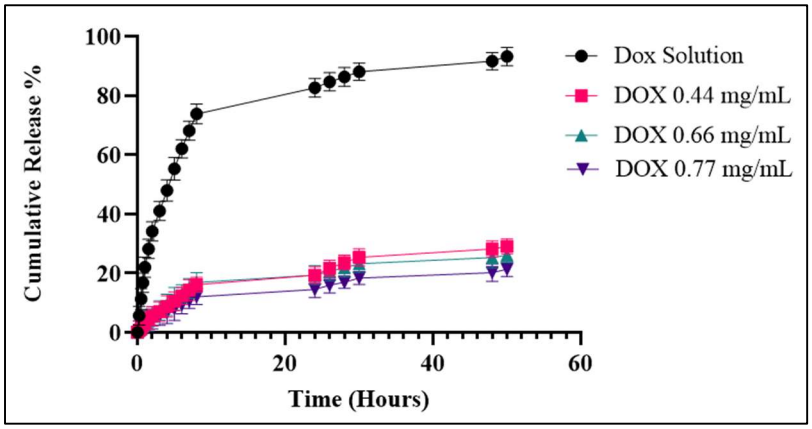

Figure 8.3. *In vitro* release study of doxorubicin from different concentrations of Doxorubicin hydrochloride ± SD (n=5)

The *in vitro* release strongly supports the finding that doxorubicin-loaded albumin nanocapsules formulation are capable of maintaining a prolonged drug release. The three formulations with different concentrations on *in vitro* drug release below 20 % in 24 hours.

After conducting an exhaustive analysis including physicochemical characterization, *in vitro* release profiles, and assessments of drug loading and encapsulation efficiency on all formulation batches, it has been determined that an initial weight of 0.77 mg/mL of drug in Doxorubicin-loaded albumin nanocapsules stable nanocapsule size of 270 nm with 0.20 PDI with negative zeta potential -31 mV. The formulation has good drug loading 5.43 % and high encapsulation efficiency 95 %. Additionally, these nanocapsules demonstrated a prolonged release pattern around 14 % of release in 24 hours and 21 % of release in 50 hours of time duration. This release mechanism is highly beneficial for treatments as it helps to maintain consistent drug concentrations in the bloodstream, reducing the need for frequent dosing and improving patient adherence to the treatment protocol. After selecting a doxorubicin concentration of 0.77 mg/mL was developed bovine serum albumin nanocapsules (BSA-NCs) using a combination of microwave and ultrasonication technologies (MW/US).

8.3 Doxorubicin-loaded BSA-NCs by Combined Microwave and Ultrasonication Technology (MW/US)

The 70 mg of Doxorubicin Hydrochloride (DOX-HCL) was dissolved in 500 µl of aqueous Span83 (1%) and N-methyl pyrrolidone in a (70:30 ratio v/v). The resulting solution was vortexed and placed in a sonication bath for 10 minutes. Then 200 µl of DOX-HCL solution was added to 4 mL of Miglyol 829. The solution was sonicated using an ultrasonication technique (US) for 60 seconds to form a water-in-oil emulsion. Simultaneously a 30 mL solution of BSA at a concentration of 8 mg/mL in PBS 0.1M at pH 8.0 containing Kolliphor HS15 (0.1% w/v) was prepared. The 2400 µl water-in-oil emulsion was dropwise added to the BSA solution. Thermal denaturation of albumin employing a microwave-assisted technology with a ramp time of 90 seconds to heat the mixture to 76°C. Simultaneously, apply ultrasonication at 20.52 KHz with a power of 15W. Allow the preparation to proceed for 12 minutes to obtain BSA-NCs. Finally, purify the DOX-BSA-NCs by dialysing them against NaCl 0.9% for 1 hour.

The ultrasonication technology and combined MW/US manufacturing technologies, when optimized, are effective for the preparation of DOX-BSA-NCs was successfully achieved a desirable size for DOX-BSA-NCs, along with a low polydispersity index of 0.20 to 0.22. These BSA-NCs also demonstrated an excellent zeta potential in the range of -30 to -32 mV. The details are reported in Table 8.2.

Table 8.2. Physiochemical Characterization of DOX-BSA NCs with two different manufacturing Technology

Manufacturing Process	Average Diameter ± SD (nm)	PDI	Zeta Potential ± SD (mv)
Ultrasonication Technology (US)	270.8 ± 4.92	0.21 ± 0.02	-31.37 ± 3.71
Combined Microwave and Ultrasonication Technology (MW/US)	202.7 ± 6.82	0.21 ± 0.02	-31.62 ± 4.22

± SD (n=5)

Ultrasonication technology has been demonstrated to have a drug loading capacity of 5.43 % and an encapsulation efficiency of 95.3% for doxorubicin-loaded albumin nanocapsules and the combined microwave and ultrasonication (MW/US) technology markedly enhances drug loading, achieving 4.12% and encapsulation efficiency was found to be 91.6%.

Table 8.3. Encapsulation Efficiency and Drug Loading of DOX-BSA NCs obtain by Different Manufacturing Process

Manufacturing Process	Formulation	(DL %)	(EE %)
Ultrasonication Technology (US)	DOX-BSA NCs	5.43 ± 0.11	95.3 ± 1.08
Combined Microwave and Ultrasonication Technology (MW/US)	DOX-BSA NCs	4.12 ± 0.16	91.6 ± 2.13

± SD (n=5)

The study investigated the *in vitro* release behaviour of DOX-BSA NCS using different manufacturing methods, namely Ultrasonication (US), and a combined approach of Microwave and Ultrasonication (MW/US), in a multi-compartment system. The results showed that DOX was released at a slower rate when prepared with US, with only 12% released after 24 hours and 23% release in 50 hours. In contrast, samples prepared using the combined MW/US technique exhibited a much faster release rate. Approximately 17% of DOX was released within the same 24-hour time and 30% of release in 50 hours of time, as shown in Figure 8.4.

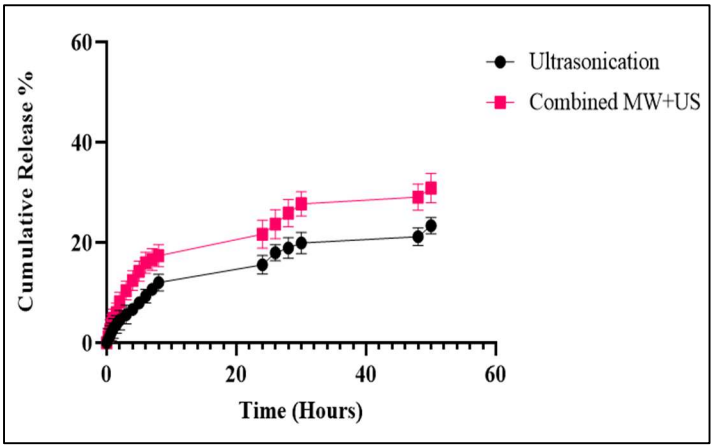

Figure 8.4. *In vitro* release study of DOX-BSA NCs with two different manufacturing methods ± SD (n=5)

8.4 ANOVA Test

A two-way ANOVA test was conducted using Graph Pad Prism to evaluate the impact of two distinct manufacturing technologies (Ultrasonication, and Combined MW/US) on the physicochemical properties of Doxorubicin-loaded to BSA nanocapsules. The properties assessed included Size, Polydispersity Index (PDI), and Zeta Potential (mV).

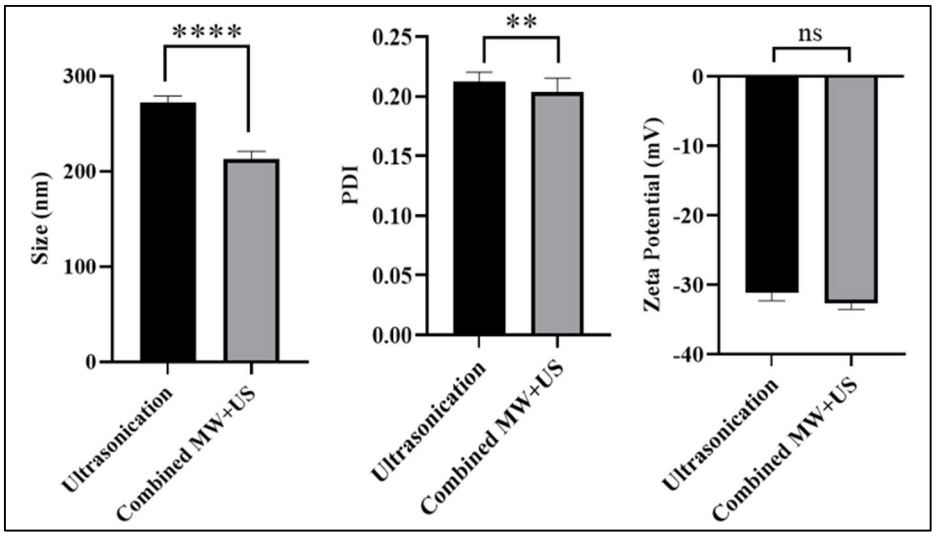

Figure 8.5. Physicochemical Characteristics Variation of DOX-BSA-NCs Obtained by Using the Different Manufacturing Methods ± SD (n=5)

The effects of Two different manufacturing processes: ultrasonication and combined microwave and ultrasonication (MW/US): size, polydispersity index (PDI), and zeta potential of nanocapsules.

Size (nm): The asterisks '****' indicates a statistically significant difference between the compared groups, with a p-value less than 0.0001, which is considered highly significant.

Polydispersity Index (PDI): is a measure of the distribution of molecular mass in a given sample. A lower PDI indicates a more uniform size distribution of particles. The asterisks '**' indicates a highly significant difference ($p < 0.0016$) between the groups.

Zeta Potential (mV): Zeta potential measures the surface charge of nanocapsules. The magnitude of the zeta potential indicates the degree of repulsion between adjacent, similarly charged particles in a dispersion. A high zeta potential confers stability. The Figure shows '' indicating a not significance level with a p-value less than 0.10, and 'ns' indicating a p-value.

After investigating in detail, the physicochemical properties and *in vitro* release patterns, was found that both Ultrasonication (US) and the combined microwave and Ultrasonication (MW/US) method are effective for drug delivery. Still, MW/US is showing a slightly fast release of DOX compared to the US technology alone. Opted for the US approach due to its higher effectiveness over the MW/US technology. The preference for the US technology is also influenced by practical challenge presented by the MW/US method, particularly in maintaining sterility. Additionally, this technology promotes a more uniform particle size distribution and precise control over particle size, thereby improving the quality and performance of the drug delivery system.

8.5 Development of Doxorubicin loaded Human Serum Albumin Nanocapsules (DOX-HSA NCs)

In this section, was developed DOX-HSA NCs using a precise double-emulsion method combined with microwave/ultrasonication (MW/US) technology. The preparation method is the same as that for DOX-BSA-NCs discussed in Section 8.3; however, in this formulation was used HSA instead of BSA. The DOX-HSA-based NCs are designed to improve drug loading, release profiles, and targeting efficiency, offering promising potential for cancer therapy.

The DOX-HSA NCs formulations have an average size of approximately 190 to 200 nm, with a negative zeta potential of approximately -31 as shown in Table 8.4. This is attributed to the carboxyl groups present in albumins.

Table 8.4. Physicochemical Characterization, Encapsulation Efficiency and Drug Loading of DOX-HSA-NCs

Formulation	Average Diameter ± SD (nm)	PDI	Zeta Potential ± SD (mv)	(DL %)	(EE %)
DOX-HSA-NCs NCs	198.7 ± 4.2	0.22 ± 0.02	-31.95 ± 5.70	3.85 ± 0.59	88.4 ± 2.21

± SD (n=3)

The study investigated the *in vitro* release behaviour of DOX-HSA NCS preparation by using, combined microwave and ultrasonication technology (MW/US) and Pure Doxorubicin HCl solution in a multi-compartment system. The results showed that DOX was released at a prolonged manner around 20 % after 24 hours from the DOX-HSA NCS but pure DOX-Solution 76% release after 24 hours, as shown in Figure 8.6.

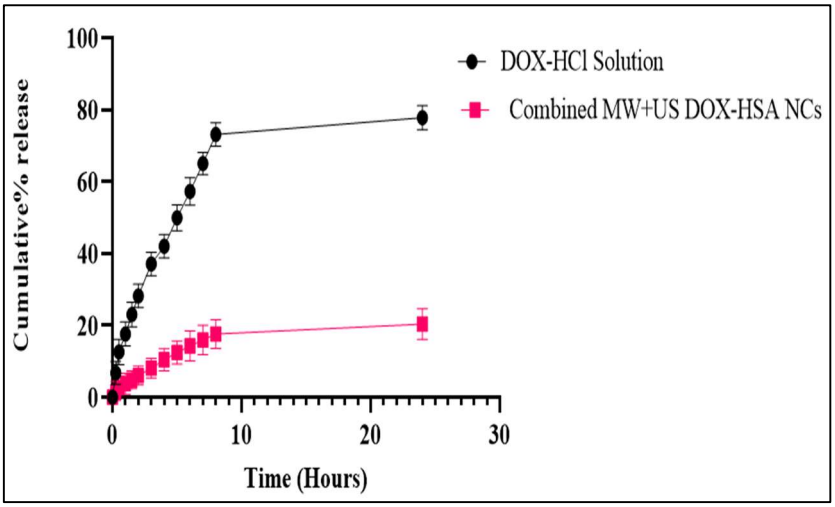

Figure 8.6. *In vitro* release study of DOX-HSA NCs with MW/US Technology

The prolonged release of doxorubicin from nanocapsules (NCs) is likely due to the slow diffusion of the drug through albumin. The utilization of this mechanism allows for the minimization of the systemic adverse effects of doxorubicin, thereby enhancing the efficiency of the nanocarriers at the targeted site.

8.6 ICOS-Fc targeted albumin-based nanocapsules as a tool for the delivery of doxorubicin in osteosarcoma cell lines

Osteosarcoma, a primary malignant bone tumour, primarily affects children and young adults, making it a significant cause of morbidity and mortality in this population [236]. As per the estimation of the American Cancer Society, more than 3,800 bone cancer cases be diagnosed in the United States in 2022 [237]. Chemotherapy was introduced in the 1970s, Doxorubicin and methotrexate were the first drugs to be used successfully, [238]. cisplatin and ifosfamide were added only later and with these, there was a significant increase in five-year disease-free survival of 35-40%. [239,240]. Despite advancements in treatment strategies, including surgical resection and adjuvant chemotherapy, the prognosis for patients with osteosarcoma remains challenging, particularly in cases of advanced or recurrent disease one of the major obstacles in osteosarcoma therapy is the development of drug resistance, leading to suboptimal treatment outcomes and limited therapeutic options. Although resistance to doxorubicin is a multifactorial phenomenon, i.e. it

depends on the occurrence of multiple mechanisms within the same cells, the most important mechanism that causes the lack or reduced response to treatment with doxorubicin is the one involving the membrane protein P-glycoprotein [241]. P-glycoprotein is the most important adverse prognostic factor for patients with osteosarcoma. [242–244]. Doxorubicin, it has several limitations, including dose-dependent cardiotoxicity, a lack of selectivity for tumour cells, and the development of cell resistance [225,234] To address these challenges, the development of albumin-based drug delivery systems that can enhance drug accumulation at the tumour site and overcome doxorubicin resistance is crucial.

In recent years, albumin-based drug delivery systems have shown great potential in improving the efficacy of chemotherapeutic agents while minimizing their systemic toxicity [245]. Furthermore, on activated CD4+ T cells, the inducible costimulatory molecule ICOS-Fc is expressed [246,247]. It is predominantly expressed on the surface of T cells and is inducible rather than constant. Upon T cell activation, triggered by recognition of an antigen, ICOS expression is upregulated. Up-regulation is crucial for fine-tuning the immune system to amplify the T-cell response when necessary. ICOS primarily functions by binding to its ligand, ICOSL, which is found on other immune cells, such as antigen-presenting cells (APCs) [171]. Which are involved in immune responses in lymphoid organs and inflammatory sites. By attaching to the appropriate ligand (ICOS-L), ICOS-Fc, a chemical, can reversibly suppress osteoclast activity and cause a reduction in bone resorption activity.[248,249]

The last part of my PhD research aimed to develop BSA-based doxorubicin-loaded Nanocapsules (DOX-BSA NCs) and conjugate them with ICOS-Fc, (DOX-BSA-ICOS-Fc NCs) by using advance ultrasonication technology. The sought to improve the targeted delivery of doxorubicin to the osteosarcoma cells line and enhance its efficacy in overcoming resistance.

8.7 Preparation of Blank BSA-NCs and DOX-BSA NCs.

Blank BSA-NCs and DOX-BSA NCs were prepared a tuned double-emulsion (W/O) using the ultrasonication technique (US) (100 kHz,500W) The preparation method is already discussed in the section 8.3 and illustrations scheme is shown below in Figure 8.7.

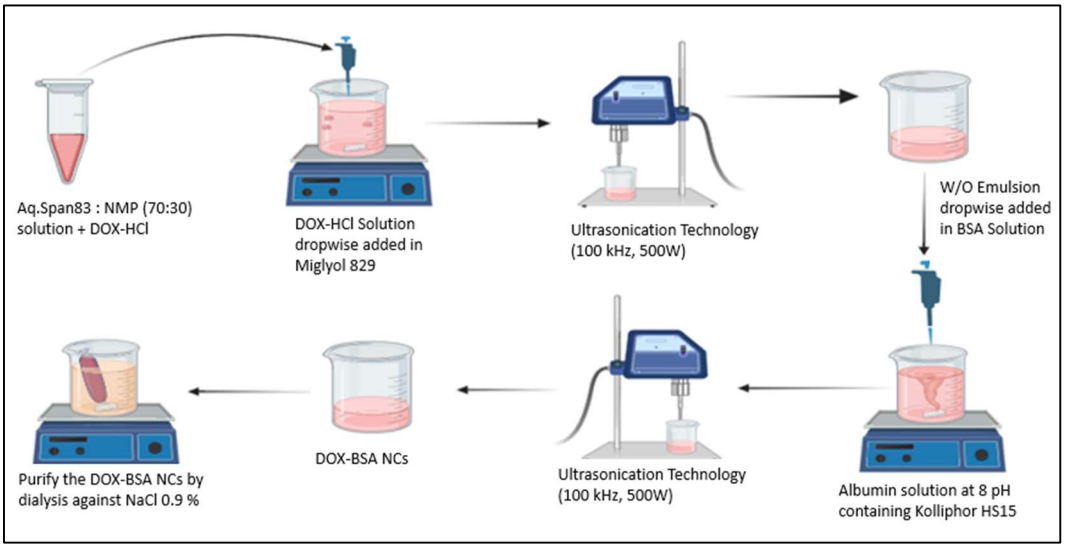

Figure 8.7. Representative scheme of the preparation by utilizing the Ultrasonication technique (20KHZ, 500W) to prepare the DOX-BSA- NCs

8.8 Bovine Serum Albumin Nanocapsules Conjugation with ICOS-Fc Human

The conjugation of BSA-NCs with ICOS-Fc involves the following procedure: Initially, 58 µL of ICOS-Fc solution (1.75 mg/mL) is combined with 42 µL of PBS (pH 7.4) in an Eppendorf tube. To this mixture, 25 µL of EDC (1-Ethyl-3-(3-dimethylaminopropyl) carbodiimide, 0.4 mg/mL in water) and 25 µL of NHS (N-Hydroxysuccinimide, 0.6 mg/mL in water) are added. The resultant mixture is then stirred for 15 minutes. Following this, 900 µL of BSA-NCs are introduced into the Eppendorf tube containing the ICOS-Fc solution. This solution is stirred at a speed of 800 RPM for 2 hours. Finally, the conjugated product is purified through dialysis against a 0.9% NaCl solution for 1 hour. This process effectively facilitates the conjugation of Blank BSA-NCs with ICOS-Fc. The process used to conjugate ICOS-Fc with BSA-NCs is also employed the same to conjugate ICOS-Fc with DOX-BSA-NCs.

EDC (1-Ethyl-3-(3-dimethylaminopropyl) carbodiimide) is a water-soluble carbodiimide that is commonly used to conjugate carboxyl groups to primary amines. Albumin, such as bovine serum albumin (BSA), has multiple carboxyl and amine groups that can participate in such conjugation reactions. When EDC is conjugated with albumin, the carbodiimide activates the carboxyl groups on the albumin, forming an O-acylisourea intermediate. This intermediate can then react with the primary amine groups to form a stable amide bond, resulting in conjugation.

8.9 Physicochemical Characterisation of Nanocapsules

The procedures for physicochemical characterisation, FTIR analysis, and *in vitro* release studies of DOX-BSA NCs have already been discussed in detail in the section 7.6. The quantification of ICOS-Fc can be achieved through the utilisation of a bicinchoninic acid (BCA) assay. This method involves the generation of a standard curve using serially diluted bovine serum albumin (BSA). Subsequently, ICOS-Fc conjugated NCs formulations are mixed with the working BCA reagent according to the BCA kit protocol as previously discussed in chapter 6. The absorbance of both standards and samples is measured at a wavelength, around 562 nm. The generated standard curve, which correlates absorbance values to known protein concentrations, is employed to determine the ICOS-Fc concentration within unknown samples based on their respective absorbance measurements.

The *In vitro* release profiles of DOX-BSA NCs and DOX-BSA ICOS-Fc NCs were examined to determine the mechanism of drug release. Four different kinetic models were used for analysis: the zero-order kinetic model, the first-order kinetic model, the simplified Higuchi model, and the Korsmeyer-Peppas model [250]. To obtain the rate constant and correlation value a graph of each model was created by using Microsoft Excel 2021 and a linear regression fit was applied. In the zero-order, the cumulative percentage of drug release was plotted against time. The cumulative percentage of drugs left against time was logarithmically shown in the first order. The Korsmeyer-Peppas model was examined by graphing the logarithm of the cumulative per cent drug release against the logarithm of time. In contrast, the Higuchi model

was evaluated by plotting the cumulative percentage of drug release against the square root of time [251].

The doxorubicin albumin Nanocapsules' hemolytic activity was assessed using mice blood. For this preparation, PBS (pH 7.4) was used to dilute the blood 1:10 v/v. As a positive control, red blood cell rupturing and additional haemoglobin release were treated by the presence of Triton x (1%). Saline solution (NaCl 0.9% w/v) was employed as a negative control. All NCs samples were diluted in 1 mL of blood with (1:10, 1:50, 1:100, 1:200, 1:400, and 1:500) and incubated for 90 min at 37 °C. Following a 20-minute centrifugation at 6000 rpm all NCs samples, the supernatant were examined at 540 nm using an ultraviolet-visible spectrophotometer (DU 730, Beckman Coulter, Fullerton, CA). The positive control, which represented 100% hemolysis, was used to compute the percentage of hemolysis [252].

A study was carried out aimed to assess the average diameter, zeta potential, and morphology of the albumin NCs formulations stored at 4°C for up to six months. Additionally, the stability of the albumin nanocapsule formulations was evaluated under physiological conditions at 37°C with Seronorm Human Plasma. Briefly, take a Seronorm Human Plasma solution 1:10 ratio v/v diluted with the PBS buffer pH 7.4, Individually, all types of NCs are diluted with the seronorm human plasma solution, mixed properly using vortex and incubate at 37°C for 1 hour and analyses all the sample on Dynamic Light Scattering (DLS).

8.10 Results

A specific type of NCs was prepared experiment a tuned double-emulsion (W/O/W) combined the ultrasonication technique using bovine serum albumin (BSA). This manufacturing method involved carefully tuning the preparation process to achieve the desired characteristics of the albumin NCs. A graphical representation of the tuned preparation method is reported in Figure 7.8. The DOX-BSA NCs were successfully prepared and conjugated with the inducible costimulatory molecule ICOS-Fc (DOX- ICOS-Fc-BSA- NCs).

The nanocapsules formulations and conjugated with ICOS-Fc have an average diameter between 250 and 290 nm, The formulations show the negative zeta

potential is about -30 m/v due to the presence of carboxyl groups of albumins. The characteristics of BSA-NCs are shown in Table 8.6 and Figure 8.5.

Table 8.5. Physicochemical Characterization of Nanocapsules

Nanocapsules	Average Diameter ± SD (nm)	PDI	Zeta Potential ± SD (mv)
Blank-BSA NCs	253.2 ± 4.1	0.22 ± 0.01	-29.32 ± 2.80
DOX-BSA NCs	270.8 ± 4.9	0.21 ± 0.02	-31.37 ± 3.72
DOX-BSA-ICOS-Fc NCs	275.6 ± 5.6	0.21 ± 0.01	-30.34 ± 3.23

± standard deviation (n=5)

NTA analysis results are reported in Figure 8.8

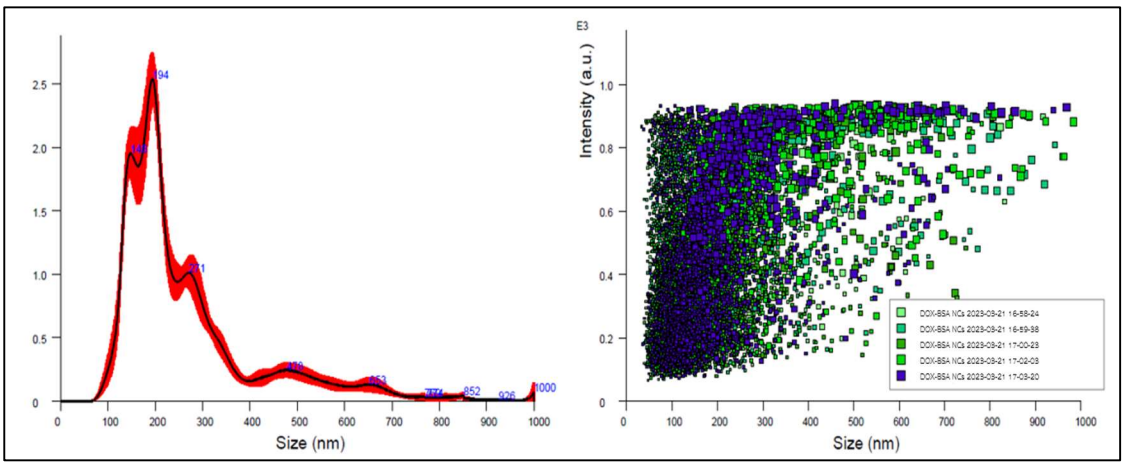

Figure 8.8. Particle size distribution analysis of DOX-BSA NCPSs by the Nanoparticle tracking analysis instrument (Nano Sight Amesbury, United Kingdom), 1) Average particle concentration/size 2) Intensity/size, for experiment.

Encapsulation efficiency and drug loading of DOX-BSA NCs and DOX-BSA NCs conjugated with ICOS-Fc were analysed by high-performance liquid chromatography (HPLC). The results of the analysis revealed a high encapsulation efficiency is about 90 to 95 % and good drug loading capacity as shown in Table 8.6.

Table 8.6 Encapsulation efficiency and Drug loading of Nanocapsules

Nanocapsules	Encapsulation Efficiency (EE %)	Drug Loading (DL %)
DOX-BSA NCs	95.01 ± 2.50	5.43 ± 0.79
DOX-BSA-ICOS-Fc NCs	93.45 ± 3.54	5.29 ± 0.62

A Fourier-transform infrared (FTIR) was used to correlate the drug and albumin with the use of FTIR spectroscopy, which allows for the characterization of molecular vibrations and interactions within a given sample. O-H Stretching around 3320-3380 cm^{-1}. This peak arises due to the stretching vibrations of hydroxyl (OH) groups present and C=O Stretching around 1610-1650 cm^{-1}. This broad peak corresponds to the carbonyl (C=O) stretching vibrations in doxorubicin. This peaks the present in the DOX-BSA NCs. It's confirmed that the albumin NCs drug incorporation through FTIR analysis is noteworthy as it provides valuable evidence of successful drug encapsulation or binding within the nanocapsule system as shown in Figure 8.9.

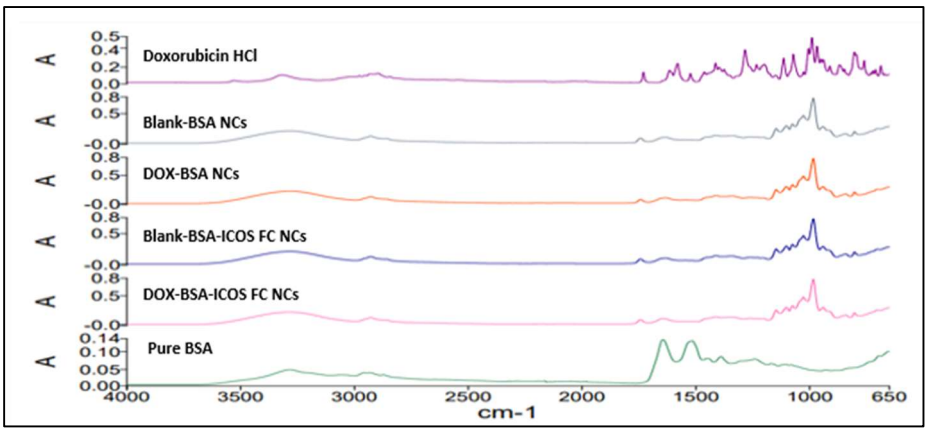

Figure 8.9. Fourier Transform Infrared Spectroscopy FTIR spectra of free DOX, DOX-loaded Nanocapsules (DOX-BSA NCs), Blank BSA Nanocapsules (Blank BSA-NCs) and both with ICOS-Fc

The *in vitro* release kinetics profile of doxorubicin from two different formulations was investigated. Figure 8.10 illustrate the *in vitro* release kinetics profiles of DOX-BSA NCs and DOX-BSA NCs conjugated with the ICOS-Fc. The results demonstrated that both formulations exhibited prolonged release of the drug over time, indicating sustained drug release compared to the doxorubicin-free solution diffusion. This indicates that the encapsulation of doxorubicin within the albumin nanocapsules, as well as the conjugation with ICOS-Fc, has influenced the release behaviour of the drug. After 24 hours, approximately 33% of the encapsulated drug was released from the DOX-BSA NCs, while about 24% of the drug was released from the DOX-BSA ICOS-Fc NCs. This suggests that the ICOS-Fc conjugation resulted in a slight reduction in the release rate of the drug in comparison to the non-conjugated DOX-BSA NCs.

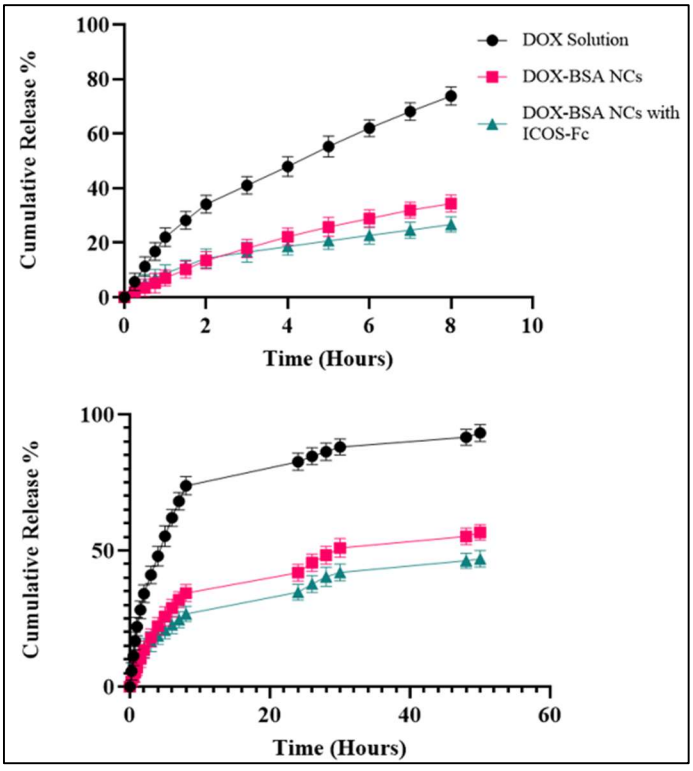

Figure 8.10. In-vitro release study of Dox-BSA NCs, Dox-BSA ICOS-Fc and Dox free solution as a release up to 8 hours and 50 hours, ± SD (n=5)

The prolonged release of doxorubicin from NCs is likely due to the slow diffusion of the drug through albumin. The aforementioned mechanism allows for the minimisation of doxorubicin's possible systemic adverse effects while simultaneously

increasing the efficiency of NCs at the targeted site. Furthermore, the drug release mechanism was investigated utilising four mathematical kinetics models: first-order kinetics, zero-order kinetics, and simplified Higuchi and Korsmeyer-Peppas models. Each kinetics model was employed to generate a graph in Microsoft Excel 2021, and the rate constant and correlation values were obtained through a linear regression fit, as illustrated in Figure 8.11. The *in vitro* release experiment using mathematical kinetics models demonstrated a preference for the first-order kinetic model in both DOX-BSA NCs and DOX-BSA ICOS-Fc NCs formulations. This indicates that the drug release from these Nanocapsules follows a first-order kinetics pattern, where the rate of release is directly proportional to the remaining drug concentration within the Nanocapsules. As the drug concentration decreases over time, the rate of release also decreases proportionally. Analysing the drug release behaviour using the first-order kinetic model allows for the estimation of release rate, prediction of the amount of drug released over time, and optimization of the formulation to achieve the desired release profile.

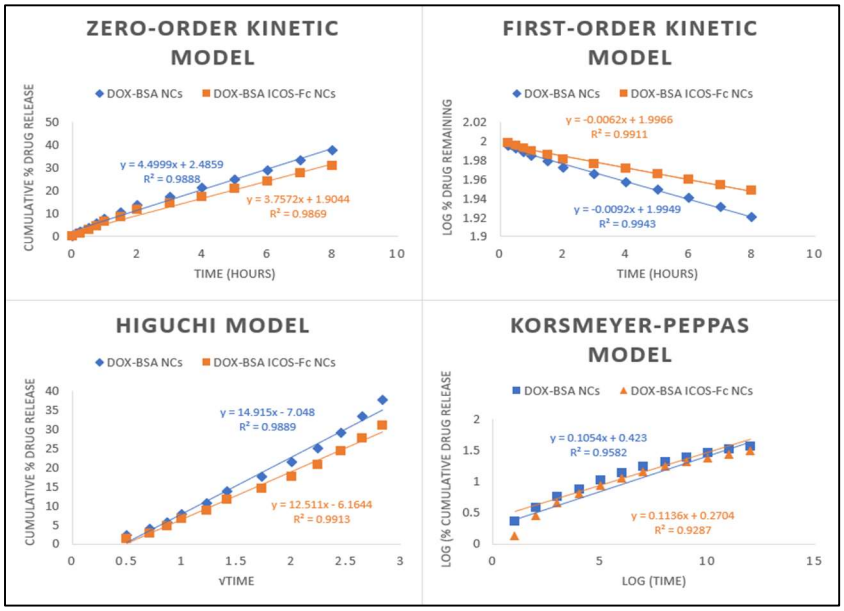

Figure 8.11. The mathematical modelling of doxorubicin release from Dox-BSA NCs and Dox-BSA ICOS-Fc NCs was performed by plotting the data and determining the preference of each kinetic model.

Table 8.8 Kinetics Model obtained R2 values

Kinetics Model	DOX-BSA NCs	DOX-BSA ICOS-Fc NCs
	R^2	
Zero-order	0.9888	0.9869
First order	0.9911	0.9943
Higuchi model	0.9889	0.9913
Korsmeyer-Peppas model	0.9582	0.9287

BSA NCs and DOX-BSA NCs were subjected to testing at various dilutions (1:10, 1:50, 1:100, 1:200, 1:400, and 1:500 v/v) to evaluate their hemolytic activity. The results indicated no significant hemolytic activity, as there was no observable damage to red blood cells when compared to the control as shown in the 8.12. These findings suggest that the tested nanocapsule formulation is biocompatible and can be safely administered in the cell lines of osteosarcoma without causing hemolytic complications.

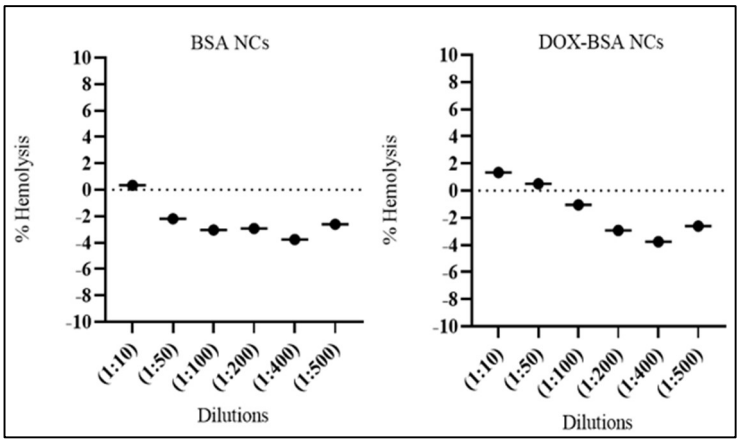

Figure 8.12 Haemolysis Study of BSA-NCs and DOX-BSA NCs

The results of the study showed that all type of albumin NCs formulations maintained their physical properties, including size, zeta potential, and morphology, for up to six months of storage at 4°C. Moreover, NCs under physiological conditions

at 37°C indicated that the formulations were stable in the presence of Seronorm Human Plasma. This indicates that the formulations were stable under these conditions, which is an important parameter for the development of stable and reliable drug delivery systems.

DOX-BSA NCs, modified with ICOS-Fc conjugation on their surface, serve a multifaceted purpose in enhancing cancer therapy. These Nanocapsules are designed to amplify the cytotoxicity of doxorubicin against U2OS cells, a type of cancer cell, by addressing a pivotal challenge: the premature removal of the drug by P-glycoproteins. By effectively shielding doxorubicin, the ICOS-Fc-conjugated Nanocapsules prevent its expulsion from cancer cells, thereby intensifying its anticancer activity. Furthermore, this targeted drug delivery system not only bolsters the efficacy of doxorubicin but also presents an avenue to mitigate the adverse effects associated with high drug dosages. By concentrating the drug payload directly at the tumour site, the system permits a reduction in the overall doxorubicin dose required, thereby diminishing the occurrence and severity of systemic side effects, which often limit the tolerability of chemotherapy.

In addition to its drug delivery function, the inclusion of ICOS-Fc on the nanocapsule surface contributes to the suppression of cellular metastasis, a critical aspect of cancer progression. ICOS-Fc serves as an immunomodulatory agent, potentially engaging the immune system to recognize and combat cancer cells, thus offering a comprehensive and multi-pronged approach to cancer therapy.

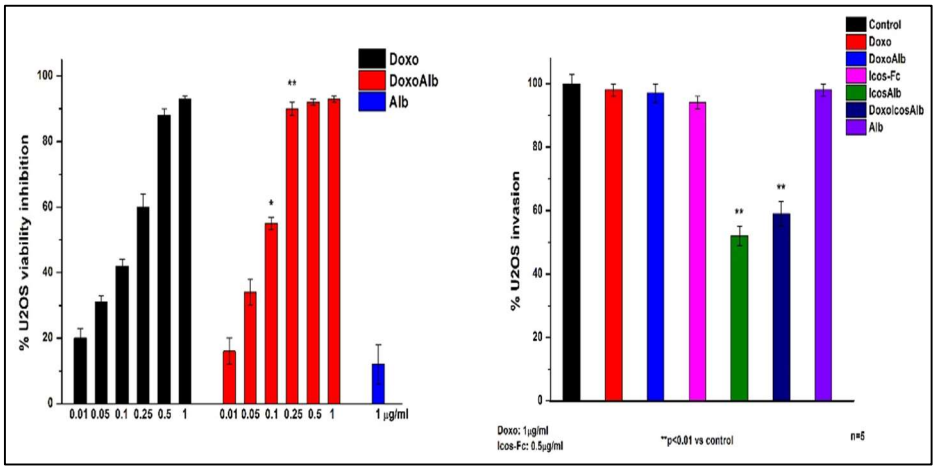

Figure 8.13. The Viability Inhibition and Invasion on Osteosarcoma cells line U2OS

DOX-BSA NCs are more effective than conventional doxorubicin in inhibiting cell growth within the dose range of 0.01-1 μg/mL after a 72-hour treatment period. This indicates their improved ability to impede cellular proliferation, which is a crucial aspect of cancer therapy. It is noteworthy that these specialized DOX-BSA NCs, which are conjugated with ICOS-Fc on their surface, can effectively inhibit the metastatic spread of cancer cells when administered at a safe concentration of only 1 μg/mL for 6 hours. This effect is similar to that of Nanocapsules that exclusively bind with ICOS-Fc. This finding has significant clinical relevance as it implies the potential to combat cancer metastasis without the use of high doses that could be harmful to the patient. Additionally, ICOS-Fc has demonstrated some effectiveness in limiting cellular invasion when used alone at a concentration of 1 μg/mL. However, it is worth noting that the anti-metastatic potential is significantly enhanced when delivered via NCs. Its activity increases twentyfold and it can effectively operate at a much lower concentration of 0.5 μg/mL. BSA-based delivery systems significantly enhance the anti-metastatic properties of ICOS-Fc, offering a promising strategy for metastasis control while mitigating the risk of adverse effects associated with higher drug concentrations.

Chapter 9: Conclusion

This PhD thesis presents a comprehensive study on the preparation and optimisation of albumin-based drug delivery systems. Improved manufacturing processes to produce albumin nanoformulation with physicochemical characteristics suitable for the design of drug delivery systems were investigated.

The research successfully demonstrates the potential of advanced manufacturing technologies, including surfactant-mediated coacervation, ultrasonication (US), microwave-assisted (MW), and combined MW/US technologies. The utilisation of advanced manufacturing technologies and meticulous process parameter tuning enabled the generation of high-quality albumin nanoparticles and nanocapsules with desirable characteristics for drug delivery applications. By fine-tuning process parameters and formulation conditions, the study achieved optimal physicochemical characteristics, including particle size, polydispersity index (PDI), zeta potential, encapsulation efficiency, in vitro drug release, and stability. These characteristics were aligned with the quality target attributes outlined in the ICH Q8 guidelines.

The research made use of both bovine serum albumin (BSA) and human serum albumin (HSA) in the development of the nanoparticles and nanocapsules. BSA was employed as a cost-effective model for initial studies, while HSA was selected due to its compatibility with human physiology. The stepwise optimisation process ensured that the same quality attributes achieved with BSA formulations were successfully adapted to HSA, thereby further validating the versatility of albumin as a nanocarrier.

A significant contribution of this thesis is the integration of sustainable, green manufacturing processes. By utilising microwave (MW), ultrasonication (US) and combined MW/US technologies, the study was successfully conducted without the use of organic solvents, thereby offering a more environmentally friendly approach to nanomedicine production.

The encapsulation of doxorubicin hydrochloride, a well-known anticancer drug, into these albumin nanocapsules, illustrates the potential therapeutic benefits of the developed systems. The surface modifications of these nanocapsules with ICOS-Fc ligands enabled targeted delivery to osteosarcoma cancer cell lines, thereby improving drug efficacy and reducing the incidence of cytotoxic side effects. This

targeted approach serves to enhance the therapeutic index of the drug, thereby representing a significant advancement in the field of cancer treatment.

This aligns with the growing need for greener albumin nanomedicine manufacturing practices, making this work not only scientifically innovative but also environmentally responsible.

References

1. Larsen, M.T.; Kuhlmann, M.; Hvam, M.L.; Howard, K.A. Albumin-Based Drug Delivery: Harnessing Nature to Cure Disease. *Mol. Cell. Ther.* **2016**, *4*, 1–12, doi:10.1186/s40591-016-0048-8.

2. Elzoghby, A.O.; Samy, W.M.; Elgindy, N.A. Albumin-Based Nanoparticles as Potential Controlled Release Drug Delivery Systems. *J. Control. Release* **2012**, *157*, 168–182, doi:10.1016/j.jconrel.2011.07.031.

3. Kratz, F. Albumin as a Drug Carrier: Design of Prodrugs, Drug Conjugates and Nanoparticles. *J. Control. Release* **2008**, *132*, 171–183, doi:10.1016/j.jconrel.2008.05.010.

4. Giovannini, I.; Chiarla, C.; Giuliante, F.; Vellone, M.; Ardito, F.; Nuzzo, G. The Relationship between Albumin, Other Plasma Proteins and Variables, and Age in the Acute Phase Response after Liver Resection in Man. *Amino Acids* **2006**, *31*, 463–469, doi:10.1007/s00726-005-0287-5.

5. Bernardi, M.; Ricci, C.S.; Zaccherini, G. Role of Human Albumin in the Management of Complications of Liver Cirrhosis. *J. Clin. Exp. Hepatol.* **2014**, *4*, 302–311, doi:10.1016/j.jceh.2014.08.007.

6. Fanali, G.; Di Masi, A.; Trezza, V.; Marino, M.; Fasano, M.; Ascenzi, P. Human Serum Albumin: From Bench to Bedside. *Mol. Aspects Med.* **2012**, *33*, 209–290, doi:10.1016/j.mam.2011.12.002.

7. Mishra, V.; Heath, R.J. Structural and Biochemical Features of Human Serum Albumin Essential for Eukaryotic Cell Culture. *Int. J. Mol. Sci.* **2021**, *22*, doi:10.3390/ijms22168411.

8. Fu, Q.; Sun, J.; Zhang, W.; Sui, X.; Yan, Z.; He, Z. Nanoparticle Albumin-Bound (NAB) Technology Is a Promising Method for Anti-Cancer Drug Delivery. *Recent Pat. Anticancer. Drug Discov.* **2009**, *4*, 262–272, doi:10.2174/157489209789206869.

9. Zsila, F. Subdomain IB Is the Third Major Drug Binding Region of Human Serum Albumin: Toward the Three-Sites Model. *Mol. Pharm.* **2013**, *10*, 1668–1682, doi:10.1021/mp400027q.

10. Naveenraj, S.; Anandan, S. Binding of Serum Albumins with Bioactive Substances - Nanoparticles to Drugs. *J. Photochem. Photobiol. C Photochem. Rev.* **2013**, *14*, 53–71, doi:10.1016/j.jphotochemrev.2012.09.001.

11. Karimi, M.; Bahrami, S.; Ravari, S.B.; Zangabad, P.S.; Mirshekari, H.; Bozorgomid, M.; Shahreza, S.; Sori, M.; Hamblin, M.R. Albumin Nanostructures as Advanced Drug Delivery Systems. *Expert Opin. Drug Deliv.* **2016**, *13*, 1609–1623, doi:10.1080/17425247.2016.1193149.

12. Hutapea, T.P.H.; Madurani, K.A.; Syahputra, M.Y.; Hudha, M.N.; Asriana, A.N.; Suprapto; Kurniawan, F. Albumin: Source, Preparation, Determination, Applications, and Prospects. *J. Sci. Adv. Mater. Devices* **2023**, *8*, 100549, doi:10.1016/j.jsamd.2023.100549.

13. Sun, D.; Xie, J.; Chen, C.J.; Liu, J.T. Analyzation of the Binding Mechanism and the Isoelectric Point of Glycated Albumin with Self-Assembled, Aptamer-Conjugated Films by Using Surface Plasmon Resonance. *Colloids Surfaces B Biointerfaces* **2022**, *214*, 112445, doi:10.1016/j.colsurfb.2022.112445.

14. Turell, L.; Botti, H.; Bonilla, L.; Torres, M.J.; Schopfer, F.; Freeman, B.A.; Armas, L.; Ricciardi, A.; Alvarez, B.; Radi, R. HPLC Separation of Human Serum Albumin Isoforms Based on Their Isoelectric Points. *J. Chromatogr. B Anal. Technol. Biomed. Life Sci.* **2014**, *944*, 144–151, doi:10.1016/j.jchromb.2013.11.019.

15. Galisteo-González, F.; Molina-Bolívar, J.A.; Navarro, S.A.; Boulaiz, H.; Aguilera-Garrido, A.; Ramírez, A.; Marchal, J.A. Albumin-Covered Lipid Nanocapsules Exhibit Enhanced Uptake Performance by Breast-Tumor Cells. *Colloids Surfaces B Biointerfaces* **2018**, *165*, 103–110, doi:10.1016/j.colsurfb.2018.02.024.

16. Li, J.M.; Chen, W.; Wang, H.; Jin, C.; Yu, X.J.; Lu, W.Y.; Cui, L.; Fu, D.L.; Ni, Q.X.; Hou, H.M. Preparation of Albumin Nanospheres Loaded with Gemcitabine and Their Cytotoxicity against BXPC-3 Cells in Vitro. *Acta Pharmacol. Sin.* **2009**, *30*, 1337–1343, doi:10.1038/aps.2009.125.

17. Sebak, S.; Mirzaei, M.; Malhotra, M.; Kulamarva, A.; Prakash, S. Human Serum Albumin Nanoparticles as an Efficient Noscapine Drug Delivery System for Potential Use in Breast Cancer: Preparation and in Vitro Analysis. *Int. J. Nanomedicine* **2010**, *5*,

525–532, doi:10.2147/IJN.S10443.

18. Kuten Pella, O.; Hornyák, I.; Horváthy, D.; Fodor, E.; Nehrer, S.; Lacza, Z. Albumin as a Biomaterial and Therapeutic Agent in Regenerative Medicine. *Int. J. Mol. Sci.* **2022**, *23*, doi:10.3390/ijms231810557.

19. Spada, A.; Emami, J.; Tuszynski, J.A.; Lavasanifar, A. The Uniqueness of Albumin as a Carrier in Nanodrug Delivery. *Mol. Pharm.* **2021**, *18*, 1862–1894, doi:10.1021/acs.molpharmaceut.1c00046.

20. Kratz, F. A Clinical Update of Using Albumin as a Drug Vehicle - A Commentary. *J. Control. Release* **2014**, *190*, 331–336, doi:10.1016/j.jconrel.2014.03.013.

21. Zheng, Y.R.; Suntharalingam, K.; Johnstone, T.C.; Yoo, H.; Lin, W.; Brooks, J.G.; Lippard, S.J. Pt(IV) Prodrugs Designed to Bind Non-Covalently to Human Serum Albumin for Drug Delivery. *J. Am. Chem. Soc.* **2014**, *136*, 8790–8798, doi:10.1021/ja5038269.

22. Bhushan, B.; Khanadeev, V.; Khlebtsov, B.; Khlebtsov, N.; Gopinath, P. Impact of Albumin Based Approaches in Nanomedicine: Imaging, Targeting and Drug Delivery. *Adv. Colloid Interface Sci.* **2017**, *246*, 13–39, doi:10.1016/j.cis.2017.06.012.

23. Spada, A.; Emami, J.; Sanaee, F.; Aminpour, M.; Paiva, I.M.; Tuszynski, J.A.; Lavasanifar, A. Albumin Nanoparticles for the Delivery of a Novel Inhibitor of β-Tubulin Polymerization. *J. Pharm. Pharm. Sci.* **2021**, *24*, 344–362, doi:10.18433/jpps31877.

24. Bertucci, C.; Domenici, E. Reversible and Covalent Binding of Drugs to Human Serum Albumin: Methodological Approaches and Physiological Relevance. *Curr. Med. Chem.* **2012**, *9*, 1463–1481, doi:10.2174/0929867023369673.

25. Acharya, V. V.; Chaudhuri, P. Modalities of Protein Denaturation and Nature of Denaturants. *Int. J. Pharm. Sci. Rev. Res.* **2021**, *69*, 19–24, doi:10.47583/ijpsrr.2021.v69i02.002.

26. Tanford, C. Protein Denaturation. In; Anfinsen, C.B., Anson, M.L., Edsall, J.T., Richards, F.M., Eds.; Advances in Protein Chemistry; Academic Press, 2003; Vol. 23, pp. 121–282.

27. Neurath, H.; Greenstein, J.P.; Putnam, F.W.; Erickson, J.O. The Chemistry of Protein Denaturation. *Chem. Rev.* **2003**, *34*, 157–265, doi:10.1021/cr60108a003.

28. Anson, M.L. Protein Denaturation and the Properties of Protein Groups. In; Anson, M.L., Edsall, J.T., Eds.; Advances in Protein Chemistry; Academic Press, 2003; Vol. 2, pp. 361–386.

29. Kunugi, S.; Tanaka, N. Cold Denaturation of Proteins under High Pressure. *Biochim. Biophys. Acta - Protein Struct. Mol. Enzymol.* **2002**, *1595*, 329–344, doi:10.1016/S0167-4838(01)00354-5.

30. Camilloni, C.; Guerini Rocco, A.; Eberini, I.; Gianazza, E.; Broglia, R.A.; Tiana, G. Urea and Guanidinium Chloride Denature Protein L in Different Ways in Molecular Dynamics Simulations. *Biophys. J.* **2008**, *94*, 4654–4661, doi:10.1529/biophysj.107.125799.

31. Almarza, J.; Rincon, L.; Bahsas, A.; Brito, F. Molecular Mechanism for the Denaturation of Proteins by Urea. *Biochemistry* **2009**, *48*, 7608–7613, doi:10.1021/bi9007116.

32. Attia, M.S.; Radwan, M.F.; Ibrahim, T.S.; Ibrahim, T.M. Development of Carvedilol-Loaded Albumin-Based Nanoparticles with Factorial Design to Optimize In Vitro and In Vivo Performance. *Pharmaceutics* **2023**, *15*, doi:10.3390/pharmaceutics15051425.

33. Daniel, R.M.; Dines, M.; Petach, H.H. The Denaturation and Degradation of Stable Enzymes at High Temperatures. *Biochem. J.* **1996**, *317*, 1–11, doi:10.1042/bj3170001.

34. Grigera, J.R.; McCarthy, A.N. The Behavior of the Hydrophobic Effect under Pressure and Protein Denaturation. *Biophys. J.* **2010**, *98*, 1626–1631, doi:10.1016/j.bpj.2009.12.4298.

35. Acampora, G.; Hermans, J. Reversible Denaturation of Sperm Whale Myoglobin. I. Dependence on Temperature, PH, and Composition1. **1967**, *21*, 1543–1547.

36. Takeda, K.; Wada, A.; Yamamoto, K.; Moriyama, Y.; Aoki, K. Conformational Change of Bovine Serum Albumin by Heat Treatment. *J. Protein Chem.* **1989**, *8*, 653–659, doi:10.1007/BF01025605.

37. Herskovits, T.T.; Gadegbeku, B.; Jaillet, H. On the Structural Stability and Solvent

Denaturation of Proteins. *J. Biol. Chem.* **1971**, *246*, 6370, doi:10.1016/s0021-9258(18)61801-0.

38. Saha, S.; Ramesh, R. Nanotechnology for Controlled Drug Delivery System. *Int. J. PharmTech Res.* **2015**, *7*, 616–628.

39. Wang, Z.; Li, Z.; Zhang, D.; Miao, L.; Huang, G. Development of Etoposide-Loaded Bovine Serum Albumin Nanosuspensions for Parenteral Delivery. *Drug Deliv.* **2015**, *22*, 79–85, doi:10.3109/10717544.2013.871600.

40. Zhang, J.-Y.; He, B.; Qu, W.; Cui, Z.; Wang, Y.; Zhang, H.; Wang, J.-C.; Zhang, Q. Preparation of the Albumin Nanoparticle System Loaded with Both Paclitaxel and Sorafenib and Its Evaluation in Vitro and in Vivo. *J. Microencapsul.* **2011**, *28*, 528–536, doi:10.3109/02652048.2011.590614.

41. Lee, J.E.; Kim, M.G.; Jang, Y.L.; Lee, M.S.; Kim, N.W.; Yin, Y.; Lee, J.H.; Lim, S.Y.; Park, J.W.; Kim, J.; et al. Self-Assembled PEGylated Albumin Nanoparticles (SPAN) as a Platform for Cancer Chemotherapy and Imaging. *Drug Deliv.* **2018**, *25*, 1570–1578, doi:10.1080/10717544.2018.1489430.

42. Wiedermann, C.J. Moderator Effect of Hypoalbuminemia in Volume Resuscitation and Plasma Expansion with Intravenous Albumin Solution. *Int. J. Mol. Sci.* **2022**, *23*, doi:10.3390/ijms232214175.

43. Gremese, E.; Bruno, D.; Varriano, V.; Perniola, S.; Petricca, L.; Ferraccioli, G. Serum Albumin Levels: A Biomarker to Be Repurposed in Different Disease Settings in Clinical Practice. *J. Clin. Med.* **2023**, *12*, doi:10.3390/jcm12186017.

44. Honary, S.; Jahanshahi, M.; Golbayani, R.; Ebrahimi, R.; Ghajar, K. Doxorubicin-Loaded Albumin Nanoparticles: Formulation and Characterization. *J. Nanosci. Nanotechnol.* **2010**, *10*, 7752–7757, doi:10.1166/jnn.2010.2832.

45. Grela, E.; Stączek, S.; Nowak, M.; Pawlikowska-Pawlega, B.; Zdybicka-Barabas, A.; Janik, S.; Cytryńska, M.; Grudzinski, W.; Gruszecki, W.I.; Luchowski, R. Enhanced Antifungal Activity of Amphotericin B Bound to Albumin: A “Trojan Horse” Effect of the Protein. *J. Phys. Chem. B* **2023**, *127*, 3632–3640, doi:10.1021/acs.jpcb.3c01168.

46. Rustgi, V.K. Albinterferon Alfa-2b, a Novel Fusion Protein of Human Albumin and

Human Interferon Alfa-2b, for Chronic Hepatitis C. *Curr. Med. Res. Opin.* **2009**, *25*, 991–1002, doi:10.1185/03007990902779186.

47. Wu, J.Z.; Williams, G.R.; Li, H.Y.; Wang, D.X.; Li, S. De; Zhu, L.M. Insulin-Loaded Plga Microspheres for Glucose-Responsive Release. *Drug Deliv.* **2017**, *24*, 1513–1525, doi:10.1080/10717544.2017.1381200.

48. Xia, T.; Jiang, X.; Deng, L.; Yang, M.; Chen, X. Albumin-Based Dynamic Double Cross-Linked Hydrogel with Self-Healing Property for Antimicrobial Application. *Colloids Surfaces B Biointerfaces* **2021**, *208*, 112042, doi:https://doi.org/10.1016/j.colsurfb.2021.112042.

49. Tessler, L.A.; Donahoe, C.D.; Garcia, D.J.; Jun, Y.-S.; Elbert, D.L.; Mitra, R.D. Nanogel Surface Coatings for Improved Single-Molecule Imaging Substrates. *J. R. Soc. Interface* **2011**, *8*, 1400–1408, doi:10.1098/rsif.2010.0669.

50. Lallemand, F.; Schmitt, M.; Bourges, J.-L.; Gurny, R.; Benita, S.; Garrigue, J.-S. Cyclosporine A Delivery to the Eye: A Comprehensive Review of Academic and Industrial Efforts. *Eur. J. Pharm. Biopharm.* **2017**, *117*, 14–28, doi:https://doi.org/10.1016/j.ejpb.2017.03.006.

51. Zhu, G.; Lynn, G.M.; Jacobson, O.; Chen, K.; Liu, Y.; Zhang, H.; Ma, Y.; Zhang, F.; Tian, R.; Ni, Q.; et al. Albumin/Vaccine Nanocomplexes That Assemble in Vivo for Combination Cancer Immunotherapy. *Nat. Commun.* **2017**, *8*, 1954, doi:10.1038/s41467-017-02191-y.

52. Hassanin, I.; Elzoghby, A. Albumin-Based Nanoparticles: A Promising Strategy to Overcome Cancer Drug Resistance. *Cancer Drug Resist.* **2020**, *3*, 930–946, doi:10.20517/cdr.2020.68.

53. Zhao, M.; Lei, C.; Yang, Y.; Bu, X.; Ma, H.; Gong, H.; Liu, J.; Fang, X.; Hu, Z.; Fang, Q. Abraxane, the Nanoparticle Formulation of Paclitaxel Can Induce Drug Resistance by Up-Regulation of P-Gp. *PLoS One* **2015**, *10*, e0131429, doi:10.1371/journal.pone.0131429.

54. Aadi Bioscience, I. Full Prescribing Information for FYARRO™ (Sirolimus Protein-Bound Particles for Injectable Suspension). **2021**, 1–19.

55. Gao, Y.; Nai, J.; Yang, Z.; Zhang, J.; Ma, S.; Zhao, Y.; Li, H.; Li, J.; Yang, Y.; Yang, M.; et al. A Novel Preparative Method for Nanoparticle Albumin-Bound Paclitaxel with High Drug Loading and Its Evaluation Both in Vitro and in Vivo. *PLoS One* **2021**, *16*, 1–25, doi:10.1371/journal.pone.0250670.

56. Squibb, B.M. ABRAXANE Patient Information. 22–23.

57. Lammers, T.; Kiessling, F.; Ashford, M.; Hennink, W.; Crommelin, D.; Strom, G. Cancer Nanomedicine: Is Targeting Our Target? *Nat. Rev. Mater.* **2016**, *1*, 1–4, doi:10.1038/natrevmats.2016.69.

58. Abraxane Approved for Metastatic Pancreatic Cancer. *Cancer Discov.* **2013**, *3*, OF3–OF3, doi:10.1158/2159-8290.CD-NB2013-137.

59. Zhao, P.; Wang, Y.; Wu, A.; Rao, Y.; Huang, Y. Roles of Albumin-Binding Proteins in Cancer Progression and Biomimetic Targeted Drug Delivery. *ChemBioChem* **2018**, *19*, 1796–1805, doi:10.1002/cbic.201800201.

60. Hama, M.; Ishima, Y.; Chuang, V.T.G.; Ando, H.; Shimizu, T.; Ishida, T. Evidence for Delivery of Abraxane via a Denatured-Albumin Transport System. *ACS Appl. Mater. Interfaces* **2021**, *13*, 19736–19744, doi:10.1021/acsami.1c03065.

61. Yuan, H.; Guo, H.; Luan, X.; He, M.; Li, F.; Burnett, J.; Truchan, N.; Sun, D. Albumin Nanoparticle of Paclitaxel (Abraxane) Decreases While Taxol Increases Breast Cancer Stem Cells in Treatment of Triple Negative Breast Cancer. *Mol. Pharm.* **2020**, *17*, 2275–2286, doi:10.1021/acs.molpharmaceut.9b01221.

62. Kampan, N.C.; Madondo, M.T.; McNally, O.M.; Quinn, M.; Plebanski, M. Paclitaxel and Its Evolving Role in the Management of Ovarian Cancer. *Biomed Res. Int.* **2015**, *2015*, 413076, doi:10.1155/2015/413076.

63. Kouchakzadeh, H.; Safavi, M.S.; Shojaosadati, S.A. *Efficient Delivery of Therapeutic Agents by Using Targeted Albumin Nanoparticles*; 1st ed.; Elsevier Inc., 2015; Vol. 98;.

64. Meng, R.; Zhu, H.; Wang, Z.; Hao, S.; Wang, B. Preparation of Drug-Loaded Albumin Nanoparticles and Its Application in Cancer Therapy. *J. Nanomater.* **2022**, *2022*, doi:10.1155/2022/3052175.

65. Sristi; Fatima, M.; Sheikh, A.; Almalki, W.H.; Talegaonkar, S.; Dubey, S.K.; Amin,

M.C.I.M.; Sahebkar, A.; Kesharwani, P. Recent Advancement on Albumin Nanoparticles in Treating Lung Carcinoma. *J. Drug Target.* **2023**, *31*, 486–499, doi:10.1080/1061186X.2023.2205609.

66. Vishnu, P.; Roy, V. Safety and Efficacy of Nab Paclitaxel in the Treatment of Patients with Breast Cancer. *Breast Cancer Basic Clin. Res.* **2011**, *5*, 53–65, doi:10.4137/BCBCR.S5857.

67. Annexure, E.C. Annex 1. *Scand. J. Rheumatol.* **2007**, *17*, 12, doi:10.3109/03009748809099213.

68. Ko, S.; Gunasekaran, S. Preparation of Sub-100-Nm Beta-Lactoglobulin (BLG) Nanoparticles. *J. Microencapsul.* **2006**, *23*, 887–898, doi:10.1080/02652040601035143.

69. Pathak, Y. V. *Surface Modification of Nanoparticles for Targeted Drug Delivery*; 2019; ISBN 9783030061159.

70. Loureiro, A.; G. Azoia, N.; C. Gomes, A.; Cavaco-Paulo, A. Albumin-Based Nanodevices as Drug Carriers. *Curr. Pharm. Des.* **2016**, *22*, 1371–1390, doi:10.2174/1381612822666160125114900.

71. Felice, B.; Prabhakaran, M.P.; Rodríguez, A.P.; Ramakrishna, S. Drug Delivery Vehicles on a Nano-Engineering Perspective. *Mater. Sci. Eng. C* **2014**, *41*, 178–195, doi:10.1016/j.msec.2014.04.049.

72. Srivastava, A.; Prajapati, A. Albumin and Functionalized Albumin Nanoparticles: Production Strategies, Characterization, and Target Indications. *Asian Biomed.* **2020**, *14*, 217–242, doi:10.1515/abm-2020-0032.

73. Li, F.Q.; Su, H.; Wang, J.; Liu, J.Y.; Zhu, Q.G.; Fei, Y.B.; Pan, Y.H.; Hu, J.H. Preparation and Characterization of Sodium Ferulate Entrapped Bovine Serum Albumin Nanoparticles for Liver Targeting. *Int. J. Pharm.* **2008**, *349*, 274–282, doi:10.1016/j.ijpharm.2007.08.001.

74. Tarhini, M.; Benlyamani, I.; Hamdani, S.; Agusti, G.; Fessi, H.; Greige-Gerges, H.; Bentaher, A.; Elaissari, A. Protein-Based Nanoparticle Preparation via Nanoprecipitation Method. *Materials (Basel).* **2018**, *11*, 1–18,

doi:10.3390/ma11030394.

75. Nguyen, H.H.; Ko, S. Preparation of Size-Controlled BSA Nanoparticles by Intermittent Addition of Desolvating Agent. *IFMBE Proc.* **2010**, *27*, 231–234, doi:10.1007/978-3-642-12020-6_58.

76. Wang, G.; Uludag, H. Recent Developments in Nanoparticle-Based Drug Delivery and Targeting Systems with Emphasis on Protein-Based Nanoparticles. *Expert Opin. Drug Deliv.* **2008**, *5*, 499–515, doi:10.1517/17425247.5.5.499.

77. Shen, Z.; Li, Y.; Kohama, K.; Oneill, B.; Bi, J. Improved Drug Targeting of Cancer Cells by Utilizing Actively Targetable Folic Acid-Conjugated Albumin Nanospheres. *Pharmacol. Res.* **2011**, *63*, 51–58, doi:10.1016/j.phrs.2010.10.012.

78. Cheng, K.; Sun, S.; Gong, X. Preparation, Characterization, and Antiproliferative Activities of Biotin-Decorated Docetaxel-Loaded Bovine Serum Albumin Nanoparticles. *Brazilian J. Pharm. Sci.* **2018**, *54*, 1–11, doi:10.1590/s2175-97902018000217295.

79. Choi, J.S.; Meghani, N. Impact of Surface Modification in BSA Nanoparticles for Uptake in Cancer Cells. *Colloids Surfaces B Biointerfaces* **2016**, *145*, 653–661, doi:10.1016/j.colsurfb.2016.05.050.

80. Abbasi, S.; Paul, A.; Prakash, S. Investigation of SiRNA-Loaded Polyethylenimine-Coated Human Serum Albumin Nanoparticle Complexes for the Treatment of Breast Cancer. *Cell Biochem. Biophys.* **2011**, *61*, 277–287, doi:10.1007/s12013-011-9201-9.

81. Zhao, D.; Zhao, X.; Zu, Y.; Li, J.; Zhang, Y.; Jiang, R.; Zhang, Z. Preparation, Characterization, and in Vitro Targeted Delivery of Folate-Decorated Paclitaxel-Loaded Bovine Serum Albumin Nanoparticles. *Int. J. Nanomedicine* **2010**, *5*, 669–677, doi:10.2147/IJN.S12918.

82. Onafuye, H.; Pieper, S.; Mulac, D.; Cinatl, J.; Wass, M.N.; Langer, K.; Michaelis, M. Doxorubicin-Loaded Human Serum Albumin Nanoparticles Overcome Transporter-Mediated Drug Resistance in Drug-Adapted Cancer Cells. *Beilstein J. Nanotechnol.* **2019**, *10*, 1707–1715, doi:10.3762/bjnano.10.166.

83. Anton, N.; Benoit, J.-P.; Saulnier, P. Design and Production of Nanoparticles

Formulated from Nano-Emulsion Templates-a Review. *J. Control. release Off. J. Control. Release Soc.* **2008**, *128*, 185–199, doi:10.1016/j.jconrel.2008.02.007.

84. Tadros, T.; Izquierdo, P.; Esquena, J.; Solans, C. Formation and Stability of Nano-Emulsions. *Adv. Colloid Interface Sci.* **2004**, *108–109*, 303–318, doi:10.1016/j.cis.2003.10.023.

85. Anton, N.; Vandamme, T.F. The Universality of Low-Energy Nano-Emulsification. *Int. J. Pharm.* **2009**, *377*, 142–147, doi:10.1016/j.ijpharm.2009.05.014.

86. Sahoo, S.K.; Parveen, S.; Panda, J.J. The Present and Future of Nanotechnology in Human Health Care. *Nanomedicine Nanotechnology, Biol. Med.* **2007**, *3*, 20–31, doi:10.1016/j.nano.2006.11.008.

87. Shimanovich, U.; Bernardes, G.J.L.; Knowles, T.P.J.; Cavaco-Paulo, A. Protein Micro- and Nano-Capsules for Biomedical Applications. *Chem. Soc. Rev.* **2014**, *43*, 1361–1371, doi:10.1039/c3cs60376h.

88. Anton, N.; Vandamme, T.F. The Universality of Low-Energy Nano-Emulsification. *Int. J. Pharm.* **2009**, *377*, 142–147, doi:10.1016/j.ijpharm.2009.05.014.

89. Anton, N.; Benoit, J.P.; Saulnier, P. Design and Production of Nanoparticles Formulated from Nano-Emulsion Templates-A Review. *J. Control. Release* **2008**, *128*, 185–199, doi:10.1016/j.jconrel.2008.02.007.

90. Giri, T.K.; Choudhary, C.; Ajazuddin; Alexander, A.; Badwaik, H.; Tripathi, D.K. Prospects of Pharmaceuticals and Biopharmaceuticals Loaded Microparticles Prepared by Double Emulsion Technique for Controlled Delivery. *Saudi Pharm. J.* **2013**, *21*, 125–141, doi:10.1016/j.jsps.2012.05.009.

91. Hawkins, M.J.; Soon-Shiong, P.; Desai, N. Protein Nanoparticles as Drug Carriers in Clinical Medicine. *Adv. Drug Deliv. Rev.* **2008**, *60*, 876–885, doi:10.1016/j.addr.2007.08.044.

92. Baier, S.; McClements, D.J. Impact of Preferential Interactions on Thermal Stability and Gelation of Bovine Serum Albumin in Aqueous Sucrose Solutions. *J. Agric. Food Chem.* **2001**, *49*, 2600–2608, doi:10.1021/jf001096j.

93. Nitta, S.K.; Numata, K. Biopolymer-Based Nanoparticles for Drug/Gene Delivery and

Tissue Engineering. *Int. J. Mol. Sci.* **2013**, *14*, 1629–1654, doi:10.3390/ijms14011629.

94. Navarra, G.; Giacomazza, D.; Leone, M.; Librizzi, F.; Militello, V.; San Biagio, P.L. Thermal Aggregation and Ion-Induced Cold-Gelation of Bovine Serum Albumin. *Eur. Biophys. J.* **2009**, *38*, 437–446, doi:10.1007/s00249-008-0389-6.

95. Nitta, S.K.; Numata, K. Biopolymer-Based Nanoparticles for Drug/Gene Delivery and Tissue Engineering. *Int. J. Mol. Sci.* **2013**, *14*, 1629–1654, doi:10.3390/ijms14011629.

96. Lee, S.H.; Heng, D.; Ng, W.K.; Chan, H.K.; Tan, R.B.H. Nano Spray Drying: A Novel Method for Preparing Protein Nanoparticles for Protein Therapy. *Int. J. Pharm.* **2011**, *403*, 192–200, doi:10.1016/j.ijpharm.2010.10.012.

97. He, X.; Xiang, N.; Zhang, J.; Zhou, J.; Fu, Y.; Gong, T.; Zhang, Z. Encapsulation of Teniposide into Albumin Nanoparticles with Greatly Lowered Toxicity and Enhanced Antitumor Activity. *Int. J. Pharm.* **2015**, *487*, 250–259, doi:10.1016/j.ijpharm.2015.04.047.

98. Chen, Y.; Liu, H.; Tang, Y.; Zhang, L.; Wu, X.; Guo, Q. Construction of Different Oil Phases - Based Nanoemulsion De- Livery Platform and Biodistribution Evaluation on Inflammato- Ry Cells and Animal Models. **2023**, 1–20, doi:10.20944/preprints202305.1164.v1.

99. Mohammad-Beigi, H.; Shojaosadati, S.A.; Morshedi, D.; Mirzazadeh, N.; Arpanaei, A. The Effects of Organic Solvents on the Physicochemical Properties of Human Serum Albumin Nanoparticles. *Iran. J. Biotechnol.* **2016**, *14*, 45–50, doi:10.15171/ijb.1168.

100. Ferrado, J.B.; Perez, A.A.; Visentini, F.F.; Islan, G.A.; Castro, G.R.; Santiago, L.G. Formation and Characterization of Self-Assembled Bovine Serum Albumin Nanoparticles as Chrysin Delivery Systems. *Colloids Surfaces B Biointerfaces* **2019**, *173*, 43–51, doi:10.1016/j.colsurfb.2018.09.046.

101. Steinhauser, I.M.; Langer, K.; Strebhardt, K.M.; Spänkuch, B. Effect of Trastuzumab-Modified Antisense Oligonucleotide-Loaded Human Serum Albumin Nanoparticles Prepared by Heat Denaturation. *Biomaterials* **2008**, *29*, 4022–4028, doi:10.1016/j.biomaterials.2008.07.001.

102. ZI, Z.; Li, X.; Duan, J.; Yang, X.-D. Targeted Treatment of Colon Cancer with Aptamer-

Guided Albumin Nanoparticles Loaded with Docetaxel. *Int. J. Nanomedicine* **2020**, *15*, 6737+.

103. Kim, T.H.; Jiang, H.H.; Youn, Y.S.; Park, C.W.; Tak, K.K.; Lee, S.; Kim, H.; Jon, S.; Chen, X.; Lee, K.C. Preparation and Characterization of Water-Soluble Albumin-Bound Curcumin Nanoparticles with Improved Antitumor Activity. *Int. J. Pharm.* **2011**, *403*, 285–291, doi:10.1016/j.ijpharm.2010.10.041.

104. Kunde, S.S.; Wairkar, S. Targeted Delivery of Albumin Nanoparticles for Breast Cancer: A Review. *Colloids Surfaces B Biointerfaces* **2022**, *213*, 112422, doi:10.1016/j.colsurfb.2022.112422.

105. Galisteo-González, F.; Molina-Bolívar, J.A. Systematic Study on the Preparation of BSA Nanoparticles. *Colloids Surfaces B Biointerfaces* **2014**, *123*, 286–292, doi:10.1016/j.colsurfb.2014.09.028.

106. Kayani, Z.; Firuzi, O.; Bordbar, A.K. Doughnut-Shaped Bovine Serum Albumin Nanoparticles Loaded with Doxorubicin for Overcoming Multidrug-Resistant in Cancer Cells. *Int. J. Biol. Macromol.* **2018**, *107*, 1835–1843, doi:10.1016/j.ijbiomac.2017.10.041.

107. Kang-Mieler, J.J.; Mieler, W.F. Thermo-Responsive Hydrogels for Ocular Drug Delivery. *Dev. Ophthalmol.* **2015**, *55*, 104–111, doi:10.1159/000434694.

108. Jithan, A.; Madhavi, K.; Madhavi, M.; Prabhakar, K. Preparation and Characterization of Albumin Nanoparticles Encapsulating Curcumin Intended for the Treatment of Breast Cancer. *Int. J. Pharm. Investig.* **2011**, *1*, 119, doi:10.4103/2230-973x.82432.

109. Clemente, N.; Boggio, E.; Gigliotti, L.C.; Raineri, D.; Ferrara, B.; Miglio, G.; Argenziano, M.; Chiocchetti, A.; Cappellano, G.; Trotta, F.; et al. Immunotherapy of Experimental Melanoma with ICOS-Fc Loaded in Biocompatible and Biodegradable Nanoparticles. *J. Control. Release* **2020**, *320*, 112–124, doi:10.1016/j.jconrel.2020.01.030.

110. Prados, J.; Melguizo, C.; Ortiz, R.; Velez, C.; J. Alvarez, P.; L. Arias, J.; A. Ruiz, M.; Gallardo, V.; Aranega, A. Doxorubicin-Loaded Nanoparticles: New Advances in Breast Cancer Therapy. *Anticancer. Agents Med. Chem.* **2012**, *12*, 1058–1070, doi:10.2174/187152012803529646.

111. Guzman-Villanueva, D.; Mendiola, M.R.; Nguyen, H.X.; Yambao, F.; Yu, N.; Weissig, V. Conjugation of Triphenylphosphonium Cation to Hydrophobic Moieties to Prepare Mitochondria-Targeting Nanocarriers. *Methods Mol. Biol.* **2019**, *2000*, 183—189, doi:10.1007/978-1-4939-9516-5_12.

112. Kothamasu, P.; Kanumur, H.; Ravur, N.; Maddu, C.; Parasuramrajam, R.; Thangavel, S. Nanocapsules: The Weapons for Novel Drug Delivery Systems. *BioImpacts* **2012**, *2*, 71–81, doi:10.5681/bi.2012.011.

113. Mayer, C. Nanocapsules as Drug Delivery Systems. *Int. J. Artif. Organs* **2005**, *28*, 1163–1171, doi:10.1177/039139880502801114.

114. Qian, K.; Wu, J.; Zhang, E.; Zhang, Y.; Fu, A. Biodegradable Double Nanocapsule as a Novel Multifunctional Carrier for Drug Delivery and Cell Imaging. *Int. J. Nanomedicine* **2015**, *10*, 4149–4157, doi:10.2147/IJN.S83731.

115. Kang, W.; Shi, Y.; Yang, Z.; Yin, X.; Zhao, Y.; Weng, L.; Teng, Z. Flexible Human Serum Albumin Nanocapsules to Enhance Drug Delivery and Cellular Uptake for Photodynamic/Chemo Cancer Therapy. *RSC Adv.* **2023**, *13*, 5609–5618, doi:10.1039/d2ra06859a.

116. Mozetič, M. Surface Modification to Improve Properties of Materials. *Materials (Basel).* **2019**, *12*, doi:10.3390/MA12030441.

117. Ruckenstein, E.; Li, Z.F. Surface Modification and Functionalization through the Self-Assembled Monolayer and Graft Polymerization. *Adv. Colloid Interface Sci.* **2005**, *113*, 43–63, doi:10.1016/j.cis.2004.07.009.

118. Arsalan Ahmed Shumaila Sarwar, Y.H.M.U.M.M.F.N.F.I.A.A.S.U.R.A.A.C.; Rehman, I.U. Surface-Modified Polymeric Nanoparticles for Drug Delivery to Cancer Cells. *Expert Opin. Drug Deliv.* **2021**, *18*, 1–24, doi:10.1080/17425247.2020.1822321.

119. Ivanova, A.; Ivanova, K.; Hoyo, J.; Heinze, T.; Sanchez-Gomez, S.; Tzanov, T. Layer-By-Layer Decorated Nanoparticles with Tunable Antibacterial and Antibiofilm Properties against Both Gram-Positive and Gram-Negative Bacteria. *ACS Appl. Mater. Interfaces* **2018**, *10*, 3314–3323, doi:10.1021/acsami.7b16508.

120. Sanità, G.; Carrese, B.; Lamberti, A. Nanoparticle Surface Functionalization: How to

Improve Biocompatibility and Cellular Internalization. *Front. Mol. Biosci.* **2020**, *7*, doi:10.3389/fmolb.2020.587012.

121. Schubert, J.; Chanana, M. Coating Matters: Review on Colloidal Stability of Nanoparticles with Biocompatible Coatings in Biological Media, Living Cells and Organisms. *Curr. Med. Chem.* **2018**, *25*, 4553–4586, doi:10.2174/0929867325666180601101859.

122. Osman, N.; Devnarain, N.; Omolo, C.A.; Fasiku, V.; Jaglal, Y.; Govender, T. Surface Modification of Nano-Drug Delivery Systems for Enhancing Antibiotic Delivery and Activity. *Wiley Interdiscip. Rev. Nanomedicine Nanobiotechnology* **2022**, *14*, 1–24, doi:10.1002/wnan.1758.

123. Elvira, C.; Gallardo, A.; San Roman, J.; Cifuentes, A. Covalent Polymer-Drug Conjugates. *Molecules* **2005**, *10*, 114–125, doi:10.3390/10010114.

124. Oriana, S.; Fracassi, A.; Archer, C.; Yamakoshi, Y. Covalent Surface Modification of Lipid Nanoparticles by Rapid Potassium Acyltrifluoroborate Amide Ligation. *Langmuir* **2018**, *34*, 13244–13251, doi:10.1021/acs.langmuir.8b01945.

125. Kuila, T.; Bose, S.; Mishra, A.K.; Khanra, P.; Kim, N.H.; Lee, J.H. Chemical Functionalization of Graphene and Its Applications. *Prog. Mater. Sci.* **2012**, *57*, 1061–1105, doi:10.1016/j.pmatsci.2012.03.002.

126. Ribeiro, H.; Da Silva, W.M.; Neves, J.C.; Calado, H.D.R.; Paniago, R.; Seara, L.M.; Mercês Camarano, D. Das; Silva, G.G. Multifunctional Nanocomposites Based on Tetraethylenepentamine-Modified Graphene Oxide/Epoxy. *Polym. Test.* **2015**, *43*, 182–192, doi:10.1016/j.polymertesting.2015.03.010.

127. Weber, C.; Coester, C.; Kreuter, J.; Langer, K. Desolvation Process and Surface Characterisation of Protein Nanoparticles. *Int. J. Pharm.* **2000**, *194*, 91–102, doi:10.1016/S0378-5173(99)00370-1.

128. Ulbrich, K.; Hekmatara, T.; Herbert, E.; Kreuter, J. Transferrin- and Transferrin-Receptor-Antibody-Modified Nanoparticles Enable Drug Delivery across the Blood-Brain Barrier (BBB). *Eur. J. Pharm. Biopharm. Off. J. Arbeitsgemeinschaft fur Pharm. Verfahrenstechnik e.V* **2009**, *71*, 251–256, doi:10.1016/j.ejpb.2008.08.021.

129. Pereverzeva, E.; Treschalin, I.; Bodyagin, D.; Maksimenko, O.; Langer, K.; Dreis, S.; Asmussen, B.; Kreuter, J.; Gelperina, S. Influence of the Formulation on the Tolerance Profile of Nanoparticle-Bound Doxorubicin in Healthy Rats: Focus on Cardio- and Testicular Toxicity. *Int. J. Pharm.* **2007**, *337*, 346–356, doi:10.1016/j.ijpharm.2007.01.031.

130. Zucchi, R.; Danesi, R. Cardiac Toxicity of Antineoplastic Anthracyclines. *Curr. Med. Chem. Anticancer. Agents* **2003**, *3*, 151–171, doi:10.2174/1568011033353434.

131. Russell, L.D.; Russell, J.A. Short-Term Morphological Response of the Rat Testis to Administration of Five Chemotherapeutic Agents. *Am. J. Anat.* **1991**, *192*, 142–168, doi:10.1002/aja.1001920205.

132. Singh, H.D.; Wang, G.; Uludağ, H.; Unsworth, L.D. Poly-L-Lysine-Coated Albumin Nanoparticles: Stability, Mechanism for Increasing in Vitro Enzymatic Resilience, and SiRNA Release Characteristics. *Acta Biomater.* **2010**, *6*, 4277–4284, doi:10.1016/j.actbio.2010.06.017.

133. Zhang, S.; Kucharski, C.; Doschak, M.R.; Sebald, W.; Uludağ, H. Polyethylenimine-PEG Coated Albumin Nanoparticles for BMP-2 Delivery. *Biomaterials* **2010**, *31*, 952–963, doi:10.1016/j.biomaterials.2009.10.011.

134. Zhang, S.; Doschak, M.R.; Uludağ, H. Pharmacokinetics and Bone Formation by BMP-2 Entrapped in Polyethylenimine-Coated Albumin Nanoparticles. *Biomaterials* **2009**, *30*, 5143–5155, doi:10.1016/j.biomaterials.2009.05.060.

135. Zhang, S.; Wang, G.; Lin, X.; Chatzinikolaidou, M.; Jennissen, H.P.; Laub, M.; Uludağ, H. Polyethylenimine-Coated Albumin Nanoparticles for BMP-2 Delivery. *Biotechnol. Prog.* **2008**, *24*, 945–956, doi:10.1002/btpr.12.

136. Badawy, M.E.I.; Rabea, E.I. A Biopolymer Chitosan and Its Derivatives as Promising Antimicrobial Agents against Plant Pathogens and Their Applications in Crop Protection. *Int. J. Carbohydr. Chem.* **2011**, *2011*, 1–29, doi:10.1155/2011/460381.

137. Younes, I.; Rinaudo, M. Chitin and Chitosan Preparation from Marine Sources. Structure, Properties and Applications. *Mar. Drugs* **2015**, *13*, 1133–1174, doi:10.3390/md13031133.

138. Kurita, K. Chitin and Chitosan: Functional Biopolymers from Marine Crustaceans. *Mar. Biotechnol. (NY).* **2006**, *8*, 203–226, doi:10.1007/s10126-005-0097-5.

139. Ways, T.M.M.; Lau, W.M.; Khutoryanskiy, V. V. Chitosan and Its Derivatives for Application in Mucoadhesive Drug Delivery Systems. *Polymers (Basel).* **2018**, *10*, doi:10.3390/polym10030267.

140. Nayak, A.; Olatunji, O.M.; Das, D.B.; Vladisavljević, G.T. Pharmaceutical Applications of Natural Polymers.; 2016.

141. Mohammed M. Mehanna, H.A.E.; Samaha, M.W. Mucoadhesive Liposomes as Ocular Delivery System: Physical, Microbiological, and in Vivo Assessment. *Drug Dev. Ind. Pharm.* **2010**, *36*, 108–118, doi:10.3109/03639040903099751.

142. Abbasi, S.; Paul, A.; Shao, W.; Prakash, S. Cationic Albumin Nanoparticles for Enhanced Drug Delivery to Treat Breast Cancer: Preparation and In Vitro Assessment . *J. Drug Deliv.* **2012**, *2012*, 1–8, doi:10.1155/2012/686108.

143. Radwan, S.E.S.; El-Moslemany, R.M.; Mehanna, R.A.; Thabet, E.H.; Abdelfattah, E.Z.A.; El-Kamel, A. Chitosan-Coated Bovine Serum Albumin Nanoparticles for Topical Tetrandrine Delivery in Glaucoma: In Vitro and in Vivo Assessment. *Drug Deliv.* **2022**, *29*, 1150–1163, doi:10.1080/10717544.2022.2058648.

144. Dodane, V.; Vilivalam, V.D. Pharmaceutical Applications of Chitosan. *Pharm. Sci. \& Technol. Today* **1998**, *1*, 246–253.

145. Maestrelli, F.; Zerrouk, N.; Chemtob, C.; Mura, P. Influence of Chitosan and Its Glutamate and Hydrochloride Salts on Naproxen Dissolution Rate and Permeation across Caco-2 Cells. *Int. J. Pharm.* **2004**, *271*, 257–267, doi:10.1016/j.ijpharm.2003.11.024.

146. Zamboulis, A.; Nanaki, S.; Michailidou, G.; Koumentakou, I.; Lazaridou, M.; Ainali, N.M.; Xanthopoulou, E.; Bikiaris, D.N. Chitosan and Its Derivatives for Ocular Delivery Formulations: Recent Advances and Developments. *Polymers (Basel).* **2020**, *12*, 9–11, doi:10.3390/polym12071519.

147. Prabaharan, M.; Rodriguez-Perez, M.A.; De Saja, J.A.; Mano, J.F. Preparation and Characterization of Poly(L-Lactic Acid)-Chitosan Hybrid Scaffolds with Drug Release

Capability. *J. Biomed. Mater. Res. - Part B Appl. Biomater.* **2007**, *81*, 427–434, doi:10.1002/jbm.b.30680.

148. Shen, Z.; Wei, W.; Zhao, Y.; Ma, G.; Dobashi, T.; Maki, Y.; Su, Z.; Wan, J. Thermosensitive Polymer-Conjugated Albumin Nanospheres as Thermal Targeting Anti-Cancer Drug Carrier. *Eur. J. Pharm. Sci. Off. J. Eur. Fed. Pharm. Sci.* **2008**, *35*, 271–282, doi:10.1016/j.ejps.2008.07.006.

149. Kouchakzadeh, H.; Shojaosadati, S.A.; Maghsoudi, A.; Vasheghani Farahani, E. Optimization of PEGylation Conditions for BSA Nanoparticles Using Response Surface Methodology. *AAPS PharmSciTech* **2010**, *11*, 1206–1211, doi:10.1208/s12249-010-9487-8.

150. Lin, W.; Garnett, M.C.; Davis, S.S.; Schacht, E.; Ferruti, P.; Illum, L. Preparation and Characterisation of Rose Bengal-Loaded Surface-Modified Albumin Nanoparticles. *J. Control. release Off. J. Control. Release Soc.* **2001**, *71*, 117–126, doi:10.1016/s0168-3659(01)00209-7.

151. Campbell, I.G.; Jones, T.A.; Foulkes, W.D.; Trowsdale, J. Folate-Binding Protein Is a Marker for Ovarian Cancer. *Cancer Res.* **1991**, *51*, 5329–5338.

152. Atkinson, S.F.; Bettinger, T.; Seymour, L.W.; Behr, J.P.; Ward, C.M. Conjugation of Folate via Gelonin Carbohydrate Residues Retains Ribosomal-Inactivating Properties of the Toxin and Permits Targeting to Folate Receptor Positive Cells. *J. Biol. Chem.* **2001**, *276*, 27930–27935, doi:10.1074/jbc.M102825200.

153. Oyewumi, M.O.; Mumper, R.J. Influence of Formulation Parameters on Gadolinium Entrapment and Tumor Cell Uptake Using Folate-Coated Nanoparticles. *Int. J. Pharm.* **2003**, *251*, 85–97, doi:10.1016/s0378-5173(02)00587-2.

154. Li, Q.; Liu, C.; Zhao, X.; Zu, Y.; Wang, Y.; Zhang, B.; Zhao, D.; Zhao, Q.; Su, L.; Gao, Y.; et al. Preparation, Characterization and Targeting of Micronized 10-Hydroxycamptothecin-Loaded Folate-Conjugated Human Serum Albumin Nanoparticles to Cancer Cells. *Int. J. Nanomedicine* **2011**, *6*, 397–405, doi:10.2147/ijn.s16144.

155. Chen, D.; Tang, Q.; Xue, W.; Xiang, J.; Zhang, L.; Wang, X. The Preparation and

Characterization of Folate-Conjugated Human Serum Albumin Magnetic Cisplatin Nanoparticles. *J. Biomed. Res.* **2010**, *24*, 26–32, doi:10.1016/S1674-8301(10)60005-X.

156. Zu, Y.; Zhang, Y.; Zhao, X.; Zhang, Q.; Liu, Y.; Jiang, R. Optimization of the Preparation Process of Vinblastine Sulfate (VBLS)-Loaded Folate-Conjugated Bovine Serum Albumin (BSA) Nanoparticles for Tumor-Targeted Drug Delivery Using Response Surface Methodology (RSM). *Int. J. Nanomedicine* **2009**, *4*, 321–333, doi:10.2147/ijn.s8501.

157. Zhang, L.; Hou, S.; Zhang, J.; Hu, W.; Wang, C. Preparation, Characterization, and in Vivo Evaluation of Mitoxantrone-Loaded, Folate-Conjugated Albumin Nanoparticles. *Arch. Pharm. Res.* **2010**, *33*, 1193–1198, doi:10.1007/s12272-010-0809-x.

158. Vandervoort, J.; Ludwig, A. Biocompatible Stabilizers in the Preparation of PLGA Nanoparticles: A Factorial Design Study. *Int. J. Pharm.* **2002**, *238*, 77–92, doi:10.1016/s0378-5173(02)00058-3.

159. Zhao, D.; Zhao, X.; Zu, Y.; Li, J.; Zhang, Y.; Jiang, R.; Zhang, Z. Preparation, Characterization, and in Vitro Targeted Delivery of Folate-Decorated Paclitaxel-Loaded Bovine Serum Albumin Nanoparticles. *Int. J. Nanomedicine* **2010**, *5*, 669–677, doi:10.2147/ijn.s12918.

160. Zu, Y.; Yuan, S.; Zhao, X.; Zhang, Y.; Zhang, X.; Jiang, R. [Preparation, activity and targeting ability evaluation in vitro on folate mediated epigallocatechin-3-gallate albumin nanoparticles]. *Yao Xue Xue Bao* **2009**, *44*, 525–531.

161. Liapis, H.; Adler, L.M.; Wick, M.R.; Rader, J.S. Expression of Alpha(v)Beta3 Integrin Is Less Frequent in Ovarian Epithelial Tumors of Low Malignant Potential in Contrast to Ovarian Carcinomas. *Hum. Pathol.* **1997**, *28*, 443–449, doi:10.1016/s0046-8177(97)90033-2.

162. Bellotti, E.; Schilling, A.L.; Little, S.R.; Decuzzi, P. Injectable Thermoresponsive Hydrogels as Drug Delivery System for the Treatment of Central Nervous System Disorders: A Review. *J. Control. Release* **2021**, *329*, 16–35, doi:10.1016/j.jconrel.2020.11.049.

163. Karmali, P.P.; Kotamraju, V.R.; Kastantin, M.; Black, M.; Missirlis, D.; Tirrell, M.;

Ruoslahti, E. Targeting of Albumin-Embedded Paclitaxel Nanoparticles to Tumors. *Nanomedicine* **2009**, *5*, 73–82, doi:10.1016/j.nano.2008.07.007.

164. Wartlick, H.; Michaelis, K.; Balthasar, S.; Strebhardt, K.; Kreuter, J.; Langer, K. Highly Specific HER2-Mediated Cellular Uptake of Antibody-Modified Nanoparticles in Tumour Cells. *J. Drug Target.* **2004**, *12*, 461–471, doi:10.1080/10611860400010697.

165. Nateghian, N.; Goodarzi, N.; Amini, M.; Atyabi, F.; Khorramizadeh, M.R.; Dinarvand, R. Biotin/Folate-Decorated Human Serum Albumin Nanoparticles of Docetaxel: Comparison of Chemically Conjugated Nanostructures and Physically Loaded Nanoparticles for Targeting of Breast Cancer. *Chem. Biol. \& Drug Des.* **2016**, *87*, 69–82, doi:https://doi.org/10.1111/cbdd.12624.

166. Anhorn, M.G.; Wagner, S.; Kreuter, J.; Langer, K.; von Briesen, H. Specific Targeting of HER2 Overexpressing Breast Cancer Cells with Doxorubicin-Loaded Trastuzumab-Modified Human Serum Albumin Nanoparticles. *Bioconjug. Chem.* **2008**, *19*, 2321–2331, doi:10.1021/bc8002452.

167. Löw, K.; Wacker, M.; Wagner, S.; Langer, K.; von Briesen, H. Targeted Human Serum Albumin Nanoparticles for Specific Uptake in EGFR-Expressing Colon Carcinoma Cells. *Nanomedicine* **2011**, *7*, 454–463, doi:10.1016/j.nano.2010.12.003.

168. Hodgson, R.; Christiansen, D.; Ierino, F.; Sandrin, M. Inducible Co-Stimulator (ICOS) in Transplantation: A Review. *Transplant. Rev.* **2022**, *36*, 100713, doi:10.1016/j.trre.2022.100713.

169. Li, D.Y.; Xiong, X.Z. ICOS+ Tregs: A Functional Subset of Tregs in Immune Diseases. *Front. Immunol.* **2020**, *11*, doi:10.3389/fimmu.2020.02104.

170. Solinas, C.; Gu-Trantien, C.; Willard-Gallo, K. The Rationale behind Targeting the ICOS-ICOS Ligand Costimulatory Pathway in Cancer Immunotherapy. *ESMO Open* **2020**, *5*, e000544, doi:10.1136/esmoopen-2019-000544.

171. Alves, G.F.; Stoppa, I.; Aimaretti, E.; Monge, C.; Mastrocola, R.; Porchietto, E.; Einaudi, G.; Collotta, D.; Bertocchi, I.; Boggio, E.; et al. ICOS-Fc as Innovative Immunomodulatory Approach to Counteract Inflammation and Organ Injury in Sepsis. *Front. Immunol.* **2022**, *13*, 1–13, doi:10.3389/fimmu.2022.992614.

172. Zhao, X.; Wang, Y.; Jiang, X.; Mo, B.; Wang, C.; Tang, M.; Rong, Y.; Zhang, G.; Hu, M.; Cai, H. Comprehensive Analysis of the Role of ICOS (CD278) in Pan-Cancer Prognosis and Immunotherapy. *BMC Cancer* **2023**, *23*, 1–15, doi:10.1186/s12885-023-10564-4.

173. Panneton, V.; Mindt, B.C.; Bouklouch, Y.; Bouchard, A.; Mohammaei, S.; Chang, J.; Diamantopoulos, N.; Witalis, M.; Li, J.; Stancescu, A.; et al. ICOS Costimulation Is Indispensable for the Differentiation of T Follicular Regulatory Cells. *Life Sci. Alliance* **2023**, *6*, 1–13, doi:10.26508/lsa.202201615.

174. Stoppa, I.; Gigliotti, C.L.; Clemente, N.; Pantham, D.; Dianzani, C.; Monge, C.; Puricelli, C.; Rolla, R.; Sutti, S.; Renò, F.; et al. ICOSL Stimulation by ICOS-Fc Accelerates Cutaneous Wound Healing In Vivo. *Int. J. Mol. Sci.* **2022**, *23*, doi:10.3390/ijms23137363.

175. Melo, P.; Montalbano, G.; Boggio, E.; Gigliotti, C.L.; Dianzani, C.; Dianzani, U.; Vitale-Brovarone, C.; Fiorilli, S. Electrospun Collagen Scaffold Bio-Functionalized with Recombinant ICOS-Fc: An Advanced Approach to Promote Bone Remodelling. *Polymers (Basel).* **2022**, *14*, doi:10.3390/polym14183780.

176. Lee, J.W.; Choi, J.; Kim, E.H.; Choi, J.; Kim, S.H.; Yang, Y. Design of SiRNA Bioconjugates for Efficient Control of Cancer-Associated Membrane Receptors. *ACS Omega* **2023**, *8*, 36435–36448, doi:10.1021/acsomega.3c05395.

177. International Council for Harmonisation EMEA/CHMP, 2009, ICH Topic Q 8 (R2) Pharmaceutical Development, Step 5: Note for Guidance on Pharmaceutical Development. *Eur. Med. Agency* **2009**, *8*.

178. Kamemura, N. Butylated Hydroxytoluene, a Food Additive, Modulates Membrane Potential and Increases the Susceptibility of Rat Thymocytes to Oxidative Stress. *Comput. Toxicol.* **2018**, *6*, 32–38, doi:10.1016/j.comtox.2018.04.001.

179. Robert, J.-L. Q8(R2): Pharmaceutical Development - ICH. *Int. Conf. Harmon. Tech. Requir. Regist. Pharm. Hum. Use, ICH-GCG ASEAN* **2010**, *8*, 26–28.

180. Sawada, T. Pharmaceutical Development. *Annu. Rep. Shionogi Res. Lab.* **2008**, *8*, 14–15, doi:10.3109/9781420081275-6.

181. Ahlert, J. ICH Q8 : Pharmaceutical Development . Regulatory Requirements Directed

by the New Note for Guidance (EMEA / CHMP / 167068 / 2004) in Comparison to the Previous Guideline (CPMP / QWP / 155 / 96). A Critical View from the Generic Pharmaceutical Industry. *ICH Harmon. Tripart. Guidel.* **2007**, 53.

182. Karanakov, L.; Tonic-Ribarska, J.; Glavas-Dodov, M.; Trajkovic-Jolevska, S. Analysis and Critical Review of ICH Q8, Q9 and Q10 from a Generic Pharmaceutical Industry View Point. *Maced. Pharm. Bull.* **2011**, *57*, 85–96, doi:10.33320/maced.pharm.bull.2011.57.010.

183. Moore, C.M. V; Ph, D. ICH Q8 / Q8R – Pharmaceutical Development • Background on ICH Q8 / Q8R • FDA Experience with QbD – Examples from CMC Pilot – Recent ONDQA Experience • Remaining Challenges • Concluding Comments. **2010**.

184. ter Horst, J.P.; Turimella, S.L.; Metsers, F.; Zwiers, A. Implementation of Quality by Design (QbD) Principles in Regulatory Dossiers of Medicinal Products in the European Union (EU) Between 2014 and 2019. *Ther. Innov. Regul. Sci.* **2021**, *55*, 583–590, doi:10.1007/s43441-020-00254-9.

185. Martins, S.; Tho, I.; Reimold, I.; Fricker, G.; Souto, E.; Ferreira, D.; Brandl, M. Brain Delivery of Camptothecin by Means of Solid Lipid Nanoparticles: Formulation Design, in Vitro and in Vivo Studies. *Int. J. Pharm.* **2012**, *439*, 49–62, doi:10.1016/j.ijpharm.2012.09.054.

186. Jenita, J.J.L.; Tibrewal, R.; Rathore, S.S.; Manjula, D.; Barnabas, W.; Mahesh, A.R. Formulation and Optimization of Albumin Nanoparticles Loaded Ivabradine Hydrochloride Using Response Surface Design. *J. Drug Deliv. Sci. Technol.* **2021**, *63*, 102461, doi:10.1016/j.jddst.2021.102461.

187. Chen, Z.; Luo, Z.; Lyu, J.; Wang, J.; Liu, Z.; Wei, J.; Lin, Y.; Zhong, Z. Preparation and Formulation Optimization of Methotrexate-Loaded Human Serum Albumin Nanoparticles Modified by Mannose. *Curr. Med. Chem.* **2021**, *28*, 5016–5029, doi:10.2174/0929867328666210118112640.

188. Yurt, F.; Özel, D.; Tunçel, A.; Gokbayrak, O.; Aktas, S. Synthesis and Optimization of the Docetaxel-Loaded and Durvalumab-Targeted Human Serum Albumin Nanoparticles, In Vitro Characterization on Triple-Negative Breast Cancer Cells. *ACS Omega* **2023**, *8*, 26287–26300, doi:10.1021/acsomega.3c02682.

189. Hanafy, N.A.N.; Abdelbadea, R.H.; Abdelaziz, A.E.; Mazyed, E.A. Formulation and Optimization of Folate-Bovine Serum Albumin-Coated Ethoniosomes of Pterostilbene as a Targeted Drug Delivery System for Lung Cancer: In Vitro and in Vivo Demonstrations. *Cancer Nanotechnol.* **2023**, *14*, 1–31, doi:10.1186/s12645-023-00197-4.

190. Dreis, S.; Rothweiler, F.; Michaelis, M.; Cinatl, J.; Kreuter, J.; Langer, K. Preparation, Characterisation and Maintenance of Drug Efficacy of Doxorubicin-Loaded Human Serum Albumin (HSA) Nanoparticles. *Int. J. Pharm.* **2007**, *341*, 207–214, doi:10.1016/j.ijpharm.2007.03.036.

191. Lomis, N.; Westfall, S.; Farahdel, L.; Malhotra, M.; Shum-Tim, D.; Prakash, S. Human Serum Albumin Nanoparticles for Use in Cancer Drug Delivery: Process Optimization and in Vitro Characterization. *Nanomaterials* **2016**, *6*, doi:10.3390/nano6060116.

192. Jachimska, B.; Pajor, A. Physico-Chemical Characterization of Bovine Serum Albumin in Solution and as Deposited on Surfaces. *Bioelectrochemistry* **2012**, *87*, 138–146, doi:10.1016/j.bioelechem.2011.09.004.

193. Younis, F.A.; Saleh, S.R.; El-Rahman, S.S.A.; Newairy, A.S.A.; El-Demellawy, M.A.; Ghareeb, D.A. Preparation, Physicochemical Characterization, and Bioactivity Evaluation of Berberine-Entrapped Albumin Nanoparticles. *Sci. Rep.* **2022**, *12*, 1–16, doi:10.1038/s41598-022-21568-8.

194. Dopierała, K.; Krajewska, M.; Weiss, M. Physicochemical Characterization of Oleanolic Acid-Human Serum Albumin Complexes for Pharmaceutical and Biosensing Applications. *Langmuir* **2020**, *36*, 3611–3623, doi:10.1021/acs.langmuir.0c00087.

195. Müller, B.G.; Leuenberger, H.; Kissel, T. Albumin Nanospheres as Carriers for Passive Drug Targeting: An Optimized Manufacturing Technique. *Pharm. Res.* 1996, *13*, 32–37.

196. Saha, M.; Sikder, P.; Saha, A.; Shah, S.; Sultana, S.; Emran, T.; Banik, A.; Islam, Z.; Islam, M.S.; Sharker, S.M.; et al. QbD Approach towards Robust Design Space for Flutamide/PiperineSelf-Emulsifying Drug Delivery System with Reduced Liver Injury. *AAPS PharmSciTech* **2022**, *23*, 1–14, doi:10.1208/s12249-022-02213-z.

197. Joshi, M.; Yadav, K.S.; Prabhakar, B. Quality by Design Approach for Development and Optimization of Rifampicin Loaded Bovine Serum Albumin Nanoparticles and Characterization. *Curr. Drug Deliv.* **2021**, *18*, 1338–1351, doi:10.2174/1567201818666210212090451.

198. Gao, F.; Chen, Z.; Zhou, L.; Xiao, X.; Wang, L.; Liu, X.; Wang, C.; Guo, Q. Preparation, Characterization and in Vitro Study of Bellidifolin Nano-Micelles. *RSC Adv.* **2022**, *12*, 21982–21989, doi:10.1039/d2ra02779h.

199. BASF Kolliphor® HS 15. *Basf* **2020**, 1–5.

200. Illum, L.; Jordan, F.; Lewis, A.L. CriticalSorb™: A Novel Efficient Nasal Delivery System for Human Growth Hormone Based on Solutol HS15. *J. Control. Release* **2012**, *162*, 194–200, doi:10.1016/j.jconrel.2012.06.014.

201. Gutiérrez-Méndez, N.; Chavez-Garay, D.R.; Leal-Ramos, M.Y. Lecithins: A Comprehensive Review of Their Properties and Their Use in Formulating Microemulsions. *J. Food Biochem.* **2022**, *46*, 1–22, doi:10.1111/jfbc.14157.

202. Ugandar R E, K.C.N. and L.D.L. In-Vitro and In-Vivo Evaluation of Directly Compressed Tablets of Simvastatin with Soy Lecithin. *World J. Pharm. Res.* **2015**, *4*, 2693–2718.

203. Jaworska, M.; Sikora, E.; Ogonowski, J. The Influence of Glicerides Oil Phase on O/W Nanoemulsion Formation by Pic Method. *Period. Polytech. Chem. Eng.* **2014**, *58*, 43–48, doi:10.3311/PPch.7299.

204. Mungali, M.; Sharma, N.; Gauri Caprylic/Capric Triglyceride. *Nat. Occur. Chem. against Alzheimer's Dis.* **2020**, 139–146, doi:10.1016/B978-0-12-819212-2.00011-6.

205. Joseph, S. PRODUCTIVITY BENEFITS OF SINGLE REACTION CHAMBER (SRC) MICROWAVE DIGESTION. 1–4.

206. Herminia López-Salazar,* Brenda Hildeliza Camacho-Díaz, Martha Lucia Arenas Ocampo, and A.R.J.-A. Microwave-Assisted Extraction of Functional Compounds from Plants: A Review.

207. Tatke, P.; Jaiswal, Y. An Overview of Microwave Assisted Extraction and Its Applications in Herbal Drug Research. *Res. J. Med. Plant* 2011, *5*, 21–31.

208. Teo, C.C.; Chong, W.P.K.; Ho, Y.S. Development and Application of Microwave-

Assisted Extraction Technique in Biological Sample Preparation for Small Molecule Analysis. *Metabolomics* **2013**, *9*, 1109–1128, doi:10.1007/s11306-013-0528-7.

209. Scheu, C.; Kaplan, W.D. Introduction to Scanning Electron Microscopy. *In-Situ Electron Microsc. Appl. Physics, Chem. Mater. Sci.* **2012**, 1–37, doi:10.1002/9783527652167.ch1.

210. Tkachenko, Y.; Niedzielski, P. FTIR as a Method for Qualitative Assessment of Solid Samples in Geochemical Research: A Review. *Molecules* **2022**, *27*, doi:10.3390/molecules27248846.

211. Britannica The Editors of Encyclopaedia. “Michelson Interferometer”. ,. *Encycl. Br.* **2024**.

212. Arzeni, C.; Pérez, O.E.; Pilosof, A.M.R. Power Ultrasound Assisted Design of Egg Albumin Nanoparticles. *Food Biophys.* **2015**, *10*, 439–446, doi:10.1007/s11483-015-9407-2.

213. Kumar, K.; Srivastav, S.; Sharanagat, V.S. Ultrasound Assisted Extraction (UAE) of Bioactive Compounds from Fruit and Vegetable Processing by-Products: A Review. *Ultrason. Sonochem.* **2021**, *70*, 105325, doi:10.1016/j.ultsonch.2020.105325.

214. Carreira-Casais, A.; Otero, P.; Garcia-Perez, P.; Garcia-Oliveira, P.; Pereira, A.G.; Carpena, M.; Soria-Lopez, A.; Simal-Gandara, J.; Prieto, M.A. Benefits and Drawbacks of Ultrasound-Assisted Extraction for the Recovery of Bioactive Compounds from Marine Algae. *Int. J. Environ. Res. Public Health* **2021**, *18*, doi:10.3390/ijerph18179153.

215. Mehta, N.; S, J.; Kumar, P.; Verma, A.K.; Umaraw, P.; Khatkar, S.K.; Khatkar, A.B.; Pathak, D.; Kaka, U.; Sazili, A.Q. Ultrasound-Assisted Extraction and the Encapsulation of Bioactive Components for Food Applications. *Foods* **2022**, *11*, doi:10.3390/foods11192973.

216. Aihua Sun, X.C. Applications and Prospects of Ultrasound-Assisted Extraction in Chinese Herbal Medicine. *Open Access J. Biomed. Sci.* **2019**, *1*, 5–15, doi:10.38125/oajbs.000103.

217. Belwal, T.; Huang, H.; Li, L.; Duan, Z.; Zhang, X.; Aalim, H.; Luo, Z. Optimization Model

for Ultrasonic-Assisted and Scale-up Extraction of Anthocyanins from Pyrus Communis 'Starkrimson' Fruit Peel. *Food Chem.* **2019**, *297*, doi:10.1016/j.foodchem.2019.124993.

218. Tamminen, J.; Holappa, J.; Vladimirovich Gradov, D.; Koiranen, T. Scaling up Continuous Ultrasound-Assisted Extractor for Plant Extracts by Using Spinach Leaves as a Test Material. *Ultrason. Sonochem.* **2022**, *90*, 106171, doi:10.1016/j.ultsonch.2022.106171.

219. Martina, K.; Tagliapietra, S.; Barge, A.; Cravotto, G. Combined Microwaves/Ultrasound, a Hybrid Technology. *Top. Curr. Chem.* **2016**, *374*, doi:10.1007/s41061-016-0082-7.

220. Cravotto, G.; Cintas, P. The Combined Use of Microwaves and Ultrasound: Improved Tools in Process Chemistry and Organic Synthesis. *Chem. - A Eur. J.* **2007**, *13*, 1902–1909, doi:10.1002/chem.200601845.

221. Baig, R.B.N.; Varma, R.S. Alternative Energy Input: Mechanochemical, Microwave and Ultrasound-Assisted Organic Synthesis. *Chem. Soc. Rev.* **2012**, *41*, 1559–1584, doi:10.1039/c1cs15204a.

222. Cravotto, G.; Cintas, P. Power Ultrasound in Organic Synthesis: Moving Cavitational Chemistry from Academia to Innovative and Large-Scale Applications. *Chem. Soc. Rev.* **2006**, *35*, 180–196, doi:10.1039/b503848k.

223. Yu, A.F.; Chan, A.T.; Steingart, R.M. Cardiac Magnetic Resonance and Cardio-Oncology: Does T 2 Signal the End of Anthracycline Cardiotoxicity? *J. Am. Coll. Cardiol.* **2019**, *73*, 792–794, doi:10.1016/j.jacc.2018.11.045.

224. Mordente, A.; Meucci, E.; Silvestrini, A.; Martorana, G.; Giardina, B. New Developments in Anthracycline-Induced Cardiotoxicity. *Curr. Med. Chem.* **2009**, *16*, 1656–1672, doi:10.2174/092986709788186228.

225. Rivankar, S. An Overview of Doxorubicin Formulations in Cancer Therapy. *J. Cancer Res. Ther.* **2014**, *10*, 853–858, doi:10.4103/0973-1482.139267.

226. Peter, S.; Alven, S.; Maseko, R.B.; Aderibigbe, B.A. Doxorubicin-Based Hybrid Compounds as Potential Anticancer Agents: A Review. *Molecules* **2022**, *27*, 1–20,

doi:10.3390/molecules27144478.

227. Kciuk, M.; Gielecińska, A.; Mujwar, S.; Kołat, D.; Kałuzińska-Kołat, Ż.; Celik, I.; Kontek, R. Doxorubicin—An Agent with Multiple Mechanisms of Anticancer Activity. *Cells* **2023**, *12*, 1–30, doi:10.3390/cells12040659.

228. Nicoletto, R.E.; Ofner, C.M. Cytotoxic Mechanisms of Doxorubicin at Clinically Relevant Concentrations in Breast Cancer Cells. *Cancer Chemother. Pharmacol.* **2022**, *89*, 285–311, doi:10.1007/s00280-022-04400-y.

229. Kciuk, M.; Gielecińska, A.; Mujwar, S.; Kołat, D.; Kałuzińska-Kołat, Ż.; Celik, I.; Kontek, R. Doxorubicin—An Agent with Multiple Mechanisms of Anticancer Activity. *Cells* **2023**, *12*, 26–32, doi:10.3390/cells12040659.

230. Sritharan, S.; Sivalingam, N. A Comprehensive Review on Time-Tested Anticancer Drug Doxorubicin. *Life Sci.* **2021**, *278*, 119527, doi:10.1016/j.lfs.2021.119527.

231. Koleini, N.; Nickel, B.E.; Edel, A.L.; Fandrich, R.R.; Ravandi, A.; Kardami, E. Oxidized Phospholipids in Doxorubicin-Induced Cardiotoxicity. *Chem. Biol. Interact.* **2019**, *303*, 35–39, doi:10.1016/j.cbi.2019.01.032.

232. Luu, A.Z.; Chowdhury, B.; Al-Omran, M.; Teoh, H.; Hess, D.A.; Verma, S. Role of Endothelium in Doxorubicin-Induced Cardiomyopathy. *JACC Basic to Transl. Sci.* **2018**, *3*, 861–870, doi:10.1016/j.jacbts.2018.06.005.

233. Ren, L.; Wang, L.; Rehberg, M.; Stoeger, T.; Zhang, J.; Chen, S. Applications and Immunological Effects of Quantum Dots on Respiratory System. *Front. Immunol.* **2022**, doi:10.3389/FIMMU.2021.795232.

234. Pautke, C.; Schieker, M.; Tischer, T.; Kolk, A.; Neth, P.; Mutschler, W.; Milz, S. Characterization of Osteosarcoma Cell Lines MG-63, Saos-2 and U-2 OS in Comparison to Human Osteoblasts. *Anticancer Res.* **2004**, *24*, 3743–3748.

235. Agrawal, K. Doxorubicin. In *xPharm: The Comprehensive Pharmacology Reference*; Enna, S.J., Bylund, D.B., Eds.; Elsevier: New York, 2007; pp. 1–5 ISBN 978-0-08-055232-3.

236. Ritter, J.; Bielack, S.S. Osteosarcoma. *Ann. Oncol.* **2010**, *21*, 320–325, doi:10.1093/annonc/mdq276.

237. American Cancer Society, I. 2023-Cancer-Facts-and-Figures 2023.

238. Yu, D.; Zhang, S.; Feng, A.; Xu, D.; Zhu, Q.; Mao, Y.; Zhao, Y.; Lv, Y.; Han, C.; Liu, R.; et al. Methotrexate, Doxorubicin, and Cisplatinum Regimen Is Still the Preferred Option for Osteosarcoma Chemotherapy: A Meta-Analysis and Clinical Observation. *Medicine (Baltimore).* **2019**, *98*, e15582, doi:10.1097/MD.0000000000015582.

239. de Kraker, J.; Voûte, P.A. Experience with Ifosfamide in Paediatric Tumours. *Cancer Chemother. Pharmacol.* **1989**, *24 Suppl 1*, S28-9, doi:10.1007/BF00253235.

240. Bacci, G.; Ferrari, S.; Lari, S.; Mercuri, M.; Donati, D.; Longhi, A.; Forni, C.; Bertoni, F.; Versari, M.; Pignotti, E. Osteosarcoma of the Limb. Amputation or Limb Salvage in Patients Treated by Neoadjuvant Chemotherapy. *J. Bone Joint Surg. Br.* **2002**, *84*, 88–92, doi:10.1302/0301-620x.84b1.12211.

241. Bramwell, V.H.C.; Anderson, D.; Charette, M.L. Doxorubicin-Based Chemotherapy for the Palliative Treatment of Adult Patients with Locally Advanced or Metastatic Soft-Tissue Sarcoma: A Meta-Analysis and Clinical Practice Guideline. *Sarcoma* **2000**, *4*, 103–112, doi:10.1080/13577140020008066.

242. Pakos, E.E.; Ioannidis, J.P.A. The Association of P-Glycoprotein with Response to Chemotherapy and Clinical Outcome in Patients with Osteosarcoma. A Meta-Analysis. *Cancer* **2003**, *98*, 581–589, doi:10.1002/cncr.11546.

243. Scherer, P.E.; Williams, S.; Fogliano, M.; Baldini, G.; Lodish, H.F. A Novel Serum Protein Similar to C1q, Produced Exclusively in Adipocytes. *J. Biol. Chem.* **1995**, *270*, 26746–26749, doi:10.1074/jbc.270.45.26746.

244. Peana, A.T.; D'Aquila, P.S.; Chessa, M.L.; Moretti, M.D.L.; Serra, G.; Pippia, P. (-)-Linalool Produces Antinociception in Two Experimental Models of Pain. *Eur. J. Pharmacol.* **2003**, *460*, 37–41, doi:10.1016/s0014-2999(02)02856-x.

245. Gu, W.; Wu, C.; Chen, J.; Xiao, Y. Nanotechnology in the Targeted Drug Delivery for Bone Diseases and Bone Regeneration. *Int. J. Nanomedicine* **2013**, *8*, 2305–2317, doi:10.2147/IJN.S44393.

246. Redoglia, V.; Dianzani, U.; Rojo, J.M.; Portolés, P.; Bragardo, M.; Wolff, H.; Buonfiglio, D.; Bonissoni, S.; Janeway, C.A. Characterization of H4: A Mouse T Lymphocyte Activation Molecule Functionally Associated with the CD3/T Cell Receptor. *Eur. J. Immunol.* **1996**, *26*, 2781–2789, doi:10.1002/eji.1830261134.

247. Buonfiglio, D.; Bragardo, M.; Bonissoni, S.; Redoglia, V.; Cauda, R.; Zupo, S.; Burgio, V.L.; Wolff, H.; Franssila, K.; Gaidano, G.; et al. Characterization of a Novel Human Surface Molecule Selectively Expressed by Mature Thymocytes, Activated T Cells and Subsets of T Cell Lymphomas. *Eur. J. Immunol.* **1999**, *29*, 2863–2874, doi:10.1002/(SICI)1521-4141(199909)29:09<2863::AID-IMMU2863>3.0.CO;2-W.

248. Fiorilli, S.; Pagani, M.; Boggio, E.; Gigliotti, C.L.; Dianzani, C.; Gauthier, R.; Pontremoli, C.; Montalbano, G.; Dianzani, U.; Vitale-Brovarone, C. Sr-Containing Mesoporous Bioactive Glasses Bio-Functionalized with Recombinant ICOS-Fc: An in Vitro Study. *Nanomaterials* **2021**, *11*, 1–23, doi:10.3390/nano11020321.

249. Gigliotti, C.L.; Boggio, E.; Clemente, N.; Shivakumar, Y.; Toth, E.; Sblattero, D.; D'Amelio, P.; Isaia, G.C.; Dianzani, C.; Yagi, J.; et al. ICOS-Ligand Triggering Impairs Osteoclast Differentiation and Function In Vitro and In Vivo. *J. Immunol.* **2016**, *197*, 3905–3916, doi:10.4049/jimmunol.1600424.

250. Rashighi, M.; Harris, J.E. HHS Public Access. *Physiol. Behav.* **2017**, *176*, 139–148, doi:10.1053/j.gastro.2016.08.014.CagY.

251. Dash, S.; Murthy, P.N.; Nath, L.; Chowdhury, P. Kinetic Modeling on Drug Release from Controlled Drug Delivery Systems. *Acta Pol. Pharm. - Drug Res.* **2010**, *67*, 217–223.

252. Ficiarà, E.; Ansari, S.A.; Argenziano, M.; Cangemi, L.; Monge, C.; Cavalli, R.; D'Agata, F. Beyond Oncological Hyperthermia: Physically Drivable Magnetic Nanobubbles as Novelmultipurpose Theranostic Carriers in the Central Nervous System. *Molecules* **2020**, *25*, doi:10.3390/molecules25092104.